

TLE202x, TLE202xA, TLE202xB, TLE202xY EXCALIBUR HIGH-SPEED LOW-POWER PRECISION OPERATIONAL AMPLIFIERS

SLOS191D – FEBRUARY 1997 – REVISED NOVEMBER 2010

- Supply Current . . . 300 μ A Max
- High Unity-Gain Bandwidth . . . 2 MHz Typ
- High Slew Rate . . . 0.45 V/ μ s Min
- Supply-Current Change Over Military Temp Range . . . 10 μ A Typ at $V_{CC} \pm = \pm 15$ V
- Specified for Both 5-V Single-Supply and ± 15 -V Operation
- Phase-Reversal Protection
- High Open-Loop Gain . . . 6.5 V/ μ V (136 dB) Typ
- Low Offset Voltage . . . 100 μ V Max
- Offset Voltage Drift With Time 0.005 μ V/mo Typ
- Low Input Bias Current . . . 50 nA Max
- Low Noise Voltage . . . 19 nV/ $\sqrt{\text{Hz}}$ Typ

description

The TLE202x, TLE202xA, and TLE202xB devices are precision, high-speed, low-power operational amplifiers using a new Texas Instruments Excalibur process. These devices combine the best features of the OP21 with highly improved slew rate and unity-gain bandwidth.

The complementary bipolar Excalibur process utilizes isolated vertical pnp transistors that yield dramatic improvement in unity-gain bandwidth and slew rate over similar devices.

The addition of a bias circuit in conjunction with this process results in extremely stable parameters with both time and temperature. This means that a precision device remains a precision device even with changes in temperature and over years of use.

This combination of excellent dc performance with a common-mode input voltage range that includes the negative rail makes these devices the ideal choice for low-level signal conditioning applications in either single-supply or split-supply configurations. In addition, these devices offer phase-reversal protection circuitry that eliminates an unexpected change in output states when one of the inputs goes below the negative supply rail.

A variety of available options includes small-outline and chip-carrier versions for high-density systems applications.

The C-suffix devices are characterized for operation from 0°C to 70°C. The I-suffix devices are characterized for operation from –40°C to 85°C. The M-suffix devices are characterized for operation over the full military temperature range of –55°C to 125°C.



Please be aware that an important notice concerning availability, standard warranty, and use in critical applications of Texas Instruments semiconductor products and disclaimers thereto appears at the end of this data sheet.

All trademarks are the property of their respective owners.

PRODUCTION DATA information is current as of publication date. Products conform to specifications per the terms of Texas Instruments standard warranty. Production processing does not necessarily include testing of all parameters.



POST OFFICE BOX 655303 • DALLAS, TEXAS 75265

Copyright © 2010, Texas Instruments Incorporated

TLE202x, TLE202xA, TLE202xB, TLE202xY EXCALIBUR HIGH-SPEED LOW-POWER PRECISION OPERATIONAL AMPLIFIERS

SLOS191D – FEBRUARY 1997 – REVISED NOVEMBER 2010

TLE2021 AVAILABLE OPTIONS

| T _A | V _{IO} max AT 25°C | PACKAGED DEVICES | | | | | | CHIP FORM [§] (Y) |
|----------------------|--------------------------------|--------------------------------------|---------------------------|---------------------------|---------------------------|-------------------------|----------------------------|----------------------------------|
| | | SMALL OUTLINE [†] (D) | SSOP [‡] (DB) | CHIP CARRIER (FK) | CERAMIC DIP (JG) | PLASTIC DIP (P) | TSSOP [‡] (PW) | |
| 0°C to 70°C | 200 μV 500 μV | TLE2021ACD TLE2021CD | TLE2021CDBLE | — | — | TLE2021ACP TLE2021CP | — TLE2021CPWLE | — TLE2021Y |
| -40°C to 85°C | 200 μV 500 μV | TLE2021AID TLE2021ID | — | — | — | TLE2021AIP TLE2021IP | — | — |
| -55°C to 125°C | 100 μV 500 μV | — TLE2021MD | — | TLE2021BMFK TLE2021MFK | TLE2021BMJG TLE2021MJG | — TLE2021MP | — | — |

[†] The D packages are available taped and reeled. To order a taped and reeled part, add the suffix R (e.g., TLE2021CDR).

[‡] The DB and PW packages are only available left-end taped and reeled.

[§] Chip forms are tested at 25°C only.

TLE2022 AVAILABLE OPTIONS

| T _A | V _{IO} max AT 25°C | PACKAGED DEVICES | | | | | | CHIP FORM [§] (Y) |
|----------------------|--------------------------------|---------------------------------------|---------------------------|--------------------------------|--|------------------------------|----------------------------|----------------------------------|
| | | SMALL OUTLINE [†] (D) | SSOP [‡] (DB) | CHIP CARRIER (FK) | CERAMIC DIP (JG) | PLASTIC DIP (P) | TSSOP [‡] (PW) | |
| 0°C to 70°C | 150 μV 300 μV 500 μV | TLE2022BCD TLE2022ACD TLE2022CD | — — TLE2022CDBLE | — | — | — TLE2022ACP TLE2022CP | — — TLE2022CPWLE | — — TLE2022Y |
| -40°C to 85°C | 150 μV 300 μV 500 μV | TLE2022BID TLE2022AID TLE2022ID | — | — | — | — TLE2022AIP TLE2022IP | — | — |
| -55°C to 125°C | 150 μV 300 μV 500 μV | — TLE2022AMD TLE2022MD | — | — TLE2022AMFK TLE2022MFK | TLE2022BMJG TLE2022AMJG TLE2022MJG | — TLE2022AMP TLE2022MP | — | — |

[†] The D packages are available taped and reeled. To order a taped and reeled part, add the suffix R (e.g., TLE2022CDR).

[‡] The DB and PW packages are only available left-end taped and reeled.

[§] Chip forms are tested at 25°C only.

TLE2024 AVAILABLE OPTIONS

| T _A | V _{IO} max AT 25°C | PACKAGED DEVICES | | | | CHIP FORM [§] (Y) |
|----------------|--------------------------------|--|--|---------------------------------------|---------------------------------------|----------------------------------|
| | | SMALL OUTLINE (DW) | CHIP CARRIER (FK) | CERAMIC DIP (J) | PLASTIC DIP (N) | |
| 0°C to 70°C | 500 μV 750 μV 1000 μV | TLE2024BCDW TLE2024ACDW TLE2024CDW | — | — | TLE2024BCN TLE2024ACN TLE2024CN | — — TLE2024Y |
| -40°C to 85°C | 500 μV 750 μV 1000 μV | TLE2024BIDW TLE2024AIDW TLE2024IDW | — | — | TLE2024BIN TLE2024AIN TLE2024IN | — |
| -55°C to 125°C | 500 μV 750 μV 1000 μV | TLE2024BMDW TLE2024AMDW TLE2024MDW | TLE2024BMFK TLE2024AMFK TLE2024MFK | TLE2024BMJ TLE2024AMJ TLE2024MJ | TLE2024BMN TLE2024AMN TLE2024MN | — |

[§] Chip forms are tested at 25°C only.



TLE202x, TLE202xA, TLE202xB, TLE202xY EXCALIBUR HIGH-SPEED LOW-POWER PRECISION OPERATIONAL AMPLIFIERS

SLOS191D – FEBRUARY 1997 – REVISED NOVEMBER 2010

TLE2021
D, DB, JG, P, OR PW PACKAGE
(TOP VIEW)



NC – No internal connection

TLE2021
FK PACKAGE
(TOP VIEW)

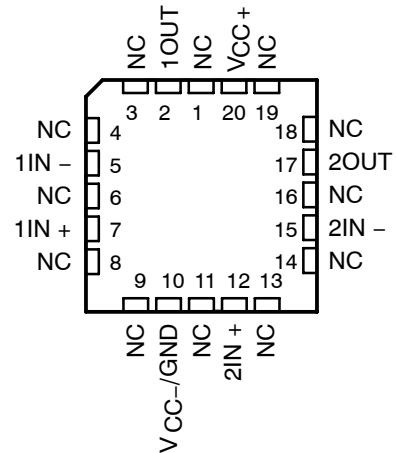


TLE2021
D, DB, JG, P, OR PW PACKAGE
(TOP VIEW)



NC – No internal connection

TLE2021
FK PACKAGE
(TOP VIEW)

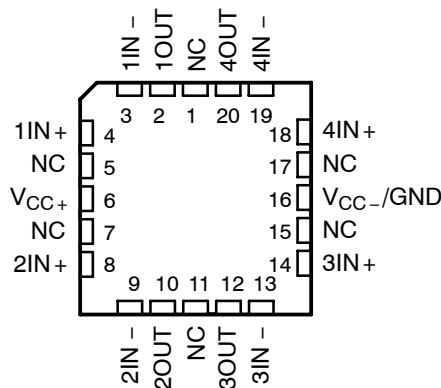


TLE2021
DW PACKAGE
(TOP VIEW)

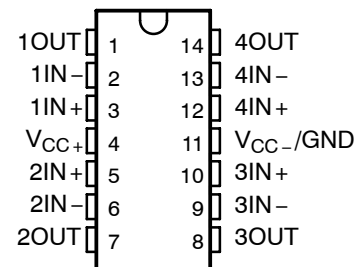


NC – No internal connection

TLE2021
FK PACKAGE
(TOP VIEW)



TLE2021
J OR N PACKAGE
(TOP VIEW)



TLE202x, TLE202xA, TLE202xB, TLE202xY EXCALIBUR HIGH-SPEED LOW-POWER PRECISION OPERATIONAL AMPLIFIERS

SLOS191D – FEBRUARY 1997 – REVISED NOVEMBER 2010

TLE2021Y chip information

This chip, when properly assembled, display characteristics similar to the TLE2021. Thermal compression or ultrasonic bonding may be used on the doped-aluminum bonding pads. This chip may be mounted with conductive epoxy or a gold-silicon preform.

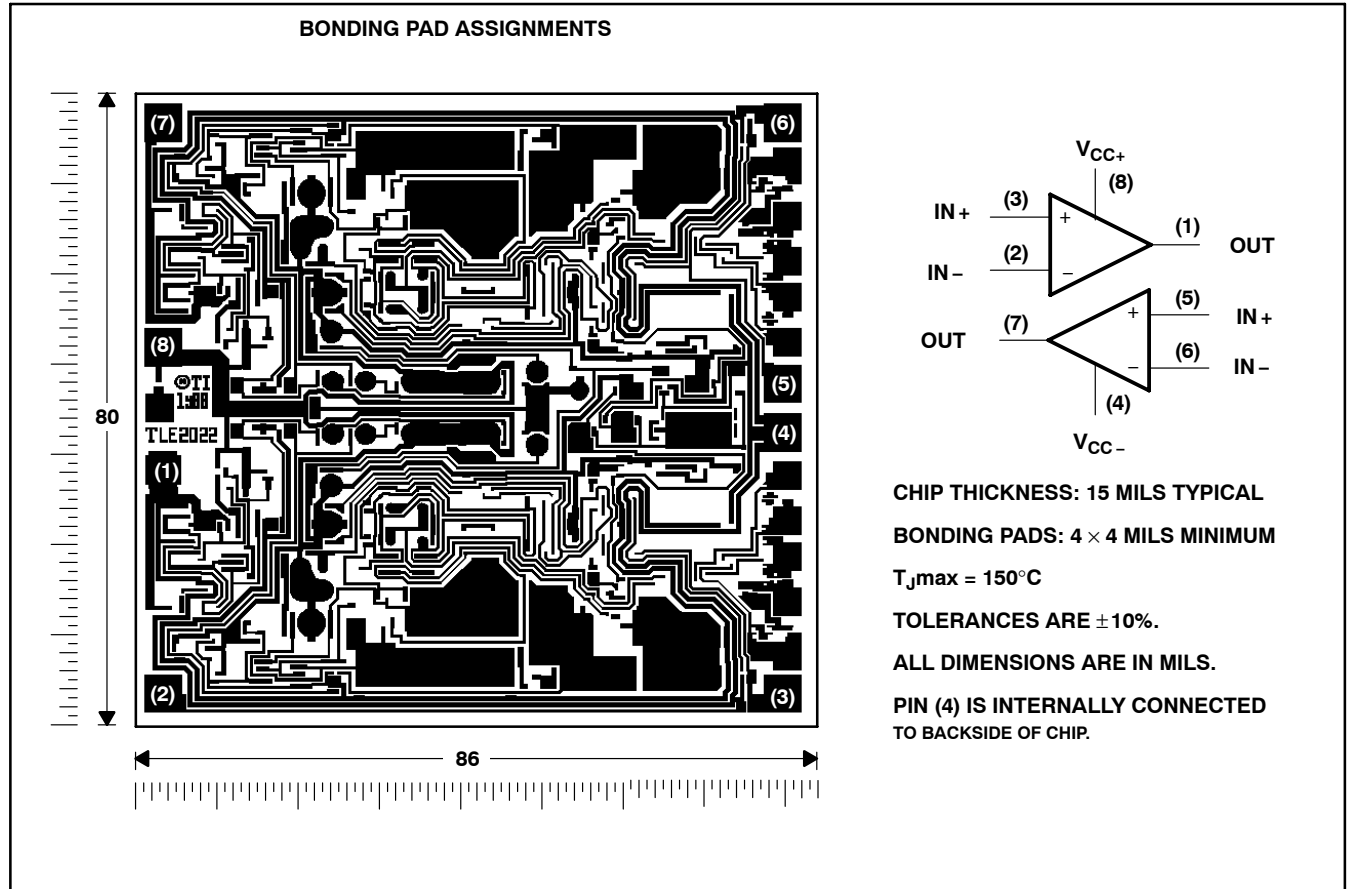


TLE202x, TLE202xA, TLE202xB, TLE202xY EXCALIBUR HIGH-SPEED LOW-POWER PRECISION OPERATIONAL AMPLIFIERS

SLOS191D – FEBRUARY 1997 – REVISED NOVEMBER 2010

TLE2022Y chip information

This chip, when properly assembled, displays characteristics similar to TLE2022. Thermal compression or ultrasonic bonding may be used on the doped-aluminum bonding pads. This chip may be mounted with conductive epoxy or a gold-silicon preform.



TLE202x, TLE202xA, TLE202xB, TLE202xY EXCALIBUR HIGH-SPEED LOW-POWER PRECISION OPERATIONAL AMPLIFIERS

SLOS191D – FEBRUARY 1997 – REVISED NOVEMBER 2010

TLE2024Y chip information

This chip, when properly assembled, displays characteristics similar to the TLE2024. Thermal compression or ultrasonic bonding may be used on the doped aluminum-bonding pads. This chip may be mounted with conductive epoxy or a gold-silicon preform.



TLE202x, TLE202xA, TLE202xB, TLE202xY EXCALIBUR HIGH-SPEED LOW-POWER PRECISION OPERATIONAL AMPLIFIERS

SLOS191D – FEBRUARY 1997 – REVISED NOVEMBER 2010

equivalent schematic (each amplifier)



| ACTUAL DEVICE COMPONENT COUNT | | | |
|-------------------------------|---------|---------|---------|
| COMPONENT | TLE2021 | TLE2022 | TLE2024 |
| Transistors | 40 | 80 | 160 |
| Resistors | 7 | 14 | 28 |
| Diodes | 4 | 8 | 16 |
| Capacitors | 4 | 8 | 16 |

TLE202x, TLE202xA, TLE202xB, TLE202xY EXCALIBUR HIGH-SPEED LOW-POWER PRECISION OPERATIONAL AMPLIFIERS

SLOS191D – FEBRUARY 1997 – REVISED NOVEMBER 2010

absolute maximum ratings over operating free-air temperature range (unless otherwise noted)[†]

| | |
|---|------------------------------|
| Supply voltage, V_{CC+} (see Note 1) | 20 V |
| Supply voltage, V_{CC-} (see Note 1) | -20 V |
| Differential input voltage, V_{ID} (see Note 2) | ± 0.6 V |
| Input voltage range, V_I (any input, see Note 1) | $\pm V_{CC}$ |
| Input current, I_I (each input) | ± 1 mA |
| Output current, I_O (each output): | |
| TLE2021 | ± 20 mA |
| TLE2022 | ± 30 mA |
| TLE2024 | ± 40 mA |
| Total current into V_{CC+} | 80 mA |
| Total current out of V_{CC-} | 80 mA |
| Duration of short-circuit current at (or below) 25°C (see Note 3) | unlimited |
| Continuous total power dissipation | See Dissipation Rating Table |
| Operating free-air temperature range, T_A : C suffix | 0°C to 70°C |
| I suffix | -40°C to 85°C |
| M suffix | -55°C to 125°C |
| Storage temperature range, T_{stg} | -65°C to 150°C |
| Case temperature for 60 seconds, T_C : FK package | 260°C |
| Lead temperature 1,6 mm (1/16 inch) from case for 10 seconds: D, DP, P, or PW package | 260°C |
| Lead temperature 1,6 mm (1/16 inch) from case for 60 seconds: JG package | 300°C |

[†] Stresses beyond those listed under “absolute maximum ratings” may cause permanent damage to the device. These are stress ratings only, and functional operation of the device at these or any other conditions beyond those indicated under “recommended operating conditions” is not implied. Exposure to absolute-maximum-rated conditions for extended periods may affect device reliability.

- NOTES:
- All voltage values, except differential voltages, are with respect to the midpoint between V_{CC+} and V_{CC-} .
 - Differential voltages are at $IN+$ with respect to $IN-$. Excessive current flows if a differential input voltage in excess of approximately ± 600 mV is applied between the inputs unless some limiting resistance is used.
 - The output may be shorted to either supply. Temperature and/or supply voltages must be limited to ensure that the maximum dissipation rating is not exceeded.

DISSIPATION RATING TABLE

| PACKAGE | $T_A \leq 25^\circ\text{C}$ POWER RATING | DERATING FACTOR ABOVE $T_A = 25^\circ\text{C}$ | $T_A = 70^\circ\text{C}$ POWER RATING | $T_A = 85^\circ\text{C}$ POWER RATING | $T_A = 125^\circ\text{C}$ POWER RATING |
|---------|---|---|--|--|---|
| D-8 | 725 mW | 5.8 mW/°C | 464 mW | 377 mW | 145 mW |
| DB-8 | 525 mW | 4.2 mW/°C | 336 mW | — | — |
| DW-16 | 1025 mW | 8.2 mW/°C | 656 mW | 533 mW | 205 mW |
| FK | 1375 mW | 11.0 mW/°C | 880 mW | 715 mW | 275 mW |
| J-14 | 1375 mW | 11.0 mW/°C | 880 mW | 715 mW | 275 mW |
| JG-8 | 1050 mW | 8.4 mW/°C | 672 mW | 546 mW | 210 mW |
| N-14 | 1150 mW | 9.2 mW/°C | 736 mW | 598 mW | 230 mW |
| P-8 | 1000 mW | 8.0 mW/°C | 640 mW | 520 mW | 200 mW |
| PW-8 | 525 mW | 4.2 mW/°C | 336 mW | — | — |

recommended operating conditions

| | | C SUFFIX | | I SUFFIX | | M SUFFIX | | UNIT |
|---------------------------------------|------------------------|----------|----------|----------|----------|----------|----------|------|
| | | MIN | MAX | MIN | MAX | MIN | MAX | |
| Supply voltage, V_{CC} | | ± 2 | ± 20 | ± 2 | ± 20 | ± 2 | ± 20 | V |
| Common-mode input voltage, V_{IC} | $V_{CC} = \pm 5$ V | 0 | 3.5 | 0 | 3.2 | 0 | 3.2 | V |
| | $V_{CC\pm} = \pm 15$ V | -15 | 13.5 | -15 | 13.2 | -15 | 13.2 | |
| Operating free-air temperature, T_A | | 0 | 70 | -40 | 85 | -55 | 125 | °C |



TLE2021 electrical characteristics at specified free-air temperature, $V_{CC} = 5\text{ V}$ (unless otherwise noted)

| PARAMETER | TEST CONDITIONS | T_A^\dagger | TLE2021C | | | TLE2021AC | | | TLE2021BC | | | UNIT |
|--|--|---------------|----------|-----------|-----|-----------|-----------|-----|-----------|-----------|---------------|------------------------------|
| | | | MIN | TYP | MAX | MIN | TYP | MAX | MIN | TYP | MAX | |
| V_{IO} Input offset voltage | | 25°C | 120 | 600 | | 100 | 300 | | 80 | 200 | μV | |
| | | Full range | | 850 | | 600 | | 300 | | | | |
| $\alpha_{V_{IO}}$ Temperature coefficient of input offset voltage | | Full range | 2 | | | 2 | | | 2 | | | $\mu\text{V}/^\circ\text{C}$ |
| Input offset voltage long-term drift (see Note 4) | $V_{IC} = 0, R_S = 50\ \Omega$ | 25°C | 0.005 | | | 0.005 | | | 0.005 | | | $\mu\text{V}/\text{mo}$ |
| I_{IO} Input offset current | | 25°C | 0.2 | 6 | | 0.2 | 6 | | 0.2 | 6 | nA | |
| | | Full range | 10 | | | 10 | | | 10 | | | |
| I_{IB} Input bias current | | 25°C | 25 | 70 | | 25 | 70 | | 25 | 70 | nA | |
| | Full range | 90 | | | 90 | | | 90 | | | | |
| V_{ICR} Common-mode input voltage range | $R_S = 50\ \Omega$ | 25°C | 0 to 3.5 | -0.3 to 4 | | 0 to 3.5 | -0.3 to 4 | | 0 to 3.5 | -0.3 to 4 | V | |
| | | Full range | 0 to 3.5 | | | 0 to 3.5 | | | 0 to 3.5 | | | |
| V_{OH} High-level output voltage | $R_L = 10\ \text{k}\Omega$ | 25°C | 4 | 4.3 | | 4 | 4.3 | | 4 | 4.3 | V | |
| | | Full range | 3.9 | | | 3.9 | | | 3.9 | | | |
| V_{OL} Low-level output voltage | | 25°C | 0.7 | | 0.8 | 0.7 | | 0.8 | 0.7 | | 0.8 | V |
| | | Full range | 0.85 | | | 0.85 | | | 0.85 | | | |
| A_{VD} Large-signal differential voltage amplification | $V_O = 1.4\text{ V to }4\text{ V}, R_L = 10\ \text{k}\Omega$ | 25°C | 0.3 | 1.5 | | 0.3 | 1.5 | | 0.3 | 1.5 | | $\text{V}/\mu\text{V}$ |
| | | Full range | 0.3 | | | 0.3 | | | 0.3 | | | |
| CMRR Common-mode rejection ratio | $V_{IC} = V_{ICR\text{min}}, R_S = 50\ \Omega$ | 25°C | 85 | 110 | | 85 | 110 | | 85 | 110 | | dB |
| | | Full range | 80 | | | 80 | | | 80 | | | |
| k_{SVR} Supply-voltage rejection ratio ($\Delta V_{CC}/\Delta V_{IO}$) | $V_{CC} = 5\text{ V to }30\text{ V}$ | 25°C | 105 | 120 | | 105 | 120 | | 105 | 120 | | dB |
| | | Full range | 100 | | | 100 | | | 100 | | | |
| I_{CC} Supply current | $V_O = 2.5\text{ V}, \text{ No load}$ | 25°C | 200 | | 300 | 200 | | 300 | 200 | | 300 | μA |
| | | Full range | 300 | | | 300 | | | 300 | | | |
| ΔI_{CC} Supply-current change over operating temperature range | | Full range | 5 | | | 5 | | | 5 | | | μA |

† Full range is 0°C to 70°C.

NOTE 4: Typical values are based on the input offset voltage shift observed through 168 hours of operating life test at $T_A = 150^\circ\text{C}$ extrapolated to $T_A = 25^\circ\text{C}$ using the Arrhenius equation and assuming an activation energy of 0.96 eV.

TLE2021 electrical characteristics at specified free-air temperature, $V_{CC} = \pm 15\text{ V}$ (unless otherwise noted)

| PARAMETER | TEST CONDITIONS | T_A^\dagger | TLE2021C | | | TLE2021AC | | | TLE2021BC | | | UNIT |
|--|---|---------------|-------------|-------------|-----|-------------|-------------|-----|-------------|-------------|------------------------|------------------------------|
| | | | MIN | TYP | MAX | MIN | TYP | MAX | MIN | TYP | MAX | |
| V_{IO} Input offset voltage | $V_{IC} = 0, R_S = 50\ \Omega$ | 25°C | | 120 | 500 | | 80 | 200 | | 40 | 100 | μV |
| | | Full range | | | 750 | | | 500 | | | 200 | |
| α_{VIO} Temperature coefficient of input offset voltage | | Full range | | 2 | | | 2 | | | 2 | | $\mu\text{V}/^\circ\text{C}$ |
| Input offset voltage long-term drift (see Note 4) | | 25°C | | 0.006 | | | 0.006 | | | 0.006 | | $\mu\text{V}/\text{mo}$ |
| I_{IO} Input offset current | | 25°C | | 0.2 | 6 | | 0.2 | 6 | | 0.2 | 6 | nA |
| | | Full range | | | 10 | | | 10 | | | 10 | |
| I_{IB} Input bias current | 25°C | | 25 | 70 | | 25 | 70 | | 25 | 70 | nA | |
| | Full range | | | 90 | | | 90 | | | 90 | | |
| V_{ICR} Common-mode input voltage range | $R_S = 50\ \Omega$ | 25°C | -15 to 13.5 | -15.3 to 14 | | -15 to 13.5 | -15.3 to 14 | | -15 to 13.5 | -15.3 to 14 | V | |
| | | Full range | -15 to 13.5 | | | -15 to 13.5 | | | -15 to 13.5 | | | |
| V_{OM+} Maximum positive peak output voltage swing | $R_L = 10\ \text{k}\Omega$ | 25°C | 14 | 14.3 | | 14 | 14.3 | | 14 | 14.3 | V | |
| | | Full range | 13.9 | | | 13.9 | | | 13.9 | | | |
| V_{OM-} Maximum negative peak output voltage swing | | 25°C | -13.7 | -14.1 | | -13.7 | -14.1 | | -13.7 | -14.1 | V | |
| | | Full range | -13.7 | | | -13.7 | | | -13.7 | | | |
| A_{VD} Large-signal differential voltage amplification | $V_O = \pm 10\ \text{V}, R_L = 10\ \text{k}\Omega$ | 25°C | 1 | 6.5 | | 1 | 6.5 | | 1 | 6.5 | $\text{V}/\mu\text{V}$ | |
| | | Full range | 1 | | | 1 | | | 1 | | | |
| CMRR Common-mode rejection ratio | $V_{IC} = V_{ICR}\ \text{min}, R_S = 50\ \Omega$ | 25°C | 100 | 115 | | 100 | 115 | | 100 | 115 | dB | |
| | | Full range | 96 | | | 96 | | | 96 | | | |
| k_{SVR} Supply-voltage rejection ratio ($\Delta V_{CC}/\Delta V_{IO}$) | $V_{CC\pm} = \pm 2.5\ \text{V}$ to $\pm 15\ \text{V}$ | 25°C | 105 | 120 | | 105 | 120 | | 105 | 120 | dB | |
| | | Full range | 100 | | | 100 | | | 100 | | | |
| I_{CC} Supply current | $V_O = 0, \text{ No load}$ | 25°C | | 240 | 350 | | 240 | 350 | | 240 | 350 | μA |
| | | Full range | | | 350 | | | 350 | | | 350 | |
| ΔI_{CC} Supply-current change over operating temperature range | | Full range | | 6 | | | 6 | | | 6 | | μA |

† Full range is 0°C to 70°C.

NOTE 4: Typical values are based on the input offset voltage shift observed through 168 hours of operating life test at $T_A = 150^\circ\text{C}$ extrapolated to $T_A = 25^\circ\text{C}$ using the Arrhenius equation and assuming an activation energy of 0.96 eV.

TLE2022 electrical characteristics at specified free-air temperature, $V_{CC} = 5\text{ V}$ (unless otherwise noted)

| PARAMETER | TEST CONDITIONS | T_A † | TLE2022C | | | TLE2022AC | | | TLE2022BC | | | UNIT |
|--|---|------------|----------|-----------|-----|-----------|-----------|-----|-----------|-----------|------------------------|------------------------------|
| | | | MIN | TYP | MAX | MIN | TYP | MAX | MIN | TYP | MAX | |
| V_{IO} Input offset voltage | $V_{IC} = 0, R_S = 50\ \Omega$ | 25°C | 600 | | | 400 | | | 250 | | | μV |
| | | Full range | 800 | | | 550 | | | 400 | | | |
| αV_{IO} Temperature coefficient of input offset voltage | | Full range | 2 | | | 2 | | | 2 | | | $\mu\text{V}/^\circ\text{C}$ |
| Input offset voltage long-term drift (see Note 4) | | 25°C | 0.005 | | | 0.005 | | | 0.005 | | | $\mu\text{V}/\text{mo}$ |
| I_{IO} Input offset current | | 25°C | 0.5 | 6 | | 0.4 | 6 | | 0.3 | 6 | | nA |
| | | Full range | 10 | | | 10 | | | 10 | | | |
| I_{IB} Input bias current | 25°C | 35 | 70 | | 33 | 70 | | 30 | 70 | | nA | |
| | Full range | 90 | | | 90 | | | 90 | | | | |
| V_{ICR} Common-mode input voltage range | $R_S = 50\ \Omega$ | 25°C | 0 to 3.5 | -0.3 to 4 | | 0 to 3.5 | -0.3 to 4 | | 0 to 3.5 | -0.3 to 4 | V | |
| | | Full range | 0 to 3.5 | | | 0 to 3.5 | | | 0 to 3.5 | | | |
| V_{OH} High-level output voltage | $R_L = 10\ \text{k}\Omega$ | 25°C | 4 | 4.3 | | 4 | 4.3 | | 4 | 4.3 | V | |
| Full range | | 3.9 | | | 3.9 | | | 3.9 | | | | |
| V_{OL} Low-level output voltage | $R_L = 10\ \text{k}\Omega$ | 25°C | 0.7 | | 0.8 | 0.7 | | 0.8 | 0.7 | | 0.8 | V |
| | | Full range | 0.85 | | | 0.85 | | | 0.85 | | | |
| A_{VD} Large-signal differential voltage amplification | $V_O = 1.4\ \text{V to } 4\ \text{V}, R_L = 10\ \text{k}\Omega$ | 25°C | 0.3 | 1.5 | | 0.4 | 1.5 | | 0.5 | 1.5 | $\text{V}/\mu\text{V}$ | |
| | | Full range | 0.3 | | | 0.4 | | | 0.5 | | | |
| CMRR Common-mode rejection ratio | $V_{IC} = V_{ICRmin}, R_S = 50\ \Omega$ | 25°C | 85 | 100 | | 87 | 102 | | 90 | 105 | dB | |
| | | Full range | 80 | | | 82 | | | 85 | | | |
| k_{SVR} Supply-voltage rejection ratio ($\Delta V_{CC} \pm / \Delta V_{IO}$) | $V_{CC} = 5\ \text{V to } 30\ \text{V}$ | 25°C | 100 | 115 | | 103 | 118 | | 105 | 120 | dB | |
| | | Full range | 95 | | | 98 | | | 100 | | | |
| I_{CC} Supply current | $V_O = 2.5\ \text{V}, \text{ No load}$ | 25°C | 450 | | 600 | 450 | | 600 | 450 | | 600 | μA |
| | | Full range | 600 | | | 600 | | | 600 | | | |
| ΔI_{CC} Supply current change over operating temperature range | | Full range | 7 | | | 7 | | | 7 | | | μA |

† Full range is 0°C to 70°C.

NOTE 4: Typical values are based on the input offset voltage shift observed through 168 hours of operating life test at $T_A = 150^\circ\text{C}$ extrapolated to $T_A = 25^\circ\text{C}$ using the Arrhenius equation and assuming an activation energy of 0.96 eV.

TLE2022 electrical characteristics at specified free-air temperature, $V_{CC} = \pm 15$ V (unless otherwise noted)

| PARAMETER | TEST CONDITIONS | T_A^\dagger | TLE2022C | | | TLE2022AC | | | TLE2022BC | | | UNIT |
|---|--|---------------|-------------|-------------|-----|-------------|-------------|-----|-------------|-------------|-----------|------------------|
| | | | MIN | TYP | MAX | MIN | TYP | MAX | MIN | TYP | MAX | |
| V_{IO} Input offset voltage | $V_{IC} = 0, R_S = 50 \Omega$ | 25°C | | 150 | 500 | | 120 | 300 | | 70 | 150 | μV |
| | | Full range | | | 700 | | | 450 | | | 300 | |
| α_{VIO} Temperature coefficient of input offset voltage | | Full range | | 2 | | | 2 | | | 2 | | $\mu V/^\circ C$ |
| Input offset voltage long-term drift (see Note 4) | | 25°C | | 0.006 | | | 0.006 | | | 0.006 | | $\mu V/mo$ |
| I_{IO} Input offset current | | 25°C | | 0.5 | 6 | | 0.4 | 6 | | 0.3 | 6 | nA |
| | | Full range | | | 10 | | | 10 | | | 10 | |
| I_{IB} Input bias current | 25°C | | 35 | 70 | | 33 | 70 | | 30 | 70 | nA | |
| | Full range | | | 90 | | | 90 | | | 90 | | |
| V_{ICR} Common-mode input voltage range | $R_S = 50 \Omega$ | 25°C | -15 to 13.5 | -15.3 to 14 | | -15 to 13.5 | -15.3 to 14 | | -15 to 13.5 | -15.3 to 14 | V | |
| | | Full range | -15 to 13.5 | | | -15 to 13.5 | | | -15 to 13.5 | | | |
| V_{OM+} Maximum positive peak output voltage swing | $R_L = 10 k\Omega$ | 25°C | 14 | 14.3 | | 14 | 14.3 | | 14 | 14.3 | V | |
| | | Full range | 13.9 | | | 13.9 | | | 13.9 | | | |
| V_{OM-} Maximum negative peak output voltage swing | | 25°C | -13.7 | -14.1 | | -13.7 | -14.1 | | -13.7 | -14.1 | V | |
| | | Full range | -13.7 | | | -13.7 | | | -13.7 | | | |
| A_{VD} Large-signal differential voltage amplification | $V_O = \pm 10$ V, $R_L = 10 k\Omega$ | 25°C | 0.8 | 4 | | 1 | 7 | | 1.5 | 10 | $V/\mu V$ | |
| | | Full range | 0.8 | | | 1 | | | 1.5 | | | |
| CMRR Common-mode rejection ratio | $V_{IC} = V_{ICRmin}, R_S = 50 \Omega$ | 25°C | 95 | 106 | | 97 | 109 | | 100 | 112 | dB | |
| | | Full range | 91 | | | 93 | | | 96 | | | |
| k_{SVR} Supply-voltage rejection ratio ($\Delta V_{CC\pm}/\Delta V_{IO}$) | $V_{CC\pm} = \pm 2.5$ V to ± 15 V | 25°C | 100 | 115 | | 103 | 118 | | 105 | 120 | dB | |
| | | Full range | 95 | | | 98 | | | 100 | | | |
| I_{CC} Supply current | $V_O = 0, \text{ No load}$ | 25°C | | 550 | 700 | | 550 | 700 | | 550 | 700 | μA |
| | | Full range | | | 700 | | | 700 | | | 700 | |
| ΔI_{CC} Supply current change over operating temperature range | | Full range | | 9 | | | 9 | | | 9 | | μA |

† Full range is 0°C to 70°C.

NOTE 4: Typical values are based on the input offset voltage shift observed through 168 hours of operating life test at $T_A = 150^\circ C$ extrapolated to $T_A = 25^\circ C$ using the Arrhenius equation and assuming an activation energy of 0.96 eV.

TLE2024 electrical characteristics at specified free-air temperature, $V_{CC} = 5\text{ V}$ (unless otherwise noted)

| PARAMETER | TEST CONDITIONS | T_A † | TLE2024C | | | TLE2024AC | | | TLE2024BC | | | UNIT |
|--|---|------------|----------|-----------|----------|-----------|----------|-----------|-----------|-----------|-----|------------------------------|
| | | | MIN | TYP | MAX | MIN | TYP | MAX | MIN | TYP | MAX | |
| V_{IO} Input offset voltage | $V_{IC} = 0,$ $R_S = 50\ \Omega$ | 25°C | 1100 | | | 850 | | | 600 | | | μV |
| | | Full range | 1300 | | | 1050 | | | 800 | | | |
| α_{VIO} Temperature coefficient of input offset voltage | | Full range | 2 | | | 2 | | | 2 | | | $\mu\text{V}/^\circ\text{C}$ |
| Input offset voltage long-term drift (see Note 4) | | 25°C | 0.005 | | | 0.005 | | | 0.005 | | | $\mu\text{V}/\text{mo}$ |
| I_{IO} Input offset current | | 25°C | 0.6 | 6 | | 0.5 | 6 | | 0.4 | 6 | | nA |
| | | Full range | 10 | | | 10 | | | 10 | | | |
| I_{IB} Input bias current | | 25°C | 45 | 70 | | 40 | 70 | | 35 | 70 | | nA |
| | | Full range | 90 | | | 90 | | | 90 | | | |
| V_{ICR} Common-mode input voltage range | $R_S = 50\ \Omega$ | 25°C | 0 to 3.5 | -0.3 to 4 | 0 to 3.5 | -0.3 to 4 | 0 to 3.5 | -0.3 to 4 | 0 to 3.5 | -0.3 to 4 | V | |
| | | Full range | 0 to 3.5 | | 0 to 3.5 | | 0 to 3.5 | | 0 to 3.5 | | | |
| V_{OH} High-level output voltage | $R_L = 10\ \text{k}\Omega$ | 25°C | 3.9 | 4.2 | | 3.9 | 4.2 | | 4 | 4.3 | | V |
| | | Full range | 3.7 | | | 3.7 | | | 3.8 | | | |
| V_{OL} Low-level output voltage | | 25°C | 0.7 | | 0.8 | | 0.7 | | 0.8 | | V | |
| | | Full range | 0.95 | | | 0.95 | | | 0.95 | | | |
| A_{VD} Large-signal differential voltage amplification | $V_O = 1.4\text{ V to }4\text{ V},$ $R_L = 10\ \text{k}\Omega$ | 25°C | 0.2 | 1.5 | | 0.3 | 1.5 | | 0.4 | 1.5 | | $\text{V}/\mu\text{V}$ |
| | | Full range | 0.1 | | | 0.1 | | | 0.1 | | | |
| CMRR Common-mode rejection ratio | $V_{IC} = V_{ICR\text{min}},$ $R_S = 50\ \Omega$ | 25°C | 80 | 90 | | 82 | 92 | | 85 | 95 | | dB |
| | | Full range | 80 | | | 82 | | | 85 | | | |
| k_{SVR} Supply-voltage rejection ratio ($\Delta V_{CC}/\Delta V_{IO}$) | $V_{CC} = 5\text{ V to }30\text{ V}$ | 25°C | 98 | 112 | | 100 | 115 | | 103 | 117 | | dB |
| | | Full range | 93 | | | 95 | | | 98 | | | |
| I_{CC} Supply current | $V_O = 2.5\text{ V},$ No load | 25°C | 800 | 1200 | | 800 | 1200 | | 800 | 1200 | | μA |
| | | Full range | 1200 | | | 1200 | | | 1200 | | | |
| ΔI_{CC} Supply current change over operating temperature range | | Full range | 15 | | | 15 | | | 15 | | | μA |

† Full range is 0°C to 70°C.

NOTE 4: Typical values are based on the input offset voltage shift observed through 168 hours of operating life test at $T_A = 150^\circ\text{C}$ extrapolated to $T_A = 25^\circ\text{C}$ using the Arrhenius equation and assuming an activation energy of 0.96 eV.

TLE2024 electrical characteristics at specified free-air temperature, $V_{CC} = \pm 15\text{ V}$ (unless otherwise noted)

| PARAMETER | TEST CONDITIONS | T_A^\dagger | TLE2024C | | | TLE2024AC | | | TLE2024BC | | | UNIT |
|---|--|---------------|-------------|-------------|-------------|-------------|-------------|-------------|------------------------|-----|-----|------------------------------|
| | | | MIN | TYP | MAX | MIN | TYP | MAX | MIN | TYP | MAX | |
| V_{IO} Input offset voltage | $V_{IC} = 0, R_S = 50\ \Omega$ | 25°C | 1000 | | | 750 | | | 500 | | | μV |
| | | Full range | 1200 | | | 950 | | | 700 | | | |
| α_{VIO} Temperature coefficient of input offset voltage | | Full range | 2 | | | 2 | | | 2 | | | $\mu\text{V}/^\circ\text{C}$ |
| Input offset voltage long-term drift (see Note 4) | | 25°C | 0.006 | | | 0.006 | | | 0.006 | | | $\mu\text{V}/\text{mo}$ |
| I_{IO} Input offset current | | 25°C | 0.6 | 6 | 0.5 | 6 | 0.4 | 6 | nA | | | |
| | | Full range | 10 | | | 10 | | | | | | |
| I_{IB} Input bias current | 25°C | 50 | 70 | 45 | 70 | 40 | 70 | nA | | | | |
| | Full range | 90 | | | 90 | | | | | | | |
| V_{ICR} Common-mode input voltage range | $R_S = 50\ \Omega$ | 25°C | -15 to 13.5 | -15.3 to 14 | -15 to 13.5 | -15.3 to 14 | -15 to 13.5 | -15.3 to 14 | V | | | |
| | | Full range | -15 to 13.5 | | -15 to 13.5 | | -15 to 13.5 | | | | | |
| V_{OM+} Maximum positive peak output voltage swing | $R_L = 10\ \text{k}\Omega$ | 25°C | 13.8 | 14.1 | 13.9 | 14.2 | 14 | 14.3 | V | | | |
| | | Full range | 13.7 | | 13.8 | | 13.9 | | | | | |
| V_{OM-} Maximum negative peak output voltage swing | | 25°C | -13.7 | -14.1 | -13.7 | -14.1 | -13.7 | -14.1 | V | | | |
| | | Full range | -13.6 | | -13.6 | | -13.6 | | | | | |
| A_{VD} Large-signal differential voltage amplification | $V_O = \pm 10\ \text{V}, R_L = 10\ \text{k}\Omega$ | 25°C | 0.4 | 2 | 0.8 | 4 | 1 | 7 | $\text{V}/\mu\text{V}$ | | | |
| | | Full range | 0.4 | | 0.8 | | 1 | | | | | |
| CMRR Common-mode rejection ratio | $V_{IC} = V_{ICRmin}, R_S = 50\ \Omega$ | 25°C | 92 | 102 | 94 | 105 | 97 | 108 | dB | | | |
| | | Full range | 88 | | 90 | | 93 | | | | | |
| k_{SVR} Supply-voltage rejection ratio ($\Delta V_{CC\pm}/\Delta V_{IO}$) | $V_{CC\pm} = \pm 2.5\ \text{V to } \pm 15\ \text{V}$ | 25°C | 98 | 112 | 100 | 115 | 103 | 117 | dB | | | |
| | | Full range | 93 | | 95 | | 98 | | | | | |
| I_{CC} Supply current | $V_O = 0, \text{ No load}$ | 25°C | 1050 | 1400 | 1050 | 1400 | 1050 | 1400 | μA | | | |
| | | Full range | 1400 | | | 1400 | | | | | | |
| ΔI_{CC} Supply current change over operating temperature range | | Full range | 20 | | | 20 | | | μA | | | |

† Full range is 0°C to 70°C.

NOTE 4: Typical values are based on the input offset voltage shift observed through 168 hours of operating life test at $T_A = 150^\circ\text{C}$ extrapolated to $T_A = 25^\circ\text{C}$ using the Arrhenius equation and assuming an activation energy of 0.96 eV.

TLE2021 electrical characteristics at specified free-air temperature, $V_{CC} = 5\text{ V}$ (unless otherwise noted)

| PARAMETER | TEST CONDITIONS | T_A † | TLE2021I | | | TLE2021AI | | | TLE2021BI | | | UNIT |
|--|--|------------|----------|-----------|-----|-----------|-----------|-----|-----------|-----------|------------------------------|---------------|
| | | | MIN | TYP | MAX | MIN | TYP | MAX | MIN | TYP | MAX | |
| V_{IO} Input offset voltage | | 25°C | | 120 | 600 | | 100 | 300 | | 80 | 200 | μV |
| | | Full range | | | 950 | | | 600 | | | 300 | |
| α_{VIO} Temperature coefficient of input offset voltage | | Full range | | 2 | | | 2 | | | 2 | $\mu\text{V}/^\circ\text{C}$ | |
| Input offset voltage long-term drift (see Note 4) | $V_{IC} = 0, R_S = 50\ \Omega$ | 25°C | | 0.005 | | | 0.005 | | | 0.005 | $\mu\text{V}/\text{mo}$ | |
| I_{IO} Input offset current | | 25°C | | 0.2 | 6 | | 0.2 | 6 | | 0.2 | 6 | nA |
| | | Full range | | | 10 | | | 10 | | | 10 | |
| I_{IB} Input bias current | | 25°C | | 25 | 70 | | 25 | 70 | | 25 | 70 | nA |
| | Full range | | | 90 | | | 90 | | | 90 | | |
| V_{ICR} Common-mode input voltage range | $R_S = 50\ \Omega$ | 25°C | 0 to 3.5 | -0.3 to 4 | | 0 to 3.5 | -0.3 to 4 | | 0 to 3.5 | -0.3 to 4 | V | |
| | | Full range | 0 to 3.2 | | | 0 to 3.2 | | | 0 to 3.2 | | | |
| V_{OH} High-level output voltage | $R_L = 10\ \text{k}\Omega$ | 25°C | 4 | 4.3 | | 4 | 4.3 | | 4 | 4.3 | V | |
| | | Full range | 3.9 | | | 3.9 | | | 3.9 | | | |
| V_{OL} Low-level output voltage | | 25°C | | 0.7 | 0.8 | | 0.7 | 0.8 | | 0.7 | 0.8 | V |
| | | Full range | | | 0.9 | | | 0.9 | | | 0.9 | |
| A_{VD} Large-signal differential voltage amplification | $V_O = 1.4\text{ V to }4\text{ V}, R_L = 10\ \text{k}\Omega$ | 25°C | 0.3 | 1.5 | | 0.3 | 1.5 | | 0.3 | 1.5 | $\text{V}/\mu\text{V}$ | |
| | | Full range | 0.25 | | | 0.25 | | | 0.25 | | | |
| CMRR Common-mode rejection ratio | $V_{IC} = V_{ICR}\ \text{min}, R_S = 50\ \Omega$ | 25°C | 85 | 110 | | 85 | 110 | | 85 | 110 | dB | |
| | | Full range | 80 | | | 80 | | | 80 | | | |
| k_{SVR} Supply-voltage rejection ratio ($\Delta V_{CC}/\Delta V_{IO}$) | $V_{CC} = 5\text{ V to }30\text{ V}$ | 25°C | 105 | 120 | | 105 | 120 | | 105 | 120 | dB | |
| | | Full range | 100 | | | 100 | | | 100 | | | |
| I_{CC} Supply current | $V_O = 2.5\text{ V},$ No load | 25°C | | 200 | 300 | | 200 | 300 | | 200 | 300 | μA |
| | | Full range | | | 300 | | | 300 | | | 300 | |
| ΔI_{CC} Supply-current change over operating temperature range | | Full range | | 6 | | | 6 | | | 6 | μA | |

† Full range is -40°C to 85°C .

NOTE 4: Typical values are based on the input offset voltage shift observed through 168 hours of operating life test at $T_A = 150^\circ\text{C}$ extrapolated to $T_A = 25^\circ\text{C}$ using the Arrhenius equation and assuming an activation energy of 0.96 eV.

TLE2021 electrical characteristics at specified free-air temperature, $V_{CC} = \pm 15\text{ V}$ (unless otherwise noted)

| PARAMETER | TEST CONDITIONS | T_A^\dagger | TLE2021I | | | TLE2021AI | | | TLE2021BI | | | UNIT |
|--|---|---------------|-------------|-------------|-----|-------------|-------------|-----|-------------|-------------|------------------------------|---------------|
| | | | MIN | TYP | MAX | MIN | TYP | MAX | MIN | TYP | MAX | |
| V_{IO} Input offset voltage | | 25°C | | 120 | 500 | | 80 | 200 | | 40 | 100 | μV |
| | | Full range | | | 850 | | | 500 | | | 200 | |
| α_{VIO} Temperature coefficient of input offset voltage | | Full range | | 2 | | | 2 | | | 2 | $\mu\text{V}/^\circ\text{C}$ | |
| Input offset voltage long-term drift (see Note 4) | $V_{IC} = 0, R_S = 50\ \Omega$ | 25°C | | 0.006 | | | 0.006 | | | 0.006 | $\mu\text{V}/\text{mo}$ | |
| | | Full range | | | | | | | | | | |
| I_{IO} Input offset current | | 25°C | | 0.2 | 6 | | 0.2 | 6 | | 0.2 | 6 | nA |
| | | Full range | | | 10 | | | 10 | | | 10 | |
| I_{IB} Input bias current | | 25°C | | 25 | 70 | | 25 | 70 | | 25 | 70 | nA |
| | | Full range | | | 90 | | | 90 | | | 90 | |
| V_{ICR} Common-mode input voltage range | $R_S = 50\ \Omega$ | 25°C | -15 to 13.5 | -15.3 to 14 | | -15 to 13.5 | -15.3 to 14 | | -15 to 13.5 | -15.3 to 14 | V | |
| | | Full range | -15 to 13.2 | | | -15 to 13.2 | | | -15 to 13.2 | | | |
| V_{OM+} Maximum positive peak output voltage swing | $R_L = 10\ \text{k}\Omega$ | 25°C | 14 | 14.3 | | 14 | 14.3 | | 14 | 14.3 | V | |
| | | Full range | 13.9 | | | 13.9 | | | 13.9 | | | |
| V_{OM-} Maximum negative peak output voltage swing | | 25°C | -13.7 | -14.1 | | -13.7 | -14.1 | | -13.7 | -14.1 | V | |
| | | Full range | -13.6 | | | -13.6 | | | -13.6 | | | |
| A_{VD} Large-signal differential voltage amplification | $V_O = 10\ \text{V}, R_L = 10\ \text{k}\Omega$ | 25°C | 1 | 6.5 | | 1 | 6.5 | | 1 | 6.5 | $\text{V}/\mu\text{V}$ | |
| | | Full range | 0.75 | | | 0.75 | | | 0.75 | | | |
| CMRR Common-mode rejection ratio | $V_{IC} = V_{ICR\ \text{min}}, R_S = 50\ \Omega$ | 25°C | 100 | 115 | | 100 | 115 | | 100 | 115 | dB | |
| | | Full range | 96 | | | 96 | | | 96 | | | |
| k_{SVR} Supply-voltage rejection ratio ($\Delta V_{CC}/\Delta V_{IO}$) | $V_{CC\pm} = \pm 2.5\ \text{V}$ to $\pm 15\ \text{V}$ | 25°C | 105 | 120 | | 105 | 120 | | 105 | 120 | dB | |
| | | Full range | 100 | | | 100 | | | 100 | | | |
| I_{CC} Supply current | $V_O = 0\ \text{V}, \text{No load}$ | 25°C | | 240 | 350 | | 240 | 350 | | 240 | 350 | μA |
| | | Full range | | | 350 | | | 350 | | | 350 | |
| ΔI_{CC} Supply-current change over operating temperature range | | Full range | | 7 | | | 7 | | | 7 | μA | |

† Full range is -40°C to 85°C .

NOTE 4: Typical values are based on the input offset voltage shift observed through 168 hours of operating life test at $T_A = 150^\circ\text{C}$ extrapolated to $T_A = 25^\circ\text{C}$ using the Arrhenius equation and assuming an activation energy of 0.96 eV.

TLE2022 electrical characteristics at specified free-air temperature, $V_{CC} = 5\text{ V}$ (unless otherwise noted)

| PARAMETER | TEST CONDITIONS | T_A^\dagger | TLE2022I | | | TLE2022AI | | | TLE2022BI | | | UNIT |
|---|---|---------------|----------|-----------|-----|-----------|-----------|-----|-----------|-----------|------------------------|------------------------------|
| | | | MIN | TYP | MAX | MIN | TYP | MAX | MIN | TYP | MAX | |
| V_{IO} Input offset voltage | $V_{IC} = 0, R_S = 50\ \Omega$ | 25°C | 600 | | | 400 | | | 250 | | | μV |
| | | Full range | 800 | | | 550 | | | 400 | | | |
| α_{VIO} Temperature coefficient of input offset voltage | | Full range | 2 | | | 2 | | | 2 | | | $\mu\text{V}/^\circ\text{C}$ |
| Input offset voltage long-term drift (see Note 4) | | 25°C | 0.005 | | | 0.005 | | | 0.005 | | | $\mu\text{V}/\text{mo}$ |
| I_{IO} Input offset current | | 25°C | 0.5 | 6 | | 0.4 | 6 | | 0.3 | 6 | | nA |
| | | Full range | 10 | | | 10 | | | 10 | | | |
| I_{IB} Input bias current | | 25°C | 35 | 70 | | 33 | 70 | | 30 | 70 | | nA |
| | | Full range | 90 | | | 90 | | | 90 | | | |
| V_{ICR} Common-mode input voltage range | $R_S = 50\ \Omega$ | 25°C | 0 to 3.5 | -0.3 to 4 | | 0 to 3.5 | -0.3 to 4 | | 0 to 3.5 | -0.3 to 4 | V | |
| | | Full range | 0 to 3.2 | | | 0 to 3.2 | | | 0 to 3.2 | | | |
| V_{OH} High-level output voltage | $R_L = 10\ \text{k}\Omega$ | 25°C | 4 | 4.3 | | 4 | 4.3 | | 4 | 4.3 | V | |
| | | Full range | 3.9 | | | 3.9 | | | 3.9 | | | |
| V_{OL} Low-level output voltage | | 25°C | | 0.7 | 0.8 | | 0.7 | 0.8 | | 0.7 | 0.8 | V |
| | | Full range | 0.9 | | | 0.9 | | | 0.9 | | | |
| A_{VD} Large-signal differential voltage amplification | $V_O = 1.4\ \text{V to } 4\ \text{V}, R_L = 10\ \text{k}\Omega$ | 25°C | 0.3 | 1.5 | | 0.4 | 1.5 | | 0.5 | 1.5 | $\text{V}/\mu\text{V}$ | |
| | | Full range | 0.2 | | | 0.2 | | | 0.2 | | | |
| CMRR Common-mode rejection ratio | $V_{IC} = V_{ICRmin}, R_S = 50\ \Omega$ | 25°C | 85 | 100 | | 87 | 102 | | 90 | 105 | dB | |
| | | Full range | 80 | | | 82 | | | 85 | | | |
| k_{SVR} Supply-voltage rejection ratio ($\Delta V_{CC\pm}/\Delta V_{IO}$) | $V_{CC} = 5\ \text{V to } 30\ \text{V}$ | 25°C | 100 | 115 | | 103 | 118 | | 105 | 120 | dB | |
| | | Full range | 95 | | | 98 | | | 100 | | | |
| I_{CC} Supply current | $V_O = 2.5\ \text{V}, \text{ No load}$ | 25°C | | 450 | 600 | | 450 | 600 | | 450 | 600 | μA |
| | | Full range | 600 | | | 600 | | | 600 | | | |
| ΔI_{CC} Supply current change over operating temperature range | | Full range | 15 | | | 15 | | | 15 | | | μA |

† Full range is -40°C to 85°C .

NOTE 4: Typical values are based on the input offset voltage shift observed through 168 hours of operating life test at $T_A = 150^\circ\text{C}$ extrapolated to $T_A = 25^\circ\text{C}$ using the Arrhenius equation and assuming an activation energy of 0.96 eV.

TLE2022 electrical characteristics at specified free-air temperature, $V_{CC} = \pm 15\text{ V}$ (unless otherwise noted)

| PARAMETER | TEST CONDITIONS | T_A^\dagger | TLE2022I | | | TLE2022AI | | | TLE2022BI | | | UNIT |
|---|--|---------------|-------------|-------------|-----|-------------|-------------|-----|-------------|-------------|------------------------|------------------------------|
| | | | MIN | TYP | MAX | MIN | TYP | MAX | MIN | TYP | MAX | |
| V_{IO} Input offset voltage | $V_{IC} = 0, R_S = 50\ \Omega$ | 25°C | | 150 | 500 | | 120 | 300 | | 70 | 150 | μV |
| | | Full range | | | 700 | | | 450 | | | 300 | |
| α_{VIO} Temperature coefficient of input offset voltage | | Full range | | 2 | | | 2 | | | 2 | | $\mu\text{V}/^\circ\text{C}$ |
| Input offset voltage long-term drift (see Note 4) | | 25°C | | 0.006 | | | 0.006 | | | 0.006 | | $\mu\text{V}/\text{mo}$ |
| I_{IO} Input offset current | | 25°C | | 0.5 | 6 | | 0.4 | 6 | | 0.3 | 6 | nA |
| | | Full range | | | 10 | | | 10 | | | 10 | |
| I_{IB} Input bias current | 25°C | | 35 | 70 | | 33 | 70 | | 30 | 70 | nA | |
| | Full range | | | 90 | | | 90 | | | 90 | | |
| V_{ICR} Common-mode input voltage range | $R_S = 50\ \Omega$ | 25°C | -15 to 13.5 | -15.3 to 14 | | -15 to 13.5 | -15.3 to 14 | | -15 to 13.5 | -15.3 to 14 | V | |
| | | Full range | -15 to 13.2 | | | -15 to 13.2 | | | -15 to 13.2 | | | |
| V_{OM+} Maximum positive peak output voltage swing | $R_L = 10\ \text{k}\Omega$ | 25°C | 14 | 14.3 | | 14 | 14.3 | | 14 | 14.3 | V | |
| | | Full range | 13.9 | | | 13.9 | | | 13.9 | | | |
| V_{OM-} Maximum negative peak output voltage swing | | 25°C | -13.7 | -14.1 | | -13.7 | -14.1 | | -13.7 | -14.1 | V | |
| | | Full range | -13.6 | | | -13.6 | | | -13.6 | | | |
| A_{VD} Large-signal differential voltage amplification | $V_O = \pm 10\ \text{V}, R_L = 10\ \text{k}\Omega$ | 25°C | 0.8 | 4 | | 1 | 7 | | 1.5 | 10 | $\text{V}/\mu\text{V}$ | |
| | | Full range | 0.8 | | | 1 | | | 1.5 | | | |
| CMRR Common-mode rejection ratio | $V_{IC} = V_{ICRmin}, R_S = 50\ \Omega$ | 25°C | 95 | 106 | | 97 | 109 | | 100 | 112 | dB | |
| | | Full range | 91 | | | 93 | | | 96 | | | |
| k_{SVR} Supply-voltage rejection ratio ($\Delta V_{CC\pm}/\Delta V_{IO}$) | $V_{CC} = \pm 2.5\ \text{V to } \pm 15\ \text{V}$ | 25°C | 100 | 115 | | 103 | 118 | | 105 | 120 | dB | |
| | | Full range | 95 | | | 98 | | | 100 | | | |
| I_{CC} Supply current | $V_O = 0, \text{ No load}$ | 25°C | | 550 | 700 | | 550 | 700 | | 550 | 700 | μA |
| | | Full range | | | 700 | | | 700 | | | 700 | |
| ΔI_{CC} Supply current change over operating temperature range | | Full range | | 30 | | | 30 | | | 30 | | μA |

† Full range is -40°C to 85°C .

NOTE 4: Typical values are based on the input offset voltage shift observed through 168 hours of operating life test at $T_A = 150^\circ\text{C}$ extrapolated to $T_A = 25^\circ\text{C}$ using the Arrhenius equation and assuming an activation energy of 0.96 eV.

TLE2024 electrical characteristics at specified free-air temperature, $V_{CC} = 5\text{ V}$ (unless otherwise noted)

| PARAMETER | TEST CONDITIONS | T_A^\dagger | TLE2024I | | | TLE2024AI | | | TLE2024BI | | | UNIT |
|---|---|---------------|----------------|-----------------|------|----------------|----------------|-----------------|----------------|-----|---------------|------------------------------|
| | | | MIN | TYP | MAX | MIN | TYP | MAX | MIN | TYP | MAX | |
| V_{IO} Input offset voltage | | 25°C | 1100 | | | 850 | | | 600 | | | μV |
| | | Full range | 1300 | | | 1050 | | | 800 | | | |
| α_{VIO} Temperature coefficient of input offset voltage | | Full range | 2 | | | 2 | | | 2 | | | $\mu\text{V}/^\circ\text{C}$ |
| Input offset voltage long-term drift (see Note 4) | $V_{IC} = 0,$ $R_S = 50\ \Omega$ | 25°C | 0.005 | | | 0.005 | | | 0.005 | | | $\mu\text{V}/\text{mo}$ |
| I_{IO} Input offset current | | 25°C | 0.6 | 6 | | 0.5 | 6 | | 0.4 | 6 | | nA |
| | Full range | 10 | | | 10 | | | 10 | | | | |
| I_{IB} Input bias current | | 25°C | 45 | | 70 | | 40 | | 70 | | nA | |
| | | Full range | 90 | | | 90 | | | 90 | | | |
| V_{ICR} Common-mode input voltage range | $R_S = 50\ \Omega$ | 25°C | 0 to 3.5 | -0.3 to 4 | | | 0 to 3.5 | -0.3 to 4 | | | V | |
| | | Full range | 0 to 3.2 | | | 0 to 3.2 | | | 0 to 3.2 | | | |
| V_{OM+} Maximum positive peak output voltage swing | $R_L = 10\ \text{k}\Omega$ | 25°C | 3.9 | 4.2 | | 3.9 | 4.2 | | 4 | 4.3 | | V |
| | | Full range | 3.7 | | | 3.7 | | | 3.8 | | | |
| V_{OM-} Maximum negative peak output voltage swing | | 25°C | 0.7 | | 0.8 | | 0.7 | | 0.8 | | V | |
| | | Full range | 0.95 | | | 0.95 | | | 0.95 | | | |
| A_{VD} Large-signal differential voltage amplification | $V_O = 1.4\text{ V to }4\text{ V},$ $R_L = 10\ \text{k}\Omega$ | 25°C | 0.2 | 1.5 | | 0.3 | 1.5 | | 0.4 | 1.5 | | $\text{V}/\mu\text{V}$ |
| | | Full range | 0.1 | | | 0.1 | | | 0.1 | | | |
| CMRR Common-mode rejection ratio | $V_{IC} = V_{ICR\text{min}},$ $R_S = 50\ \Omega$ | 25°C | 80 | 90 | | 82 | 92 | | 85 | 95 | | dB |
| | | Full range | 80 | | | 82 | | | 85 | | | |
| k_{SVR} Supply-voltage rejection ratio ($\Delta V_{CC\pm}/\Delta V_{IO}$) | $V_{CC\pm} = \pm 2.5\text{ V to } \pm 15\text{ V}$ | 25°C | 98 | 112 | | 100 | 115 | | 103 | 117 | | dB |
| | | Full range | 93 | | | 95 | | | 98 | | | |
| I_{CC} Supply current | $V_O = 0,$ No load | 25°C | 800 | | 1200 | | 800 | | 1200 | | μA | |
| | | Full range | 1200 | | | 1200 | | | 1200 | | | |
| ΔI_{CC} Supply current change over operating temperature range | | Full range | 30 | | | 30 | | | 30 | | | μA |

† Full range is -40°C to 85°C .

NOTE 4: Typical values are based on the input offset voltage shift observed through 168 hours of operating life test at $T_A = 150^\circ\text{C}$ extrapolated to $T_A = 25^\circ\text{C}$ using the Arrhenius equation and assuming an activation energy of 0.96 eV.

TLE2024 electrical characteristics at specified free-air temperature, $V_{CC} = \pm 15$ V (unless otherwise noted)

| PARAMETER | TEST CONDITIONS | T_A^\dagger | TLE2024I | | | TLE2024AI | | | TLE2024BI | | | UNIT |
|---|--|---------------|-------------|-------------|-------------|-------------|-------------|-------------|------------|---------|-----|------------------|
| | | | MIN | TYP | MAX | MIN | TYP | MAX | MIN | TYP | MAX | |
| V_{IO} Input offset voltage | $V_{IC} = 0, R_S = 50 \Omega$ | 25°C | 1000 | | | 750 | | | 500 | | | μV |
| | | Full range | 1200 | | | 950 | | | 700 | | | |
| α_{VIO} Temperature coefficient of input offset voltage | | Full range | 2 | | | 2 | | | 2 | | | $\mu V/^\circ C$ |
| Input offset voltage long-term drift (see Note 4) | | 25°C | 0.006 | | | 0.006 | | | 0.006 | | | $\mu V/mo$ |
| I_{IO} Input offset current | | 25°C | 0.6 | 6 | 0.5 | 6 | 0.4 | 6 | nA | | | |
| | | Full range | 10 | | | 10 | | | | | | |
| I_{IB} Input bias current | | 25°C | 50 | 70 | 45 | 70 | 40 | 70 | nA | | | |
| | | Full range | 90 | | | 90 | | | | | | |
| V_{ICR} Common-mode input voltage range | $R_S = 50 \Omega$ | 25°C | -15 to 13.5 | -15.3 to 14 | -15 to 13.5 | -15.3 to 14 | -15 to 13.5 | -15.3 to 14 | V | | | |
| | | Full range | -15 to 13.2 | | -15 to 13.2 | | -15 to 13.2 | | | | | |
| V_{OM+} Maximum positive peak output voltage swing | $R_L = 10 k\Omega$ | 25°C | 13.8 | 14.1 | 13.9 | 14.2 | 14 | 14.3 | V | | | |
| | | Full range | 13.7 | | | 13.8 | | | | | | |
| V_{OM-} Maximum negative peak output voltage swing | | 25°C | -13.7 | -14.1 | -13.7 | -14.1 | -13.7 | -14.1 | V | | | |
| | | Full range | -13.6 | | | -13.6 | | | | | | |
| A_{VD} Large-signal differential voltage amplification | $V_O = \pm 10$ V, $R_L = 10 k\Omega$ | 25°C | 0.4 | 2 | 0.8 | 4 | 1 | 7 | V/ μV | | | |
| | | Full range | 0.4 | | | 0.8 | | | | | | |
| CMRR Common-mode rejection ratio | $V_{IC} = V_{ICRmin}, R_S = 50 \Omega$ | 25°C | 92 | 102 | 94 | 105 | 97 | 108 | dB | | | |
| | | Full range | 88 | | | 90 | | | | | | |
| k_{SVR} Supply-voltage rejection ratio ($\Delta V_{CC\pm}/\Delta V_{IO}$) | $V_{CC\pm} = \pm 2.5$ V to ± 15 V | 25°C | 98 | 112 | 100 | 115 | 103 | 117 | dB | | | |
| | | Full range | 93 | | | 95 | | | | | | |
| I_{CC} Supply current | $V_O = 0, \text{ No load}$ | 25°C | 1050 | 1400 | 1050 | 1400 | 1050 | 1400 | μA | | | |
| | | Full range | 1400 | | | 1400 | | | | | | |
| ΔI_{CC} Supply current change over operating temperature range | | Full range | 50 | | | 50 | | | 50 | μA | | |

† Full range is $-40^\circ C$ to $85^\circ C$.

NOTE 4: Typical values are based on the input offset voltage shift observed through 168 hours of operating life test at $T_A = 150^\circ C$ extrapolated to $T_A = 25^\circ C$ using the Arrhenius equation and assuming an activation energy of 0.96 eV.

TLE2021 electrical characteristics at specified free-air temperature, $V_{CC} = 5\text{ V}$ (unless otherwise noted)

| PARAMETER | | TEST CONDITIONS | T_A^\dagger | TLE2021M | | | TLE2021BM | | | UNIT |
|---|---|--|---|------------|----------|-----------|-----------|----------|------------------------------|------------------------|
| | | | | MIN | TYP | MAX | MIN | TYP | MAX | |
| V_{IO} | Input offset voltage | $V_{IC} = 0,$ $R_S = 50\ \Omega$ | 25°C | 120 | 600 | | 80 | 200 | μV | |
| | | | Full range | | 1100 | | 300 | | | |
| α_{VIO} | Temperature coefficient of input offset voltage | | Full range | 2 | | | 2 | | $\mu\text{V}/^\circ\text{C}$ | |
| Input offset voltage long-term drift (see Note 4) | | | 25°C | 0.005 | | | 0.005 | | $\mu\text{V}/\text{mo}$ | |
| I_{IO} | Input offset current | | 25°C | 0.2 | 6 | | 0.2 | 6 | nA | |
| | | | Full range | | 10 | | 10 | | | |
| I_{IB} | Input bias current | | 25°C | 25 | 70 | | 25 | 70 | nA | |
| | | | Full range | | 90 | | 90 | | | |
| V_{ICR} | Common-mode input voltage range | | $R_S = 50\ \Omega$ | 25°C | 0 to 3.5 | -0.3 to 4 | | 0 to 3.5 | -0.3 to 4 | V |
| | | | | Full range | 0 to 3.2 | | | 0 to 3.2 | | |
| V_{OH} | High-level output voltage | $R_L = 10\ \text{k}\Omega$ | 25°C | 4 | 4.3 | | 4 | 4.3 | V | |
| | | | Full range | 3.8 | | | 3.8 | | | |
| V_{OL} | Low-level output voltage | | 25°C | | 0.7 | 0.8 | | 0.7 | 0.8 | V |
| | | | Full range | | 0.95 | | 0.95 | | | |
| A_{VD} | Large-signal differential voltage amplification | | $V_O = 1.4\text{ V to }4\text{ V},$ $R_L = 10\ \text{k}\Omega$ | 25°C | 0.3 | 1.5 | | 0.3 | 1.5 | $\text{V}/\mu\text{V}$ |
| | | | | Full range | 0.1 | | | 0.1 | | |
| CMRR | Common-mode rejection ratio | $V_{IC} = V_{ICRmin},$ $R_S = 50\ \Omega$ | 25°C | 85 | 110 | | 85 | 110 | dB | |
| | | | Full range | 80 | | | 80 | | | |
| k_{SVR} | Supply-voltage rejection ratio ($\Delta V_{CC\pm}/\Delta V_{IO}$) | $V_{CC} = 5\text{ V to }30\text{ V}$ | 25°C | 105 | 120 | | 105 | 120 | dB | |
| | | | Full range | 100 | | | 100 | | | |
| I_{CC} | Supply current | $V_O = 2.5\text{ V},$ No load | 25°C | 170 | 230 | | 170 | 230 | μA | |
| | | | Full range | | 230 | | 230 | | | |
| ΔI_{CC} | Supply current change over operating temperature range | | Full range | | 9 | | 9 | | μA | |

† Full range is -55°C to 125°C .

NOTE 4: Typical values are based on the input offset voltage shift observed through 168 hours of operating life test at $T_A = 150^\circ\text{C}$ extrapolated to $T_A = 25^\circ\text{C}$ using the Arrhenius equation and assuming an activation energy of 0.96 eV.

TLE2021 electrical characteristics at specified free-air temperature, $V_{CC} = \pm 15$ V (unless otherwise noted)

| PARAMETER | TEST CONDITIONS | T_A † | TLE2021M | | | TLE2021BM | | | UNIT |
|---|--|------------|-------------|-------------|------|-------------|-------------|------------|------------|
| | | | MIN | TYP | MAX | MIN | TYP | MAX | |
| V_{IO} Input offset voltage | $V_{IC} = 0, R_S = 50 \Omega$ | 25°C | | 120 | 500 | | 40 | 100 | μ V |
| | | Full range | | | 1000 | | | 200 | |
| α_{VIO} Temperature coefficient of input offset voltage | | Full range | | 2 | | | 2 | | μ V/°C |
| Input offset voltage long-term drift (see Note 4) | | 25°C | | 0.006 | | | 0.006 | | μ V/mo |
| I_{IO} Input offset current | | 25°C | | 0.2 | 6 | | 0.2 | 6 | nA |
| | | Full range | | | 10 | | | 10 | |
| I_{IB} Input bias current | 25°C | | 25 | 70 | | 25 | 70 | nA | |
| | Full range | | | 90 | | | 90 | | |
| V_{ICR} Common-mode input voltage range | $R_S = 50 \Omega$ | 25°C | -15 to 13.5 | -15.3 to 14 | | -15 to 13.5 | -15.3 to 14 | V | |
| | | Full range | -15 to 13.2 | | | -15 to 13.2 | | | |
| V_{OM+} Maximum positive peak output voltage swing | $R_L = 10 k\Omega$ | 25°C | 14 | 14.3 | | 14 | 14.3 | V | |
| | | Full range | 13.8 | | | 13.8 | | | |
| V_{OM-} Maximum negative peak output voltage swing | | 25°C | -13.7 | -14.1 | | -13.7 | -14.1 | V | |
| | | Full range | -13.6 | | | -13.6 | | | |
| A_{VD} Large-signal differential voltage amplification | $V_O = \pm 10$ V, $R_L = 10 k\Omega$ | 25°C | 1 | 6.5 | | 1 | 6.5 | V/ μ V | |
| | | Full range | 0.5 | | | 0.5 | | | |
| CMRR Common-mode rejection ratio | $V_{IC} = V_{ICRmin}, R_S = 50 \Omega$ | 25°C | 100 | 115 | | 100 | 115 | dB | |
| | | Full range | 96 | | | 96 | | | |
| k_{SVR} Supply-voltage rejection ratio ($\Delta V_{CC\pm}/\Delta V_{IO}$) | $V_{CC\pm} = \pm 2.5$ V to ± 15 V | 25°C | 105 | 120 | | 105 | 120 | dB | |
| | | Full range | 100 | | | 100 | | | |
| I_{CC} Supply current | $V_O = 0, \text{ No load}$ | 25°C | | 200 | 300 | | 200 | 300 | μ A |
| | | Full range | | | 300 | | | 300 | |
| ΔI_{CC} Supply current change over operating temperature range | | Full range | | 10 | | | 10 | | μ A |

† Full range is -55°C to 125°C.

NOTE 4: Typical values are based on the input offset voltage shift observed through 168 hours of operating life test at $T_A = 150^\circ\text{C}$ extrapolated to $T_A = 25^\circ\text{C}$ using the Arrhenius equation and assuming an activation energy of 0.96 eV.

TLE2022 electrical characteristics at specified free-air temperature, $V_{CC} = 5\text{ V}$ (unless otherwise noted)

| PARAMETER | TEST CONDITIONS | T_A^\dagger | TLE2022M | | | TLE2022AM | | | TLE2022BM | | | UNIT |
|---|---|---------------|----------|-----------|-----|-----------|-----------|-----|-----------|-----------|------------------------|------------------------------|
| | | | MIN | TYP | MAX | MIN | TYP | MAX | MIN | TYP | MAX | |
| V_{IO} Input offset voltage | $V_{IC} = 0, R_S = 50\ \Omega$ | 25°C | 600 | | | 400 | | | 250 | | | μV |
| | | Full range | 800 | | | 550 | | | 400 | | | |
| α_{VIO} Temperature coefficient of input offset voltage | | Full range | 2 | | | 2 | | | 2 | | | $\mu\text{V}/^\circ\text{C}$ |
| Input offset voltage long-term drift (see Note 4) | | 25°C | 0.005 | | | 0.005 | | | 0.005 | | | $\mu\text{V}/\text{mo}$ |
| I_{IO} Input offset current | | 25°C | 0.5 | 6 | | 0.4 | 6 | | 0.3 | 6 | | nA |
| | | Full range | 10 | | | 10 | | | 10 | | | |
| I_{IB} Input bias current | 25°C | 35 | 70 | | 33 | 70 | | 30 | 70 | | nA | |
| | Full range | 90 | | | 90 | | | 90 | | | | |
| V_{ICR} Common-mode input voltage range | $R_S = 50\ \Omega$ | 25°C | 0 to 3.5 | -0.3 to 4 | | 0 to 3.5 | -0.3 to 4 | | 0 to 3.5 | -0.3 to 4 | V | |
| | | Full range | 0 to 3.2 | | | 0 to 3.2 | | | 0 to 3.2 | | | |
| V_{OH} High-level output voltage | $R_L = 10\ \text{k}\Omega$ | 25°C | 4 | 4.3 | | 4 | 4.3 | | 4 | 4.3 | V | |
| | | Full range | 3.8 | | | 3.8 | | | 3.8 | | | |
| V_{OL} Low-level output voltage | | 25°C | 0.7 | 0.8 | | 0.7 | 0.8 | | 0.7 | 0.8 | V | |
| | | Full range | 0.95 | | | 0.95 | | | 0.95 | | | |
| A_{VD} Large-signal differential voltage amplification | $V_O = 1.4\ \text{V to } 4\ \text{V}, R_L = 10\ \text{k}\Omega$ | 25°C | 0.3 | 1.5 | | 0.4 | 1.5 | | 0.5 | 1.5 | $\text{V}/\mu\text{V}$ | |
| | | Full range | 0.1 | | | 0.1 | | | 0.1 | | | |
| CMRR Common-mode rejection ratio | $V_{IC} = V_{ICRmin}, R_S = 50\ \Omega$ | 25°C | 85 | 100 | | 87 | 102 | | 90 | 105 | dB | |
| | | Full range | 80 | | | 82 | | | 85 | | | |
| k_{SVR} Supply-voltage rejection ratio ($\Delta V_{CC\pm}/\Delta V_{IO}$) | $V_{CC} = 5\ \text{V to } 30\ \text{V}$ | 25°C | 100 | 115 | | 103 | 118 | | 105 | 120 | dB | |
| | | Full range | 95 | | | 98 | | | 100 | | | |
| I_{CC} Supply current | $V_O = 2.5\ \text{V}, \text{ No load}$ | 25°C | 450 | 600 | | 450 | 600 | | 450 | 600 | μA | |
| | | Full range | 600 | | | 600 | | | 600 | | | |
| ΔI_{CC} Supply current change over operating temperature range | | Full range | 37 | | | 37 | | | 37 | | | μA |

† Full range is -55°C to 125°C .

NOTE 4: Typical values are based on the input offset voltage shift observed through 168 hours of operating life test at $T_A = 150^\circ\text{C}$ extrapolated to $T_A = 25^\circ\text{C}$ using the Arrhenius equation and assuming an activation energy of 0.96 eV.

TLE2022 electrical characteristics at specified free-air temperature, $V_{CC} = \pm 15$ V (unless otherwise noted)

| PARAMETER | TEST CONDITIONS | T_A^\dagger | TLE2022M | | | TLE2022AM | | | TLE2022BM | | | UNIT |
|---|--|---------------|-------------|-------------|-----|-------------|-------------|-----|-------------|-------------|-----------|-------------------|
| | | | MIN | TYP | MAX | MIN | TYP | MAX | MIN | TYP | MAX | |
| V_{IO} Input offset voltage | $V_{IC} = 0, R_S = 50 \Omega$ | 25°C | | 150 | 500 | | 120 | 300 | | 70 | 150 | μV |
| | | Full range | | | 700 | | | 450 | | | 300 | |
| $^{\circ}V_{IO}$ Temperature coefficient of input offset voltage | | Full range | | 2 | | | 2 | | | 2 | | $\mu V/^{\circ}C$ |
| Input offset voltage long-term drift (see Note 4) | | 25°C | | 0.006 | | | 0.006 | | | 0.006 | | $\mu V/mo$ |
| I_{IO} Input offset current | | 25°C | | 0.5 | 6 | | 0.4 | 6 | | 0.3 | 6 | nA |
| | | Full range | | | 10 | | | 10 | | | 10 | |
| I_{IB} Input bias current | 25°C | | 35 | 70 | | 33 | 70 | | 30 | 70 | nA | |
| | Full range | | | 90 | | | 90 | | | 90 | | |
| V_{ICR} Common-mode input voltage range | $R_S = 50 \Omega$ | 25°C | -15 to 13.5 | -15.3 to 14 | | -15 to 13.5 | -15.3 to 14 | | -15 to 13.5 | -15.3 to 14 | V | |
| | | Full range | -15 to 13.2 | | | -15 to 13.2 | | | -15 to 13.2 | | | |
| V_{OM+} Maximum positive peak output voltage swing | $R_L = 10 k\Omega$ | 25°C | 14 | 14.3 | | 14 | 14.3 | | 14 | 14.3 | V | |
| | | Full range | 13.9 | | | 13.9 | | | 13.9 | | | |
| V_{OM-} Maximum negative peak output voltage swing | | 25°C | -13.7 | -14.1 | | -13.7 | -14.1 | | -13.7 | -14.1 | V | |
| | | Full range | -13.6 | | | -13.6 | | | -13.6 | | | |
| A_{VD} Large-signal differential voltage amplification | $V_O = \pm 10$ V, $R_L = 10 k\Omega$ | 25°C | 0.8 | 4 | | 1 | 7 | | 1.5 | 10 | $V/\mu V$ | |
| | | Full range | 0.8 | | | 1 | | | 1.5 | | | |
| CMRR Common-mode rejection ratio | $V_{IC} = V_{ICRmin}, R_S = 50 \Omega$ | 25°C | 95 | 106 | | 97 | 109 | | 100 | 112 | dB | |
| | | Full range | 91 | | | 93 | | | 96 | | | |
| k_{SVR} Supply-voltage rejection ratio ($\Delta V_{CC\pm}/\Delta V_{IO}$) | $V_{CC\pm} = \pm 2.5$ V to ± 15 V | 25°C | 100 | 115 | | 103 | 118 | | 105 | 120 | dB | |
| | | Full range | 95 | | | 98 | | | 100 | | | |
| I_{CC} Supply current | $V_O = 0, \text{ No load}$ | 25°C | | 550 | 700 | | 550 | 700 | | 550 | 700 | μA |
| | | Full range | | | 700 | | | 700 | | | 700 | |
| ΔI_{CC} Supply current change over operating temperature range | | Full range | | 60 | | | 60 | | | 60 | | μA |

† Full range is $-55^{\circ}C$ to $125^{\circ}C$.

NOTE 4: Typical values are based on the input offset voltage shift observed through 168 hours of operating life test at $T_A = 150^{\circ}C$ extrapolated to $T_A = 25^{\circ}C$ using the Arrhenius equation and assuming an activation energy of 0.96 eV.

TLE2024 electrical characteristics at specified free-air temperature, $V_{CC} = 5\text{ V}$ (unless otherwise noted)

| PARAMETER | TEST CONDITIONS | T_A † | TLE2024M | | | TLE2024AM | | | TLE2024BM | | | UNIT |
|---|--|------------|----------|-----------|----------|-----------|----------|-----------|-----------|-----|------------------------|------------------------------|
| | | | MIN | TYP | MAX | MIN | TYP | MAX | MIN | TYP | MAX | |
| V_{IO} Input offset voltage | | 25°C | 1100 | | | 850 | | | 600 | | | μV |
| | | Full range | 1300 | | | 1050 | | | 800 | | | |
| α_{VIO} Temperature coefficient of input offset voltage | | Full range | 2 | | | 2 | | | 2 | | | $\mu\text{V}/^\circ\text{C}$ |
| Input offset voltage long-term drift (see Note 4) | $V_{IC} = 0,$ $R_S = 50\ \Omega$ | 25°C | 0.005 | | | 0.005 | | | 0.005 | | | $\mu\text{V}/\text{mo}$ |
| I_{IO} Input offset current | | 25°C | 0.6 | 6 | 0.5 | 6 | 0.4 | 6 | | | | nA |
| | Full range | 10 | | | 10 | | | 10 | | | | |
| I_{IB} Input bias current | | 25°C | 45 | 70 | 40 | 70 | 35 | 70 | | | nA | |
| | | Full range | 90 | | | 90 | | | 90 | | | |
| V_{ICR} Common-mode input voltage range | $R_S = 50\ \Omega$ | 25°C | 0 to 3.5 | -0.3 to 4 | 0 to 3.5 | -0.3 to 4 | 0 to 3.5 | -0.3 to 4 | | | V | |
| | | Full range | 0 to 3.2 | | 0 to 3.2 | | 0 to 3.2 | | | | | |
| V_{OM+} Maximum positive peak output voltage swing | $R_L = 10\ \text{k}\Omega$ | 25°C | 3.9 | 4.2 | 3.9 | 4.2 | 4 | 4.3 | | | V | |
| | | Full range | 3.7 | | | 3.7 | | | 3.8 | | | |
| V_{OM-} Maximum negative peak output voltage swing | | 25°C | 0.7 | | 0.8 | | 0.7 | | 0.8 | | V | |
| | | Full range | 0.95 | | | 0.95 | | | 0.95 | | | |
| A_{VD} Large-signal differential voltage amplification | $V_O = 1.4\ \text{V to } 4\ \text{V},$ $R_L = 10\ \text{k}\Omega$ | 25°C | 0.2 | 1.5 | 0.3 | 1.5 | 0.4 | 1.5 | | | $\text{V}/\mu\text{V}$ | |
| | | Full range | 0.1 | | | 0.1 | | | 0.1 | | | |
| CMRR Common-mode rejection ratio | $V_{IC} = V_{ICR\text{min}},$ $R_S = 50\ \Omega$ | 25°C | 80 | 90 | 82 | 92 | 85 | 95 | | | dB | |
| | | Full range | 80 | | | 82 | | | 85 | | | |
| k_{SVR} Supply-voltage rejection ratio ($\Delta V_{CC\pm}/\Delta V_{IO}$) | $V_{CC\pm} = \pm 2.5\ \text{V to } \pm 15\ \text{V}$ | 25°C | 98 | 112 | 100 | 115 | 103 | 117 | | | dB | |
| | | Full range | 93 | | | 95 | | | 98 | | | |
| I_{CC} Supply current | $V_O = 0,$ No load | 25°C | 800 | 1200 | 800 | 1200 | 800 | 1200 | | | μA | |
| | | Full range | 1200 | | | 1200 | | | 1200 | | | |
| ΔI_{CC} Supply current change over operating temperature range | | Full range | 50 | | | 50 | | | 50 | | | μA |

† Full range is -55°C to 125°C .

NOTE 4: Typical values are based on the input offset voltage shift observed through 168 hours of operating life test at $T_A = 150^\circ\text{C}$ extrapolated to $T_A = 25^\circ\text{C}$ using the Arrhenius equation and assuming an activation energy of 0.96 eV.

TLE2024 electrical characteristics at specified free-air temperature, $V_{CC} = \pm 15$ V (unless otherwise noted)

| PARAMETER | TEST CONDITIONS | T_A^\dagger | TLE2024M | | | TLE2024AM | | | TLE2024BM | | | UNIT |
|---|--|---------------|-------------|-------------|-----|-------------|-------------|-----|-------------|-------------|------------|------------------|
| | | | MIN | TYP | MAX | MIN | TYP | MAX | MIN | TYP | MAX | |
| V_{IO} Input offset voltage | $V_{IC} = 0, R_S = 50 \Omega$ | 25°C | 1000 | | | 750 | | | 500 | | | μV |
| | | Full range | 1200 | | | 950 | | | 700 | | | |
| α_{VIO} Temperature coefficient of input offset voltage | | Full range | 2 | | | 2 | | | 2 | | | $\mu V/^\circ C$ |
| Input offset voltage long-term drift (see Note 4) | | 25°C | 0.006 | | | 0.006 | | | 0.006 | | | $\mu V/mo$ |
| I_{IO} Input offset current | | 25°C | 0.6 | 6 | | 0.5 | 6 | | 0.4 | 6 | | nA |
| | | Full range | 10 | | | 10 | | | 10 | | | |
| I_{IB} Input bias current | 25°C | 50 | 70 | | 45 | 70 | | 40 | 70 | | nA | |
| | Full range | 90 | | | 90 | | | 90 | | | | |
| V_{ICR} Common-mode input voltage range | $R_S = 50 \Omega$ | 25°C | -15 to 13.5 | -15.3 to 14 | | -15 to 13.5 | -15.3 to 14 | | -15 to 13.5 | -15.3 to 14 | V | |
| | | Full range | -15 to 13.2 | | | -15 to 13.2 | | | -15 to 13.2 | | | |
| V_{OM+} Maximum positive peak output voltage swing | $R_L = 10 k\Omega$ | 25°C | 13.8 | 14.1 | | 13.9 | 14.2 | | 14 | 14.3 | V | |
| | | Full range | 13.7 | | | 13.7 | | | 13.8 | | | |
| V_{OM-} Maximum negative peak output voltage swing | | 25°C | -13.7 | -14.1 | | -13.7 | -14.1 | | -13.7 | -14.1 | V | |
| | | Full range | -13.6 | | | -13.6 | | | -13.6 | | | |
| A_{VD} Large-signal differential voltage amplification | $V_O = \pm 10$ V, $R_L = 10 k\Omega$ | 25°C | 0.4 | 2 | | 0.8 | 4 | | 1 | 7 | V/ μV | |
| | | Full range | 0.4 | | | 0.8 | | | 1 | | | |
| CMRR Common-mode rejection ratio | $V_{IC} = V_{ICRmin}, R_S = 50 \Omega$ | 25°C | 92 | 102 | | 94 | 105 | | 97 | 108 | dB | |
| | | Full range | 88 | | | 90 | | | 93 | | | |
| k_{SVR} Supply-voltage rejection ratio ($\Delta V_{CC\pm}/\Delta V_{IO}$) | $V_{CC\pm} = \pm 2.5$ V to ± 15 V | 25°C | 98 | 112 | | 100 | 115 | | 103 | 117 | dB | |
| | | Full range | 93 | | | 95 | | | 98 | | | |
| I_{CC} Supply current | $V_O = 0, \text{ No load}$ | 25°C | 1050 | 1400 | | 1050 | 1400 | | 1050 | 1400 | μA | |
| | | Full range | 1400 | | | 1400 | | | 1400 | | | |
| ΔI_{CC} Supply current change over operating temperature range | | Full range | 85 | | | 85 | | | 85 | | | μA |

† Full range is $-55^\circ C$ to $125^\circ C$.

NOTE 4: Typical values are based on the input offset voltage shift observed through 168 hours of operating life test at $T_A = 150^\circ C$ extrapolated to $T_A = 25^\circ C$ using the Arrhenius equation and assuming an activation energy of 0.96 eV.

TLE2021 operating characteristics, $V_{CC} = 5\text{ V}$, $T_A = 25^\circ\text{C}$

| PARAMETER | TEST CONDITIONS | T_A | C SUFFIX | | | I SUFFIX | | | M SUFFIX | | | UNIT |
|-------------|---|---|----------|-----|-----|----------|-----|-----|----------|-----|-----|------------------------|
| | | | MIN | TYP | MAX | MIN | TYP | MAX | MIN | TYP | MAX | |
| SR | Slew rate at unity gain | $V_O = 1\text{ V to }3\text{ V}$, See Figure 1 | 25°C | | | 0.5 | | | 0.5 | | | $\text{V}/\mu\text{s}$ |
| V_n | Equivalent input noise voltage (see Figure 2) | $f = 10\text{ Hz}$ | 25°C | | | 21 50 | | | 21 50 | | | nV/Hz |
| | | $f = 1\text{ kHz}$ | 25°C | | | 17 30 | | | 17 30 | | | |
| $V_{N(PP)}$ | Peak-to-peak equivalent input noise voltage | $f = 0.1\text{ to }1\text{ Hz}$ | 25°C | | | 0.16 | | | 0.16 | | | μV |
| | | $f = 0.1\text{ to }10\text{ Hz}$ | 25°C | | | 0.47 | | | 0.47 | | | |
| I_n | Equivalent input noise current | | 25°C | | | 0.09 | | | 0.09 | | | pA/Hz |
| B_1 | Unity-gain bandwidth | See Figure 3 | 25°C | | | 1.2 | | | 1.2 | | | MHz |
| ϕ_m | Phase margin at unity gain | See Figure 3 | 25°C | | | 42° | | | 42° | | | |

TLE2021 operating characteristics at specified free-air temperature, $V_{CC} = \pm 15\text{ V}$

| PARAMETER | TEST CONDITIONS | T_A^\dagger | C SUFFIX | | | I SUFFIX | | | M SUFFIX | | | UNIT |
|-------------|---|---|------------|-----|-----|-----------|-----|-----|-----------|-----|-----|------------------------|
| | | | MIN | TYP | MAX | MIN | TYP | MAX | MIN | TYP | MAX | |
| SR | Slew rate at unity gain | $V_O = 1\text{ V to }3\text{ V}$, See Figure 1 | 25°C | | | 0.45 0.65 | | | 0.45 0.65 | | | $\text{V}/\mu\text{s}$ |
| | | | Full range | | | 0.45 | | | 0.42 | | | |
| V_n | Equivalent input noise voltage (see Figure 2) | $f = 10\text{ Hz}$ | 25°C | | | 19 50 | | | 19 50 | | | nV/Hz |
| | | $f = 1\text{ kHz}$ | 25°C | | | 15 30 | | | 15 30 | | | |
| $V_{N(PP)}$ | Peak-to-peak equivalent input noise voltage | $f = 0.1\text{ to }1\text{ Hz}$ | 25°C | | | 0.16 | | | 0.16 | | | μV |
| | | $f = 0.1\text{ to }10\text{ Hz}$ | 25°C | | | 0.47 | | | 0.47 | | | |
| I_n | Equivalent input noise current | | 25°C | | | 0.09 | | | 0.09 | | | pA/Hz |
| B_1 | Unity-gain bandwidth | See Figure 3 | 25°C | | | 2 | | | 2 | | | MHz |
| ϕ_m | Phase margin at unity gain | See Figure 3 | 25°C | | | 46° | | | 46° | | | |

[†] Full range is 0°C to 70°C for the C-suffix devices, –40°C to 85°C for the I-suffix devices, and –55°C to 125°C for the M-suffix devices.

TLE2022 operating characteristics, $V_{CC} = 5\text{ V}$, $T_A = 25^\circ\text{C}$

| PARAMETER | TEST CONDITIONS | C SUFFIX | | | I SUFFIX | | | M SUFFIX | | | UNIT |
|-------------|---|---|-----|-----|----------|-----|-----|----------|-----|-----|------------------------------|
| | | MIN | TYP | MAX | MIN | TYP | MAX | MIN | TYP | MAX | |
| SR | Slew rate at unity gain | $V_O = 1\text{ V to }3\text{ V}$, See Figure 1 | | | 0.5 | | | 0.5 | | | $\text{V}/\mu\text{s}$ |
| V_n | Equivalent input noise voltage (see Figure 2) | f = 10 Hz | | | 21 | | | 21 | | | $\text{nV}/\sqrt{\text{Hz}}$ |
| | | f = 1 kHz | | | 17 | | | 17 | | | |
| $V_{N(PP)}$ | Peak-to-peak equivalent input noise voltage | f = 0.1 to 1 Hz | | | 0.16 | | | 0.16 | | | μV |
| | | f = 0.1 to 10 Hz | | | 0.47 | | | 0.47 | | | |
| I_n | Equivalent input noise current | 0.1 | | | 0.1 | | | 0.1 | | | $\text{pA}/\sqrt{\text{Hz}}$ |
| B_1 | Unity-gain bandwidth | See Figure 3 | | | 1.7 | | | 1.7 | | | MHz |
| ϕ_m | Phase margin at unity gain | See Figure 3 | | | 47° | | | 47° | | | |

TLE2022 operating characteristics at specified free-air temperature, $V_{CC} = \pm 15\text{ V}$

| PARAMETER | TEST CONDITIONS | T_A | C SUFFIX† | | | I SUFFIX† | | | M SUFFIX† | | | UNIT |
|-------------|---|---|------------------|-----|-----|-----------|-----|-----|-----------|-----|-----|------------------------------|
| | | | MIN | TYP | MAX | MIN | TYP | MAX | MIN | TYP | MAX | |
| SR | Slew rate at unity gain | $V_O = \pm 10\text{ V}$, See Figure 1 | 25°C | | | 0.45 | | | 0.45 | | | $\text{V}/\mu\text{s}$ |
| | | | Full range | | | 0.45 | | | 0.42 | | | |
| V_n | Equivalent input noise voltage (see Figure 2) | 25°C | f = 10 Hz | | | 19 | | | 19 | | | $\text{nV}/\sqrt{\text{Hz}}$ |
| | | | f = 1 kHz | | | 15 | | | 15 | | | |
| $V_{N(PP)}$ | Peak-to-peak equivalent input noise voltage | 25°C | f = 0.1 to 1 Hz | | | 0.16 | | | 0.16 | | | μV |
| | | | f = 0.1 to 10 Hz | | | 0.47 | | | 0.47 | | | |
| I_n | Equivalent input noise current | 25°C | 0.1 | | | 0.1 | | | 0.1 | | | $\text{pA}/\sqrt{\text{Hz}}$ |
| B_1 | Unity-gain bandwidth | 25°C | See Figure 3 | | | 2.8 | | | 2.8 | | | MHz |
| ϕ_m | Phase margin at unity gain | 25°C | See Figure 3 | | | 52° | | | 52° | | | |

† Full range is 0°C to 70°C for the C-suffix devices, -40°C to 85°C for the I suffix devices and -55°C to 125°C for the I-suffix devices.

TLE2024 operating characteristics, $V_{CC} = 5\text{ V}$, $T_A = 25^\circ\text{C}$

| PARAMETER | TEST CONDITIONS | C SUFFIX | | | I SUFFIX | | | M SUFFIX | | | UNIT |
|-------------|---|---|-----|-----|----------|-----|-----|----------|-----|-----|------------------------------|
| | | MIN | TYP | MAX | MIN | TYP | MAX | MIN | TYP | MAX | |
| SR | Slew rate at unity gain | $V_O = 1\text{ V to }3\text{ V}$, See Figure 1 | | | 0.5 | | | 0.5 | | | $\text{V}/\mu\text{s}$ |
| V_n | Equivalent input noise voltage (see Figure 2) | f = 10 Hz | | | 21 50 | | | 21 50 | | | $\text{nV}/\sqrt{\text{Hz}}$ |
| | | f = 1 kHz | | | 17 30 | | | 17 30 | | | |
| $V_{N(PP)}$ | Peak-to-peak equivalent input noise voltage | f = 0.1 to 1 Hz | | | 0.16 | | | 0.16 | | | μV |
| | | f = 0.1 to 10 Hz | | | 0.47 | | | 0.47 | | | |
| I_n | Equivalent input noise current | | | | 0.1 | | | 0.1 | | | $\text{pA}/\sqrt{\text{Hz}}$ |
| B_1 | Unity-gain bandwidth | See Figure 3 | | | 1.7 | | | 1.7 | | | MHz |
| ϕ_m | Phase margin at unity gain | See Figure 3 | | | 47° | | | 47° | | | |

TLE2024 operating characteristics at specified free-air temperature, $V_{CC} = \pm 15\text{ V}$ (unless otherwise noted)

| PARAMETER | TEST CONDITIONS | T_A | C SUFFIX† | | | I SUFFIX† | | | M SUFFIX† | | | UNIT |
|-------------|---|--|------------------|-----|-----|-----------|-----|-----|-----------|-----|-----|------------------------------|
| | | | MIN | TYP | MAX | MIN | TYP | MAX | MIN | TYP | MAX | |
| SR | Slew rate at unity gain | $V_O = \pm 10\text{ V}$, See Figure 1 | 25°C | | | 0.45 0.7 | | | 0.45 0.7 | | | $\text{V}/\mu\text{s}$ |
| | | | Full range | | | 0.45 | | | 0.42 | | | |
| V_n | Equivalent input noise voltage (see Figure 2) | f = 10 Hz | 25°C | | | 19 50 | | | 19 50 | | | $\text{nV}/\sqrt{\text{Hz}}$ |
| | | | f = 1 kHz | | | 15 30 | | | 15 30 | | | |
| $V_{N(PP)}$ | Peak-to-peak equivalent input noise voltage | f = 0.1 to 1 Hz | 25°C | | | 0.16 | | | 0.16 | | | μV |
| | | | f = 0.1 to 10 Hz | | | 0.47 | | | 0.47 | | | |
| I_n | Equivalent input noise current | 25°C | | | | 0.1 | | | 0.1 | | | $\text{pA}/\sqrt{\text{Hz}}$ |
| B_1 | Unity-gain bandwidth | 25°C | See Figure 3 | | | 2.8 | | | 2.8 | | | MHz |
| ϕ_m | Phase margin at unity gain | 25°C | See Figure 3 | | | 52° | | | 52° | | | |

† Full range is 0°C to 70°C for the C-suffix devices, -40°C to 85°C for the I suffix devices and -55°C to 125°C for the I-suffix devices.

TLE202x, TLE202xA, TLE202xB, TLE202xY EXCALIBUR HIGH-SPEED LOW-POWER PRECISION OPERATIONAL AMPLIFIERS

SLOS191D – FEBRUARY 1997 – REVISED NOVEMBER 2010

TLE2021Y electrical characteristics at $V_{CC} = 5\text{ V}$, $T_A = 25^\circ\text{C}$ (unless otherwise noted)

| PARAMETER | TEST CONDITIONS | TLE2021Y | | | UNIT | |
|---|--|----------|------------------|-----|-------------------------|----|
| | | MIN | TYP | MAX | | |
| V_{IO} Input offset voltage | $V_{IC} = 0$, $R_S = 50\ \Omega$ | | 150 | | μV | |
| Input offset voltage long-term drift (see Note 4) | | | 0.005 | | $\mu\text{V}/\text{mo}$ | |
| I_{IO} Input offset current | | | | 0.5 | | nA |
| I_{IB} Input bias current | | | | 35 | | nA |
| V_{ICR} Common-mode input voltage range | $R_S = 50\ \Omega$ | | - 0.3 to 4 | | V | |
| V_{OH} Maximum high-level output voltage | $R_L = 10\ \text{k}\Omega$ | | 4.3 | | V | |
| V_{OL} Maximum low-level output voltage | | | | 0.7 | | V |
| A_{VD} Large-signal differential voltage amplification | $V_O = 1.4\ \text{to}\ 4\ \text{V}$, $R_L = 10\ \text{k}\Omega$ | | 1.5 | | $\text{V}/\mu\text{V}$ | |
| CMRR Common-mode rejection ratio | $V_{IC} = V_{ICR}\ \text{min}$, $R_S = 50\ \Omega$ | | 100 | | dB | |
| k_{SVR} Supply-voltage rejection ratio ($\Delta V_{CC\pm}/\Delta V_{IO}$) | $V_{CC} = 5\ \text{V}\ \text{to}\ 30\ \text{V}$ | | 115 | | dB | |
| I_{CC} Supply current | $V_O = 2.5\ \text{V}$, No load | | 400 | | μA | |

NOTE 4: Typical values are based on the input offset voltage shift observed through 168 hours of operating life test at $T_A = 150^\circ\text{C}$ extrapolated to $T_A = 25^\circ\text{C}$ using the Arrhenius equation and assuming an activation energy of 0.96 eV.

TLE2021Y operating characteristics at $V_{CC} = 5\text{ V}$, $T_A = 25^\circ\text{C}$

| PARAMETER | TEST CONDITIONS | TLE2021Y | | | UNIT |
|---|---|----------|------|-----|------------------------------|
| | | MIN | TYP | MAX | |
| SR Slew rate at unity gain | $V_O = 1\ \text{V}\ \text{to}\ 3\ \text{V}$ | | 0.5 | | $\text{V}/\mu\text{s}$ |
| V_n Equivalent input noise voltage | $f = 10\ \text{Hz}$ | | 21 | | $\text{nV}/\sqrt{\text{Hz}}$ |
| | $f = 1\ \text{kHz}$ | | 17 | | |
| $V_{N(PP)}$ Peak-to-peak equivalent input noise voltage | $f = 0.1\ \text{to}\ 1\ \text{Hz}$ | | 0.16 | | μV |
| | $f = 0.1\ \text{to}\ 10\ \text{Hz}$ | | 0.47 | | |
| I_n Equivalent input noise current | | | 0.1 | | $\text{pA}/\sqrt{\text{Hz}}$ |
| B_1 Unity-gain bandwidth | | | 1.7 | | MHz |
| ϕ_m Phase margin at unity gain | | | 47° | | |



TLE202x, TLE202xA, TLE202xB, TLE202xY EXCALIBUR HIGH-SPEED LOW-POWER PRECISION OPERATIONAL AMPLIFIERS

SLOS191D – FEBRUARY 1997 – REVISED NOVEMBER 2010

TLE2022Y electrical characteristics, $V_{CC} = 5\text{ V}$, $T_A = 25^\circ\text{C}$ (unless otherwise noted)

| PARAMETER | TEST CONDITIONS | TLE2022Y | | | UNIT |
|---|---|----------|------------------|-----|-------------------------|
| | | MIN | TYP | MAX | |
| V_{IO} Input offset voltage | $V_{IC} = 0$, $R_S = 50\ \Omega$ | | 150 | 600 | μV |
| Input offset voltage long-term drift (see Note 4) | | | 0.005 | | $\mu\text{V}/\text{mo}$ |
| I_{IO} Input offset current | | | 0.5 | | nA |
| I_{IB} Input bias current | | | 35 | | nA |
| V_{ICR} Common-mode input voltage range | $R_S = 50\ \Omega$ | | - 0.3 to 4 | | V |
| V_{OH} Maximum high-level output voltage | $R_L = 10\ \text{k}\Omega$ | | 4.3 | | V |
| V_{OL} Maximum low-level output voltage | | | 0.7 | | V |
| A_{VD} Large-signal differential voltage amplification | $V_O = 1.4\ \text{to}\ 4\ \text{V}$, $R_L = 10\ \text{k}\Omega$ | | 1.5 | | $\text{V}/\mu\text{V}$ |
| CMRR Common-mode rejection ratio | $V_{IC} = V_{ICR}\ \text{min}$, $R_S = 50\ \Omega$ | | 100 | | dB |
| k_{SVR} Supply-voltage rejection ratio ($\Delta V_{CC\pm} / \Delta V_{IO}$) | $V_{CC} = 5\ \text{V}\ \text{to}\ 30\ \text{V}$ | | 115 | | dB |
| I_{CC} Supply current | $V_O = 2.5\ \text{V}$, No load | | 450 | | μA |

NOTE 4: Typical values are based on the input offset voltage shift observed through 168 hours of operating life test at $T_A = 150^\circ\text{C}$ extrapolated to $T_A = 25^\circ\text{C}$ using the Arrhenius equation and assuming an activation energy of 0.96 eV.

TLE2022Y operating characteristics, $V_{CC} = 5\ \text{V}$, $T_A = 25^\circ\text{C}$

| PARAMETER | TEST CONDITIONS | TLE2022Y | | | UNIT |
|---|---|----------|------|-----|------------------------------|
| | | MIN | TYP | MAX | |
| SR Slew rate at unity gain | $V_O = 1\ \text{V}\ \text{to}\ 3\ \text{V}$, See Figure 1 | | 0.5 | | $\text{V}/\mu\text{s}$ |
| V_n Equivalent input noise voltage (see Figure 2) | $f = 10\ \text{Hz}$ | | 21 | | $\text{nV}/\sqrt{\text{Hz}}$ |
| | $f = 1\ \text{kHz}$ | | 17 | | |
| $V_{N(PP)}$ Peak-to-peak equivalent input noise voltage | $f = 0.1\ \text{to}\ 1\ \text{Hz}$ | | 0.16 | | μV |
| | $f = 0.1\ \text{to}\ 10\ \text{Hz}$ | | 0.47 | | |
| I_n Equivalent input noise current | | | 0.1 | | $\text{pA}/\sqrt{\text{Hz}}$ |
| B_1 Unity-gain bandwidth | See Figure 3 | | 1.7 | | MHz |
| ϕ_m Phase margin at unity gain | See Figure 3 | | 47° | | |



TLE202x, TLE202xA, TLE202xB, TLE202xY EXCALIBUR HIGH-SPEED LOW-POWER PRECISION OPERATIONAL AMPLIFIERS

SLOS191D – FEBRUARY 1997 – REVISED NOVEMBER 2010

TLE2024Y electrical characteristics, $V_{CC} = 5\text{ V}$, $T_A = 25^\circ\text{C}$ (unless otherwise noted)

| PARAMETER | TEST CONDITIONS | TLE2024Y | | | UNIT |
|--|--|----------|-----------------|-----|-------------------------|
| | | MIN | TYP | MAX | |
| Input offset voltage long-term drift (see Note 4) | | | 0.005 | | $\mu\text{V}/\text{mo}$ |
| I_{IO} Input offset current | $V_{IC} = 0$, $R_S = 50\ \Omega$ | | 0.6 | | nA |
| I_{IB} Input bias current | | | 45 | | nA |
| V_{ICR} Common-mode input voltage range | $R_S = 50\ \Omega$ | | -0.3 to 4 | | V |
| V_{OH} High-level output voltage | $R_L = 10\ \text{k}\Omega$ | | 4.2 | | V |
| V_{OL} Low-level output voltage | | | 0.7 | | V |
| A_{VD} Large-signal differential voltage amplification | $V_O = 1.4\text{ V to }4\text{ V}$, $R_L = 10\ \text{k}\Omega$ | | 1.5 | | $\text{V}/\mu\text{V}$ |
| CMRR Common-mode rejection ratio | $V_{IC} = V_{ICRmin}$, $R_S = 50\ \Omega$ | | 90 | | dB |
| k_{SVR} Supply-voltage rejection ratio ($\Delta V_{CC}/\Delta V_{IO}$) | $V_{CC} = 5\text{ V to }30\text{ V}$ | | 112 | | dB |
| I_{CC} Supply current | $V_O = 2.5\text{ V}$, No load | | 800 | | μA |

NOTE 4. Typical values are based on the input offset voltage shift observed through 168 hours of operating life test at $T_A = 150^\circ\text{C}$ extrapolated to $T_A = 25^\circ\text{C}$ using the Arrhenius equation and assuming an activation energy of 0.96 eV.

TLE2024Y operating characteristics, $V_{CC} = 5\text{ V}$, $T_A = 25^\circ\text{C}$

| PARAMETER | TEST CONDITIONS | TLE2024Y | | | UNIT |
|---|---|----------|------|-----|------------------------------|
| | | MIN | TYP | MAX | |
| SR Slew rate at unity gain | $V_O = 1\text{ V to }3\text{ V}$, See Figure 1 | | 0.5 | | $\text{V}/\mu\text{s}$ |
| V_n Equivalent input noise voltage (see Figure 2) | $f = 10\text{ Hz}$ | | 21 | | $\text{nV}/\sqrt{\text{Hz}}$ |
| | $f = 1\text{ kHz}$ | | 17 | | |
| $V_{N(PP)}$ Peak-to-peak equivalent input noise voltage | $f = 0.1\text{ to }1\text{ Hz}$ | | 0.16 | | μV |
| | $f = 0.1\text{ to }10\text{ Hz}$ | | 0.47 | | |
| I_n Equivalent input noise current | | | 0.1 | | $\text{pA}/\sqrt{\text{Hz}}$ |
| B_1 Unity-gain bandwidth | See Figure 3 | | 1.7 | | MHz |
| ϕ_m Phase margin at unity gain | See Figure 3 | | 47° | | |

PARAMETER MEASUREMENT INFORMATION



(a) SINGLE SUPPLY



(b) SPLIT SUPPLY

NOTE A: C_L includes fixture capacitance.

Figure 1. Slew-Rate Test Circuit

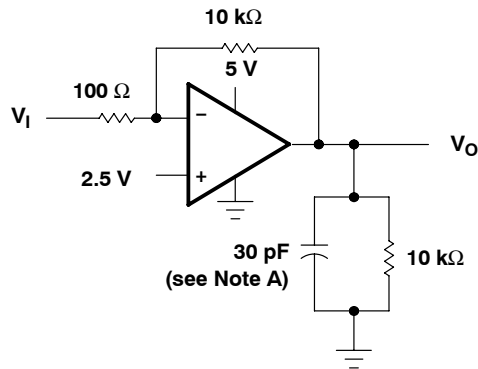


(a) SINGLE SUPPLY

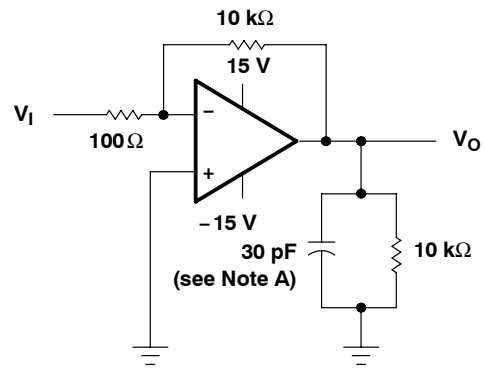


(b) SPLIT SUPPLY

Figure 2. Noise-Voltage Test Circuit



(a) SINGLE SUPPLY



(b) SPLIT SUPPLY

NOTE A: C_L includes fixture capacitance.

Figure 3. Unity-Gain Bandwidth and Phase-Margin Test Circuit

TLE202x, TLE202xA, TLE202xB, TLE202xY EXCALIBUR HIGH-SPEED LOW-POWER PRECISION OPERATIONAL AMPLIFIERS

SLOS191D – FEBRUARY 1997 – REVISED NOVEMBER 2010

PARAMETER MEASUREMENT INFORMATION



NOTE A: C_L includes fixture capacitance.

Figure 4. Small-Signal Pulse-Response Test Circuit

typical values

Typical values presented in this data sheet represent the median (50% point) of device parametric performance.

TLE202x, TLE202xA, TLE202xB, TLE202xY
EXCALIBUR HIGH-SPEED LOW-POWER PRECISION
OPERATIONAL AMPLIFIERS

SLOS191D – FEBRUARY 1997 – REVISED NOVEMBER 2010

TYPICAL CHARACTERISTICS

Table of Graphs

| | | | FIGURE |
|-------------|---|---|----------------------------|
| V_{IO} | Input offset voltage | Distribution | 5, 6, 7 |
| I_{IB} | Input bias current | vs Common-mode input voltage vs Free-air temperature | 8, 9, 10 11, 12, 13 |
| I_I | Input current | vs Differential input voltage | 14 |
| V_{OM} | Maximum peak output voltage | vs Output current vs Free-air temperature | 15, 16, 17 18 |
| V_{OH} | High-level output voltage | vs High-level output current vs Free-air temperature | 19, 20 21 |
| V_{OL} | Low-level output voltage | vs Low-level output current vs Free-air temperature | 22 23 |
| $V_{O(PP)}$ | Maximum peak-to-peak output voltage | vs Frequency | 24, 25 |
| A_{VD} | Large-signal differential voltage amplification | vs Frequency vs Free-air temperature | 26 27, 28, 29 |
| I_{OS} | Short-circuit output current | vs Supply voltage vs Free-air temperature | 30 – 33 34 – 37 |
| I_{CC} | Supply current | vs Supply voltage vs Free-air temperature | 38, 39, 40 41, 42, 43 |
| CMRR | Common-mode rejection ratio | vs Frequency | 44, 45, 46 |
| SR | Slew rate | vs Free-air temperature | 47, 48, 49 |
| | Voltage-follower small-signal pulse response | | 50, 51 |
| | Voltage-follower large-signal pulse response | | 52 – 57 |
| $V_{N(PP)}$ | Peak-to-peak equivalent input noise voltage | 0.1 to 1 Hz 0.1 to 10 Hz | 58 59 |
| V_n | Equivalent input noise voltage | vs Frequency | 60 |
| B_1 | Unity-gain bandwidth | vs Supply voltage vs Free-air temperature | 61, 62 63, 64 |
| ϕ_m | Phase margin | vs Supply voltage vs Load capacitance vs Free-air temperature | 65, 66 67, 68 69, 70 |
| | Phase shift | vs Frequency | 26 |



TLE202x, TLE202xA, TLE202xB, TLE202xY EXCALIBUR HIGH-SPEED LOW-POWER PRECISION OPERATIONAL AMPLIFIERS

SLOS191D – FEBRUARY 1997 – REVISED NOVEMBER 2010

TYPICAL CHARACTERISTICS

**DISTRIBUTION OF TLE2021
INPUT OFFSET VOLTAGE**

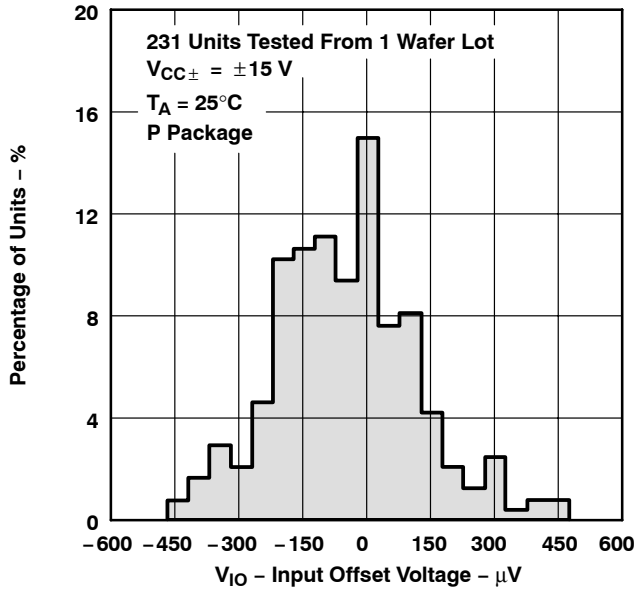


Figure 5

**DISTRIBUTION OF TLE2022
INPUT OFFSET VOLTAGE**

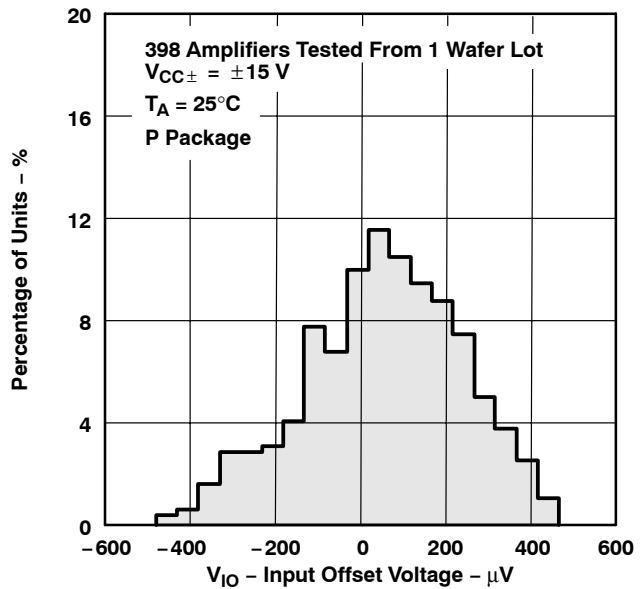


Figure 6

**DISTRIBUTION OF TLE2024
INPUT OFFSET VOLTAGE**

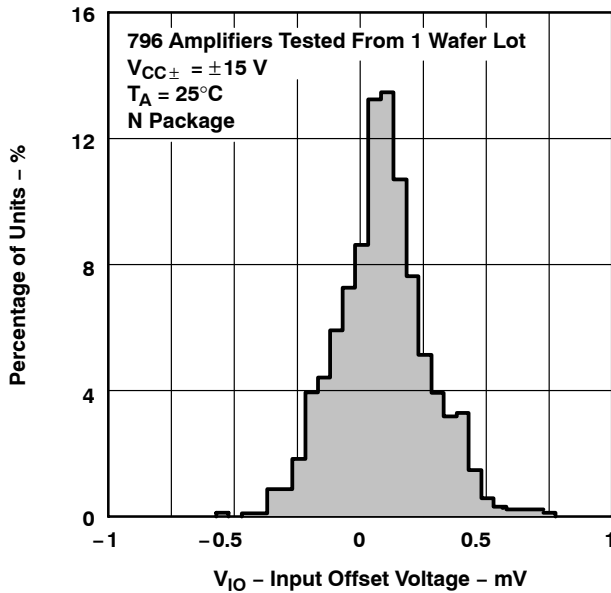


Figure 7

**TLE2021
INPUT BIAS CURRENT
vs
COMMON-MODE INPUT VOLTAGE**

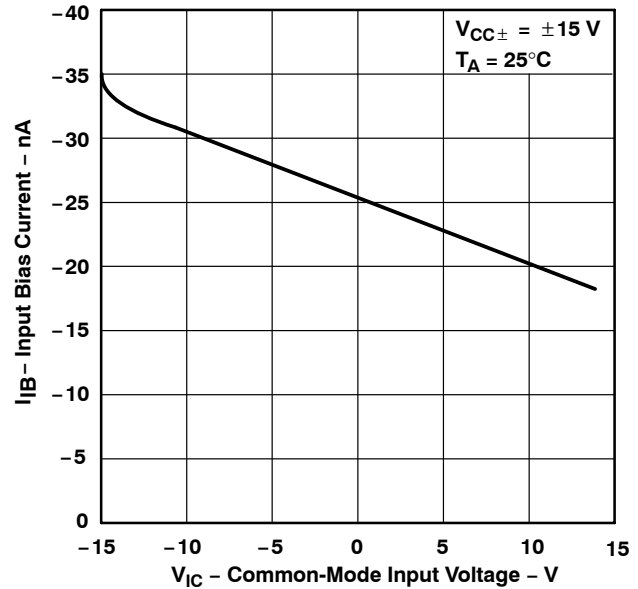
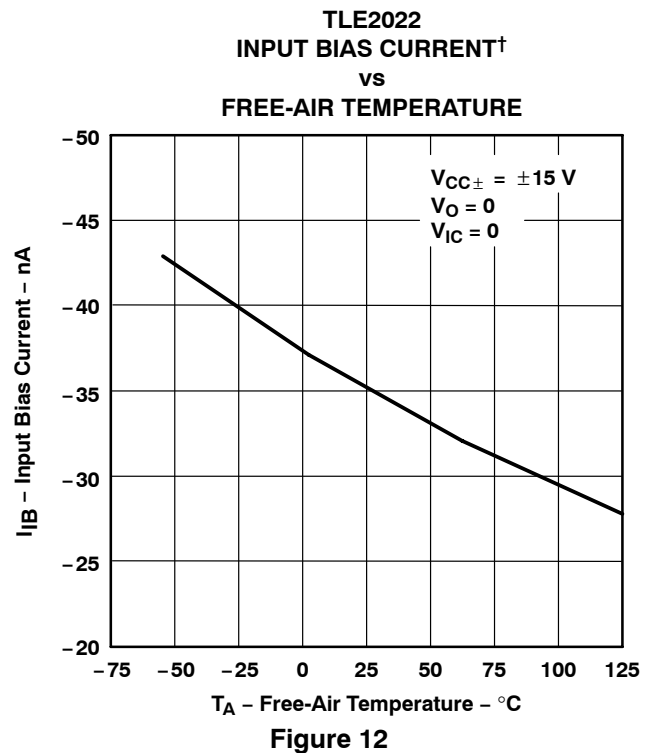
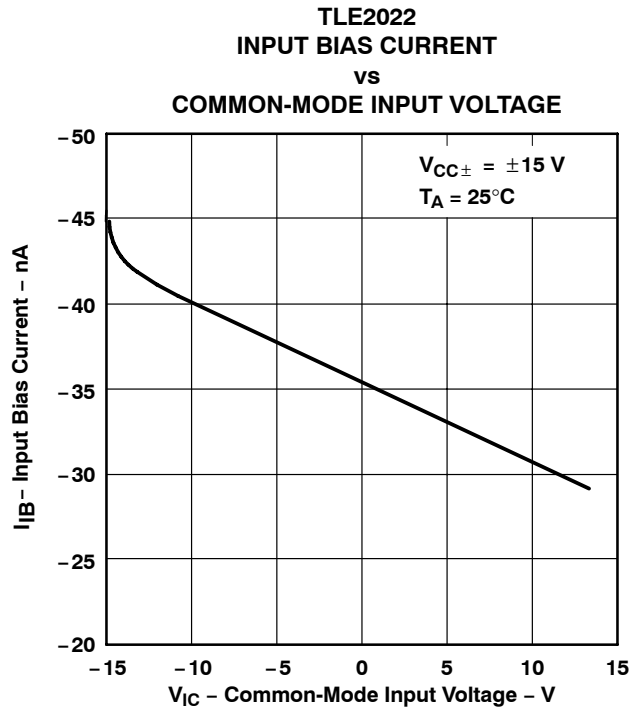


Figure 8

TLE202x, TLE202xA, TLE202xB, TLE202xY EXCALIBUR HIGH-SPEED LOW-POWER PRECISION OPERATIONAL AMPLIFIERS

SLOS191D – FEBRUARY 1997 – REVISED NOVEMBER 2010

TYPICAL CHARACTERISTICS

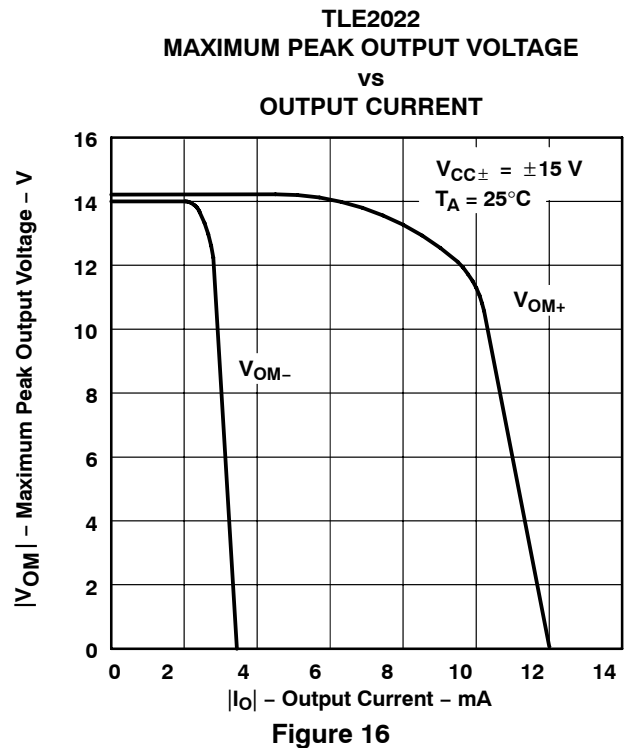
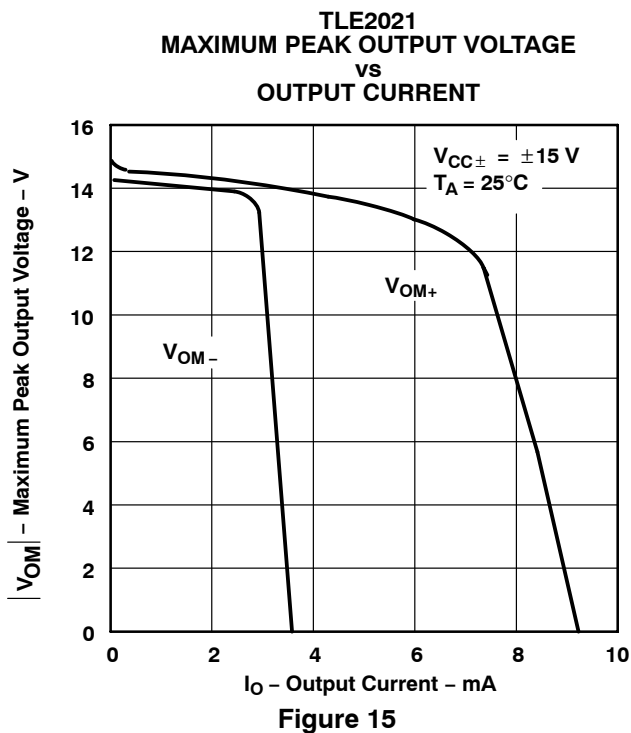
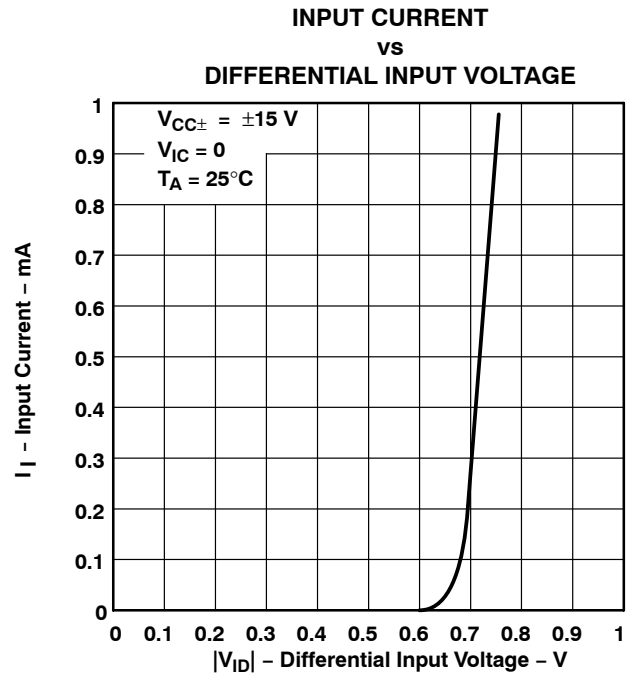


† Data at high and low temperatures are applicable only within the rated operating free-air temperature ranges of the various devices.

TLE202x, TLE202xA, TLE202xB, TLE202xY EXCALIBUR HIGH-SPEED LOW-POWER PRECISION OPERATIONAL AMPLIFIERS

SLOS191D – FEBRUARY 1997 – REVISED NOVEMBER 2010

TYPICAL CHARACTERISTICS

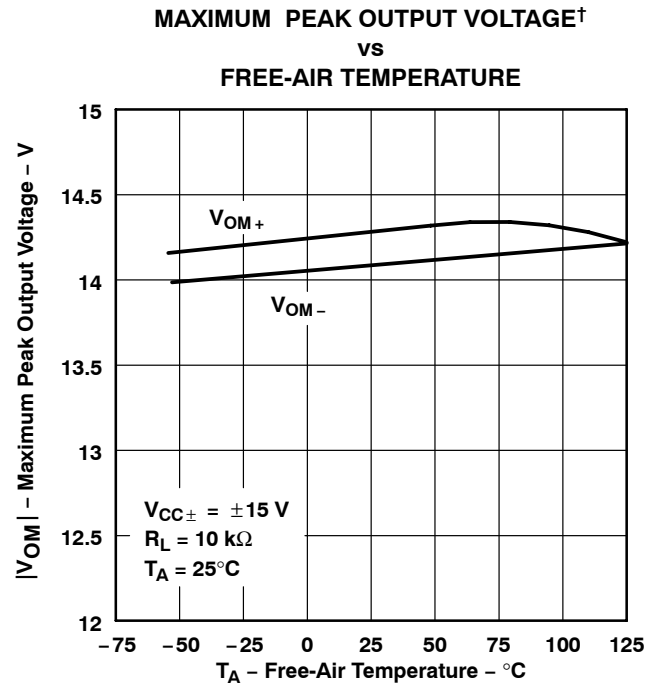
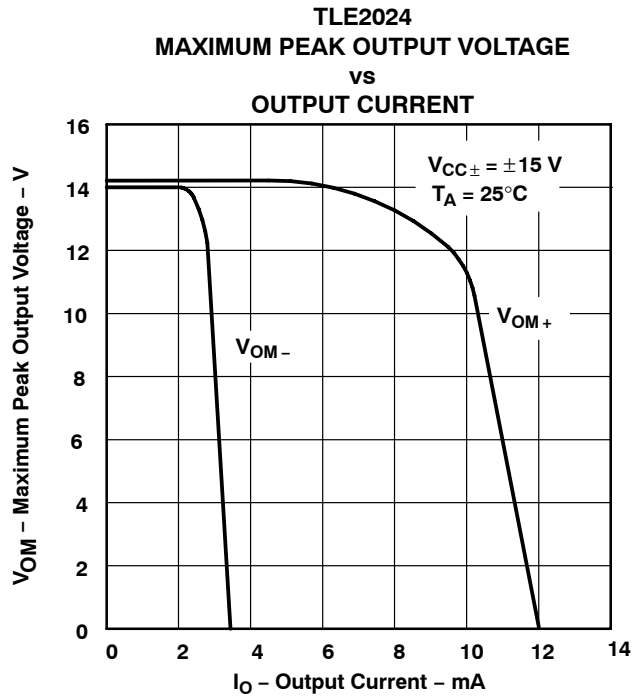


† Data at high and low temperatures are applicable only within the rated operating free-air temperature ranges of the various devices.

TLE202x, TLE202xA, TLE202xB, TLE202xY EXCALIBUR HIGH-SPEED LOW-POWER PRECISION OPERATIONAL AMPLIFIERS

SLOS191D – FEBRUARY 1997 – REVISED NOVEMBER 2010

TYPICAL CHARACTERISTICS

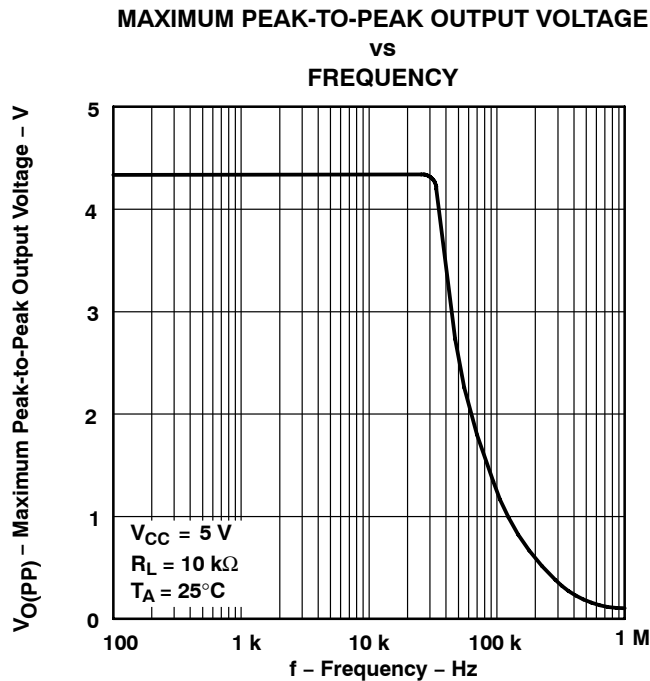
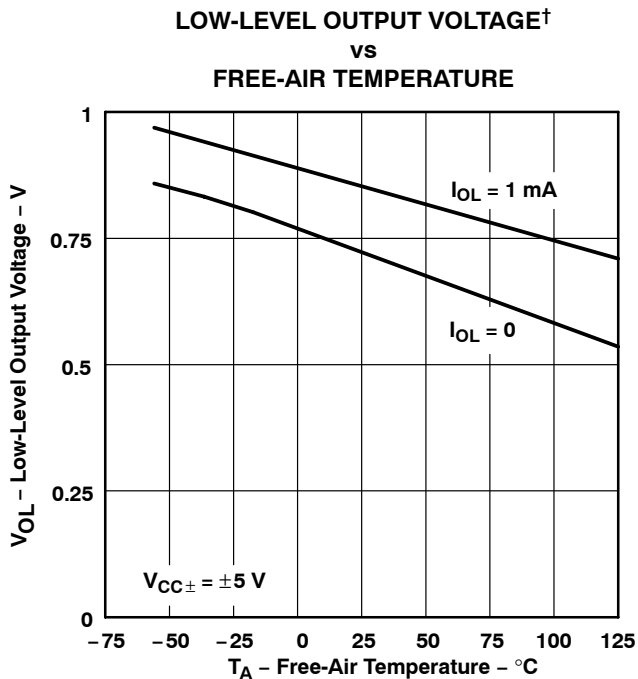


† Data at high and low temperatures are applicable only within the rated operating free-air temperature ranges of the various devices.

TLE202x, TLE202xA, TLE202xB, TLE202xY EXCALIBUR HIGH-SPEED LOW-POWER PRECISION OPERATIONAL AMPLIFIERS

SLOS191D – FEBRUARY 1997 – REVISED NOVEMBER 2010

TYPICAL CHARACTERISTICS



[†] Data at high and low temperatures are applicable only within the rated operating free-air temperature ranges of the various devices.



TLE202x, TLE202xA, TLE202xB, TLE202xY EXCALIBUR HIGH-SPEED LOW-POWER PRECISION OPERATIONAL AMPLIFIERS

SLOS191D – FEBRUARY 1997 – REVISED NOVEMBER 2010

TYPICAL CHARACTERISTICS

MAXIMUM PEAK-TO-PEAK OUTPUT VOLTAGE vs FREQUENCY

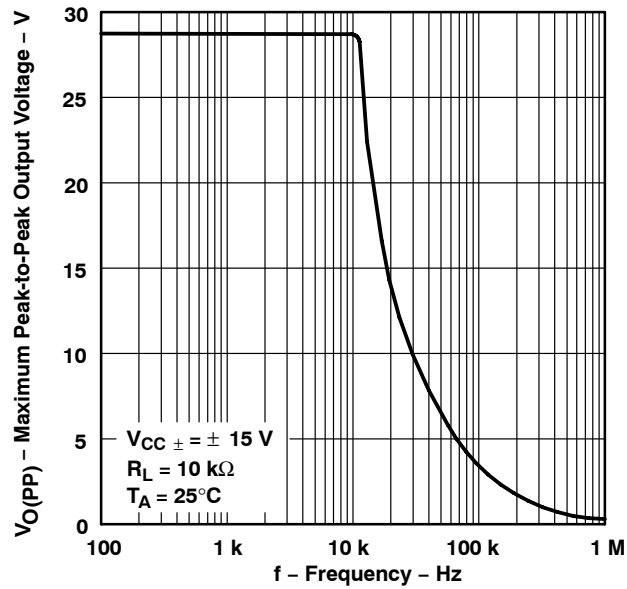


Figure 25

LARGE-SIGNAL DIFFERENTIAL VOLTAGE AMPLIFICATION AND PHASE SHIFT vs FREQUENCY



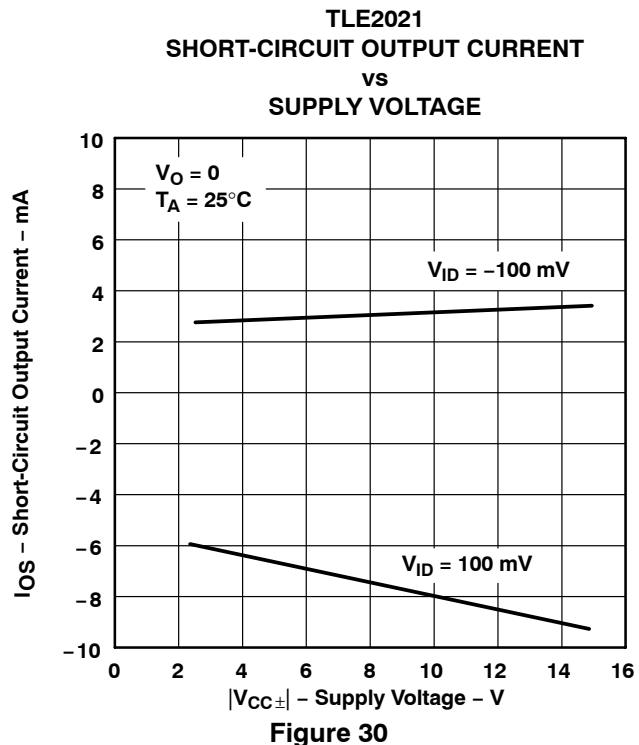
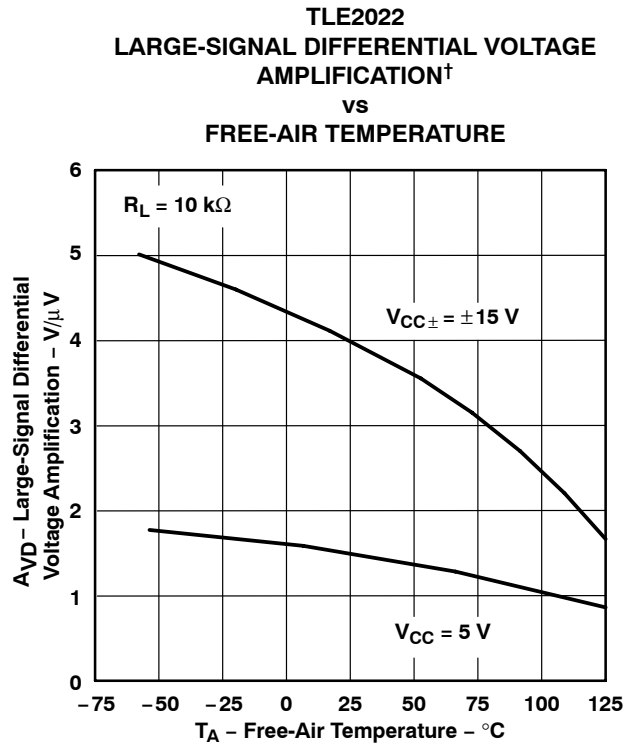
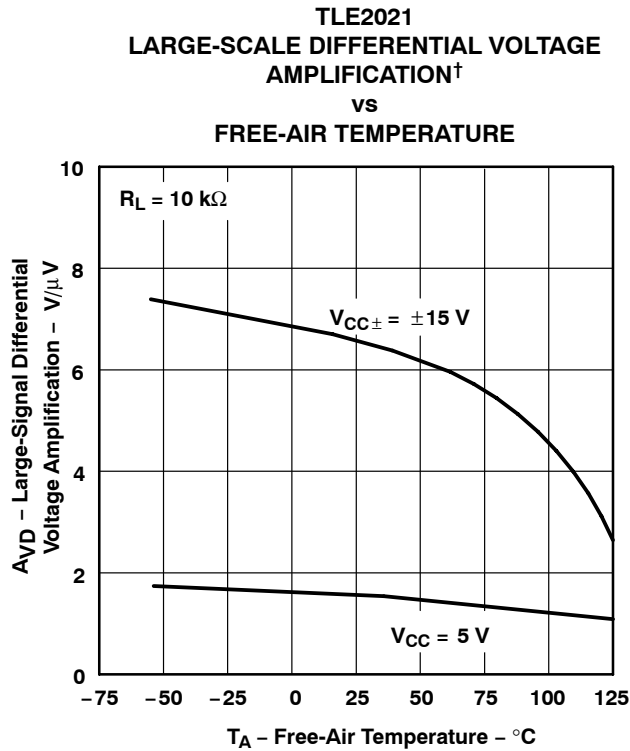
Figure 26



TLE202x, TLE202xA, TLE202xB, TLE202xY EXCALIBUR HIGH-SPEED LOW-POWER PRECISION OPERATIONAL AMPLIFIERS

SLOS191D – FEBRUARY 1997 – REVISED NOVEMBER 2010

TYPICAL CHARACTERISTICS

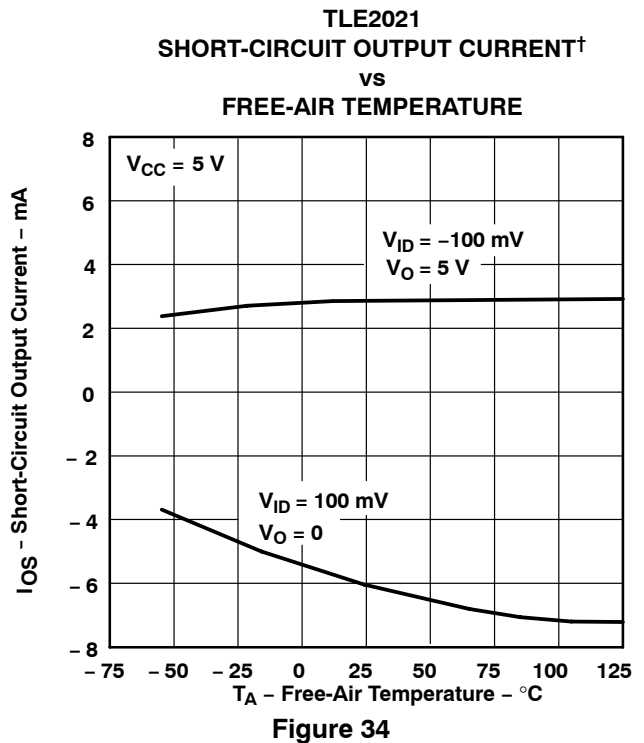
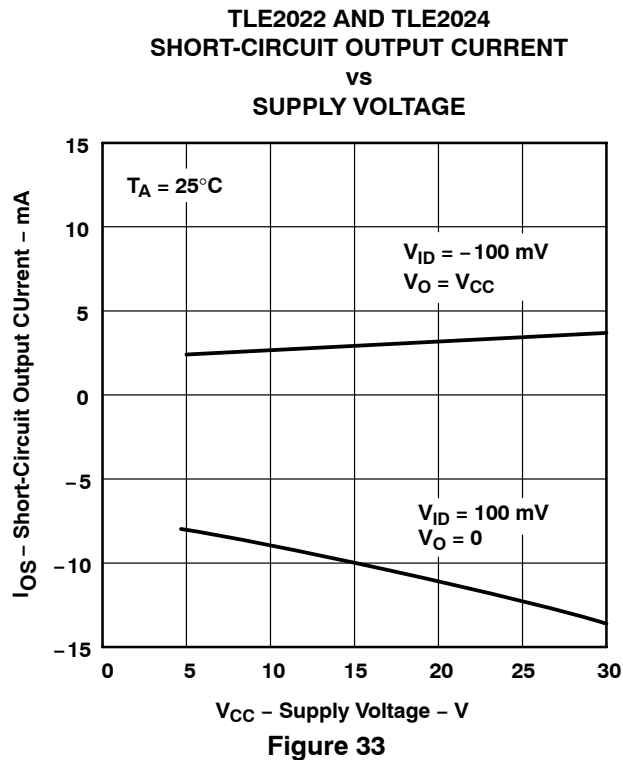
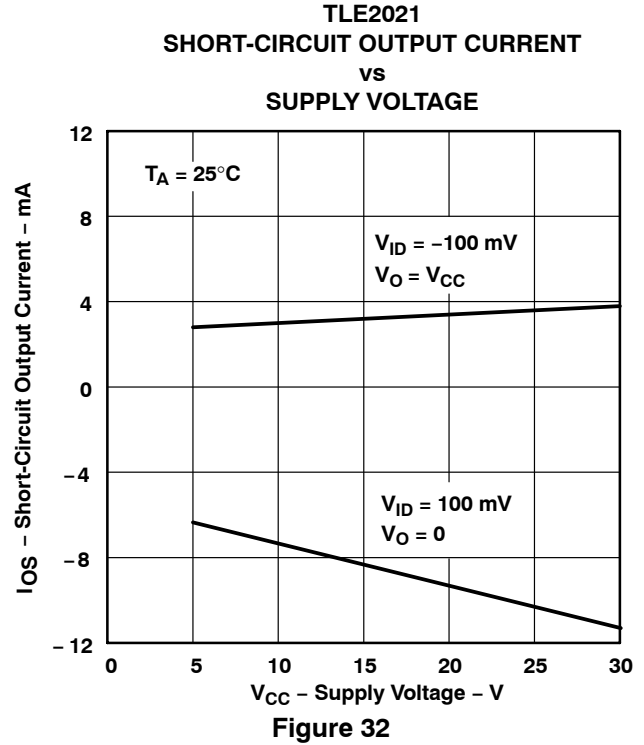
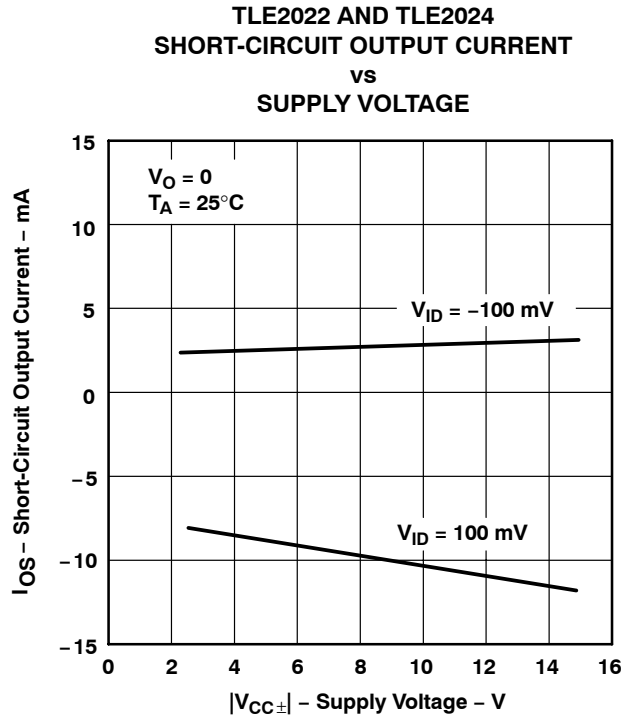


† Data at high and low temperatures are applicable only within the rated operating free-air temperature ranges of the various devices.

TLE202x, TLE202xA, TLE202xB, TLE202xY EXCALIBUR HIGH-SPEED LOW-POWER PRECISION OPERATIONAL AMPLIFIERS

SLOS191D – FEBRUARY 1997 – REVISED NOVEMBER 2010

TYPICAL CHARACTERISTICS



† Data at high and low temperatures are applicable only within the rated operating free-air temperature ranges of the various devices.

TLE202x, TLE202xA, TLE202xB, TLE202xY EXCALIBUR HIGH-SPEED LOW-POWER PRECISION OPERATIONAL AMPLIFIERS

SLOS191D – FEBRUARY 1997 – REVISED NOVEMBER 2010

TYPICAL CHARACTERISTICS

**TLE2022 AND TLE2024
SHORT-CIRCUIT OUTPUT CURRENT†
vs
FREE-AIR TEMPERATURE**



Figure 35

**TLE2021
SHORT-CIRCUIT OUTPUT CURRENT†
vs
FREE-AIR TEMPERATURE**



Figure 36

**TLE2022 AND TLE2024
SHORT-CIRCUIT OUTPUT CURRENT†
vs
FREE-AIR TEMPERATURE**



Figure 37

**TLE2021
SUPPLY CURRENT
vs
SUPPLY VOLTAGE**



Figure 38

† Data at high and low temperatures are applicable only within the rated operating free-air temperature ranges of the various devices.

TLE202x, TLE202xA, TLE202xB, TLE202xY EXCALIBUR HIGH-SPEED LOW-POWER PRECISION OPERATIONAL AMPLIFIERS

SLOS191D – FEBRUARY 1997 – REVISED NOVEMBER 2010

TYPICAL CHARACTERISTICS



Figure 39

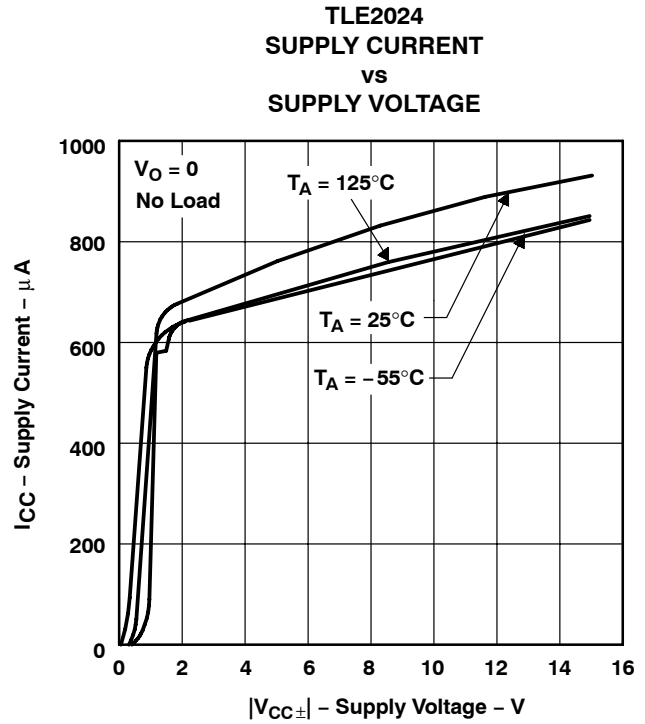


Figure 40

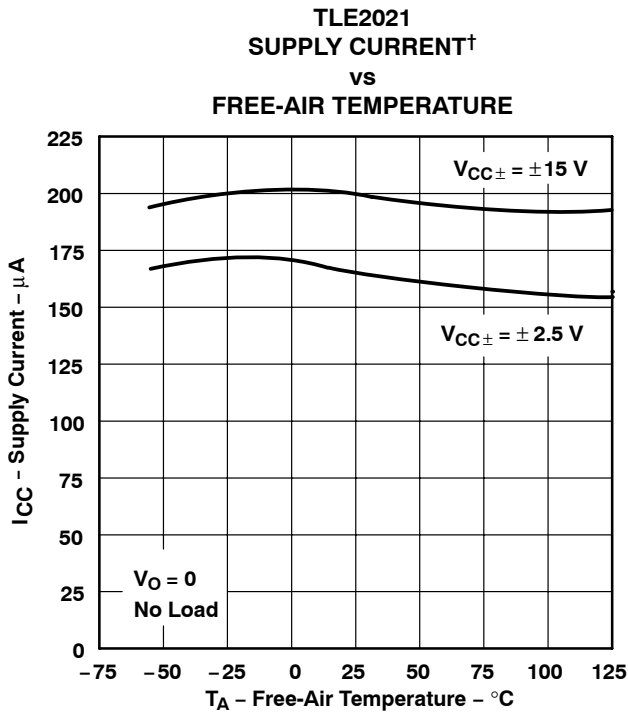


Figure 41

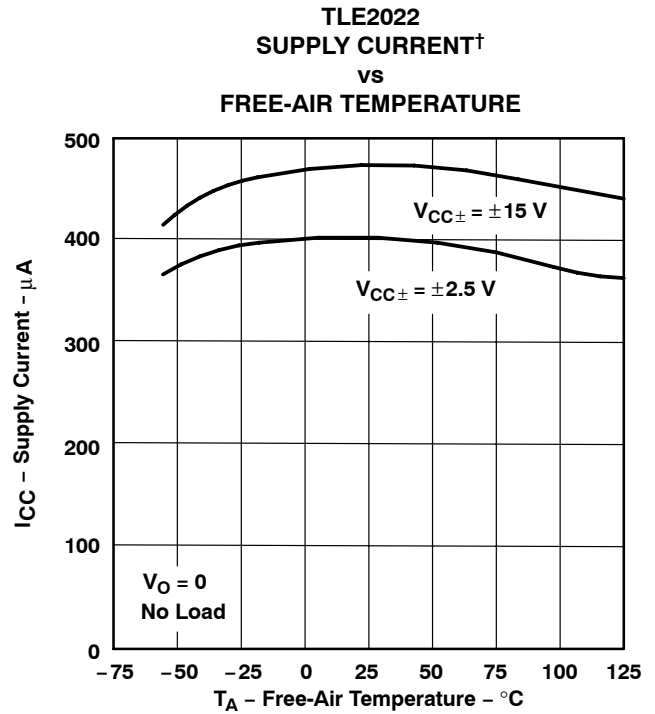


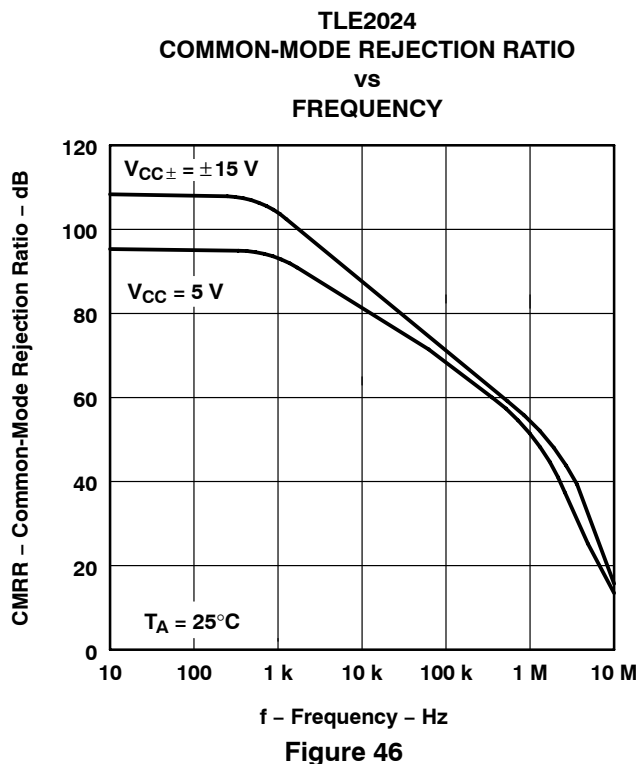
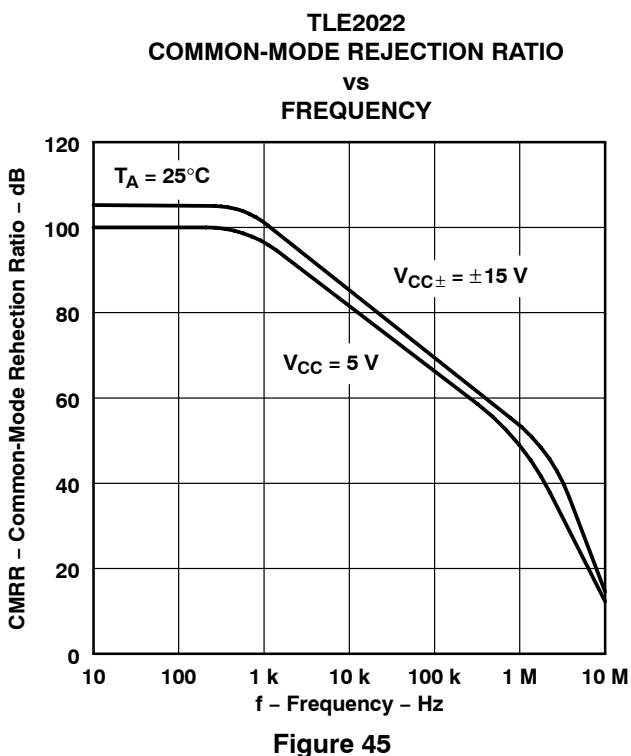
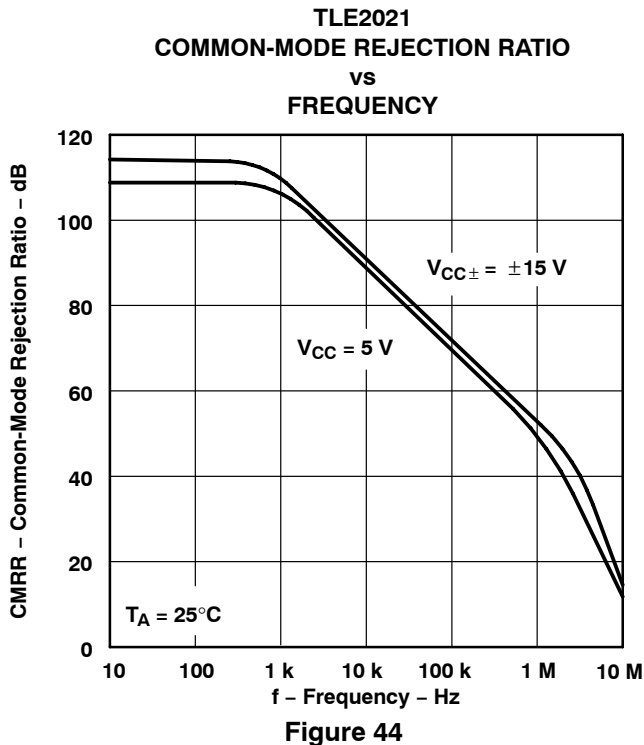
Figure 42

† Data at high and low temperatures are applicable only within the rated operating free-air temperature ranges of the various devices.

TLE202x, TLE202xA, TLE202xB, TLE202xY EXCALIBUR HIGH-SPEED LOW-POWER PRECISION OPERATIONAL AMPLIFIERS

SLOS191D – FEBRUARY 1997 – REVISED NOVEMBER 2010

TYPICAL CHARACTERISTICS



† Data at high and low temperatures are applicable only within the rated operating free-air temperature ranges of the various devices.

TLE202x, TLE202xA, TLE202xB, TLE202xY EXCALIBUR HIGH-SPEED LOW-POWER PRECISION OPERATIONAL AMPLIFIERS

SLOS191D – FEBRUARY 1997 – REVISED NOVEMBER 2010

TYPICAL CHARACTERISTICS



† Data at high and low temperatures are applicable only within the rated operating free-air temperature ranges of the various devices.

TLE202x, TLE202xA, TLE202xB, TLE202xY EXCALIBUR HIGH-SPEED LOW-POWER PRECISION OPERATIONAL AMPLIFIERS

SLOS191D – FEBRUARY 1997 – REVISED NOVEMBER 2010

TYPICAL CHARACTERISTICS

**VOLTAGE-FOLLOWER
SMALL-SIGNAL
PULSE RESPONSE**

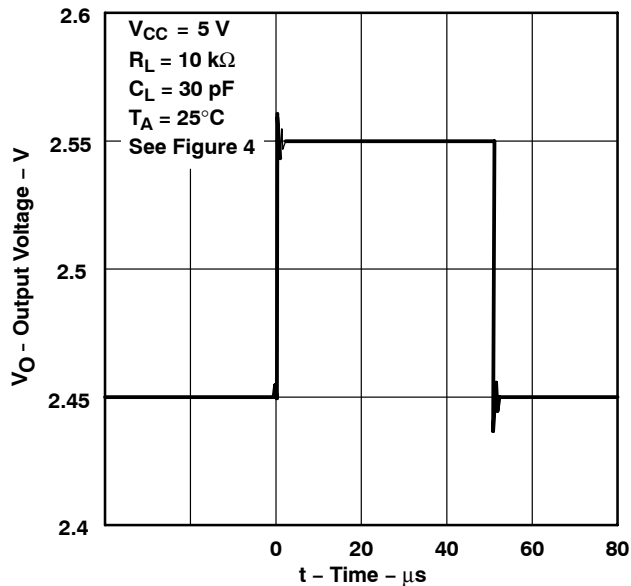


Figure 51

**TLE2021
VOLTAGE-FOLLOWER LARGE-SIGNAL
PULSE RESPONSE**

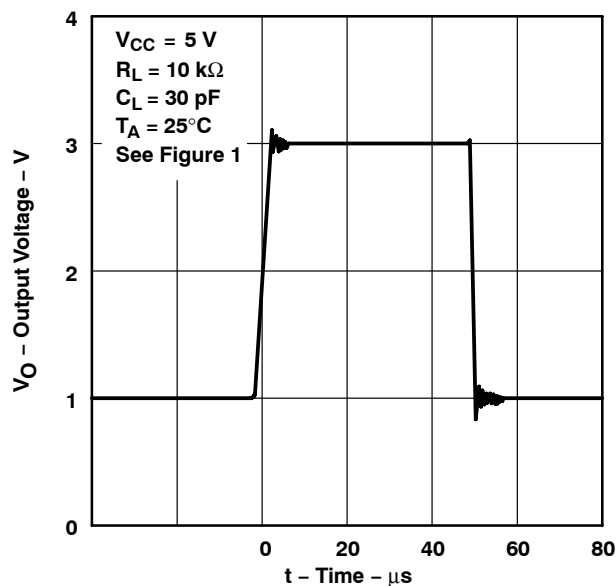


Figure 52

**TLE2022
VOLTAGE-FOLLOWER LARGE-SIGNAL
PULSE RESPONSE**

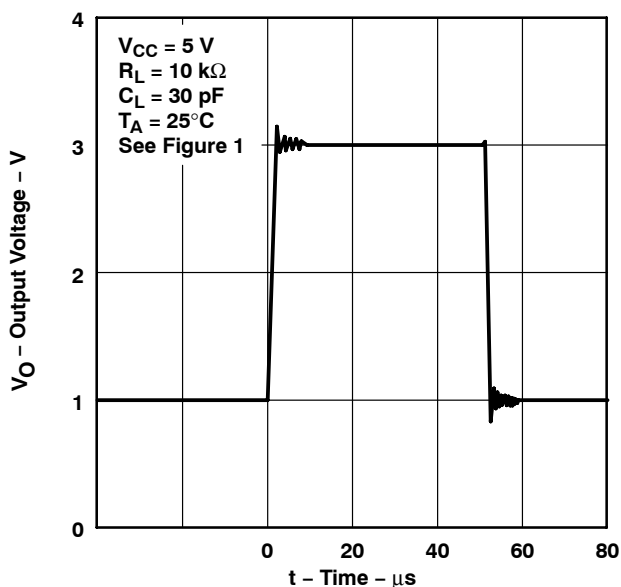


Figure 53

**TLE2024
VOLTAGE-FOLLOWER LARGE-SCALE
PULSE RESPONSE**

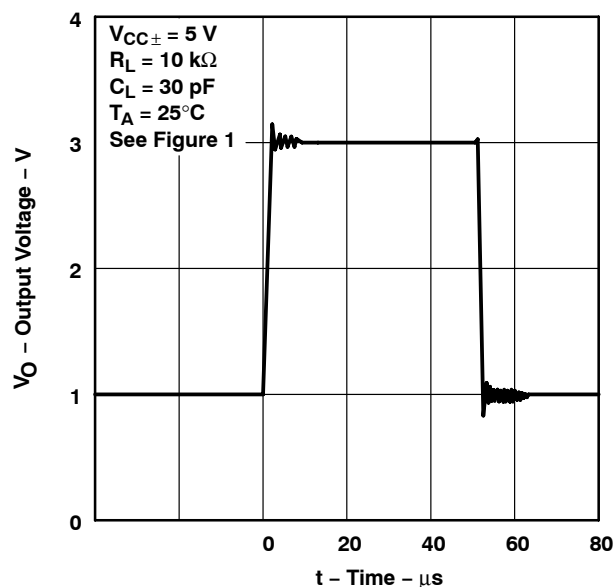


Figure 54

TLE202x, TLE202xA, TLE202xB, TLE202xY EXCALIBUR HIGH-SPEED LOW-POWER PRECISION OPERATIONAL AMPLIFIERS

SLOS191D – FEBRUARY 1997 – REVISED NOVEMBER 2010

TYPICAL CHARACTERISTICS



Figure 55



Figure 56



Figure 57



Figure 58

TLE202x, TLE202xA, TLE202xB, TLE202xY EXCALIBUR HIGH-SPEED LOW-POWER PRECISION OPERATIONAL AMPLIFIERS

SLOS191D – FEBRUARY 1997 – REVISED NOVEMBER 2010

TYPICAL CHARACTERISTICS

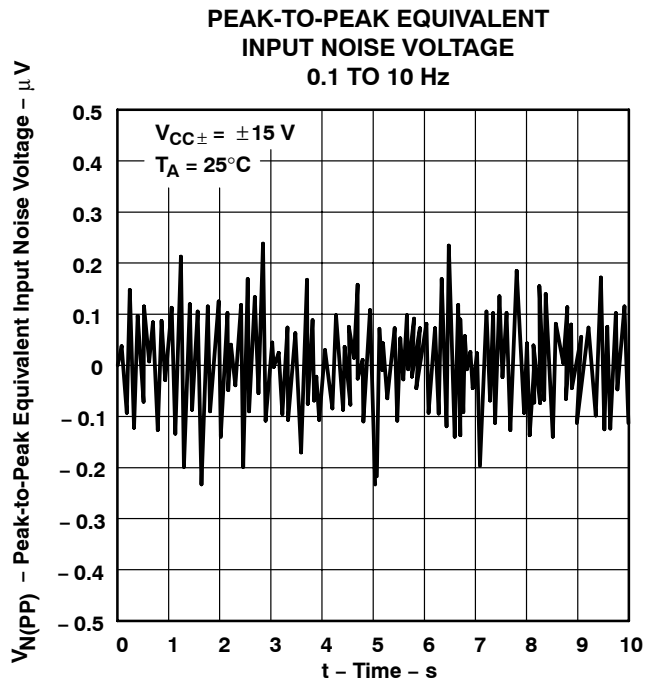


Figure 59

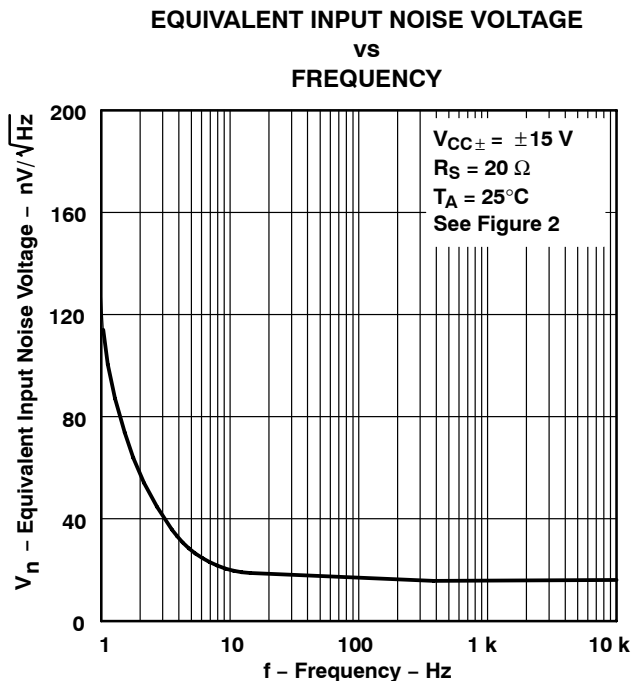


Figure 60

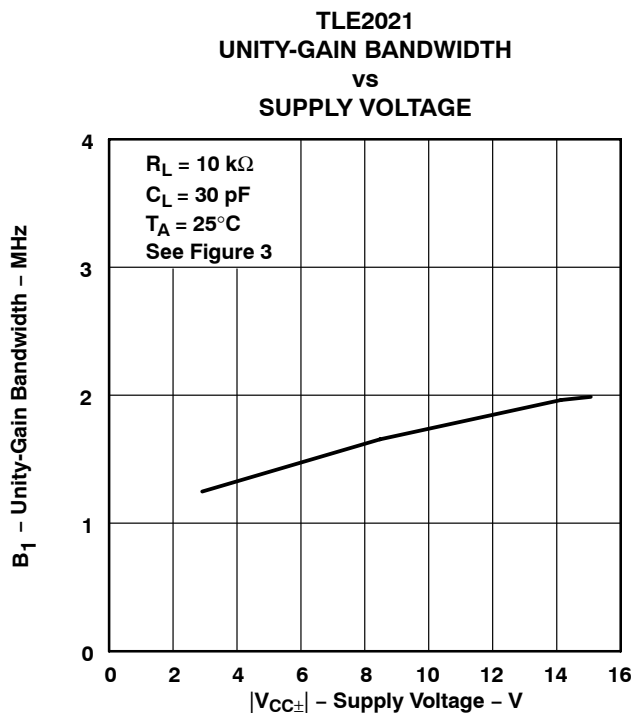


Figure 61

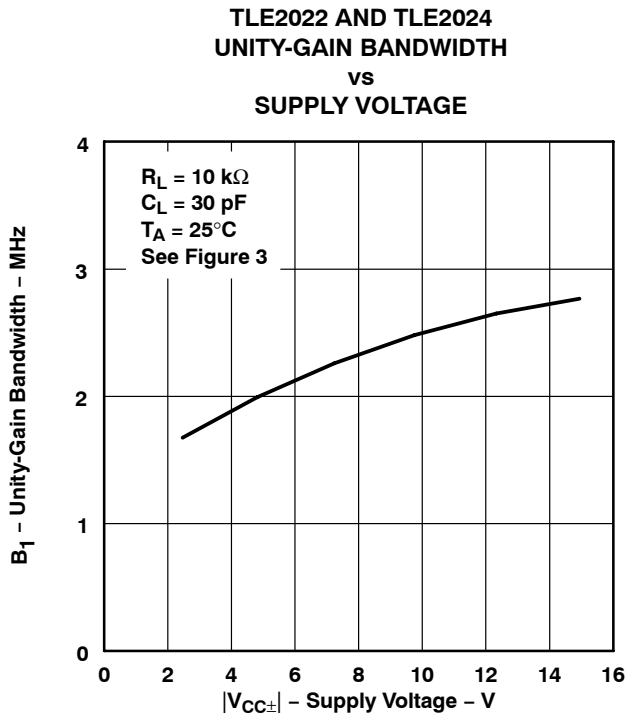
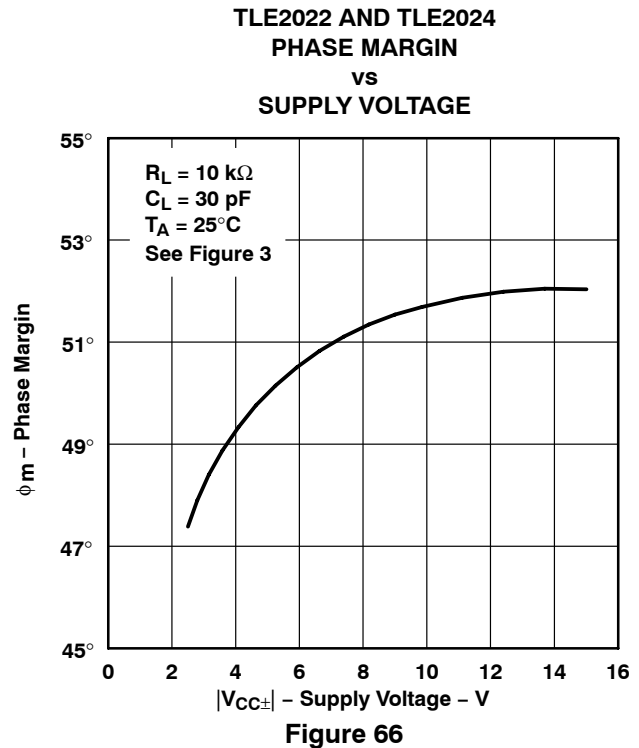
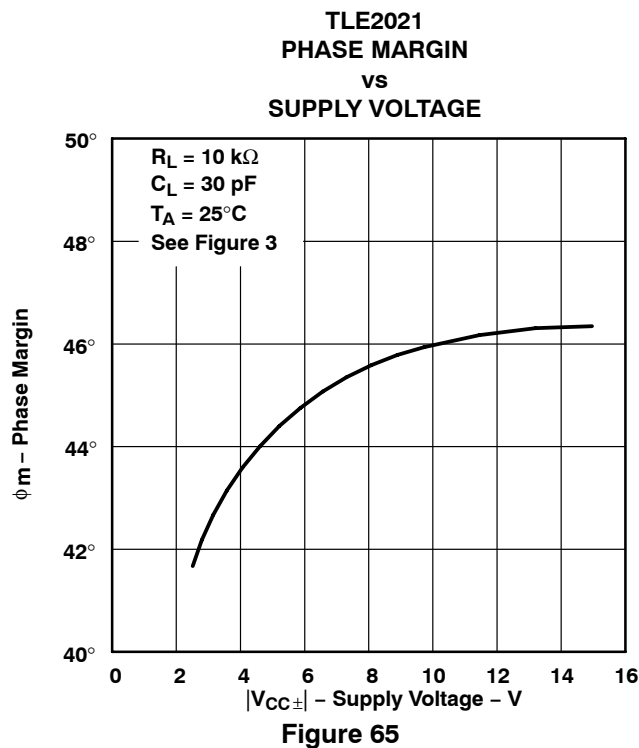
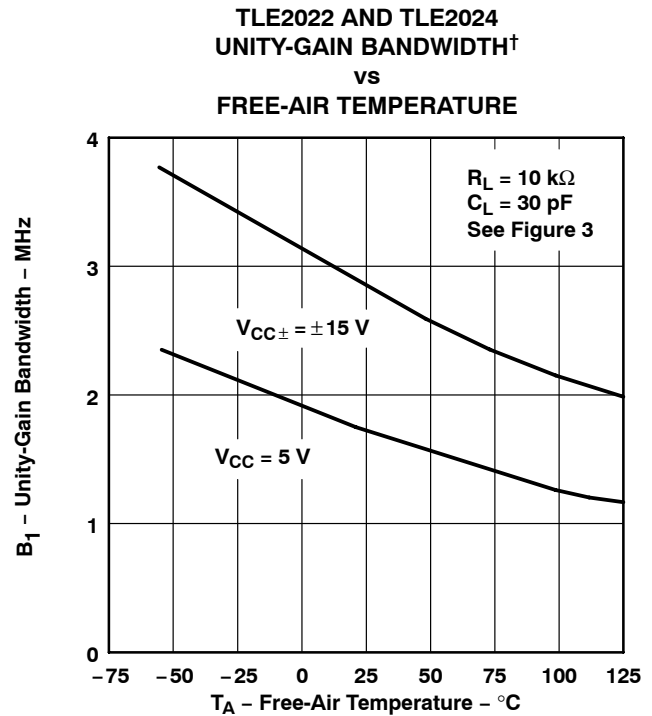


Figure 62

TLE202x, TLE202xA, TLE202xB, TLE202xY EXCALIBUR HIGH-SPEED LOW-POWER PRECISION OPERATIONAL AMPLIFIERS

SLOS191D – FEBRUARY 1997 – REVISED NOVEMBER 2010

TYPICAL CHARACTERISTICS



† Data at high and low temperatures are applicable only within the rated operating free-air temperature ranges of the various devices.

TLE202x, TLE202xA, TLE202xB, TLE202xY EXCALIBUR HIGH-SPEED LOW-POWER PRECISION OPERATIONAL AMPLIFIERS

SLOS191D – FEBRUARY 1997 – REVISED NOVEMBER 2010

TYPICAL CHARACTERISTICS

**TLE2021
PHASE MARGIN
vs
LOAD CAPACITANCE**



Figure 67

**TLE2022 AND TLE2024
PHASE MARGIN
vs
LOAD CAPACITANCE**



Figure 68

**TLE2021
PHASE MARGIN†
vs
FREE-AIR TEMPERATURE**



Figure 69

**TLE2022 AND TLE2024
PHASE MARGIN†
vs
FREE-AIR TEMPERATURE**



Figure 70

† Data at high and low temperatures are applicable only within the rated operating free-air temperature ranges of the various devices.

APPLICATION INFORMATION

voltage-follower applications

The TLE202x circuitry includes input-protection diodes to limit the voltage across the input transistors; however, no provision is made in the circuit to limit the current if these diodes are forward biased. This condition can occur when the device is operated in the voltage-follower configuration and driven with a fast, large-signal pulse. It is recommended that a feedback resistor be used to limit the current to a maximum of 1 mA to prevent degradation of the device. This feedback resistor forms a pole with the input capacitance of the device. For feedback resistor values greater than 10 k Ω , this pole degrades the amplifier phase margin. This problem can be alleviated by adding a capacitor (20 pF to 50 pF) in parallel with the feedback resistor (see Figure 71).



Figure 71. Voltage Follower

Input offset voltage nulling

The TLE202x series offers external null pins that further reduce the input offset voltage. The circuit in Figure 72 can be connected as shown if this feature is desired. When external nulling is not needed, the null pins may be left disconnected.

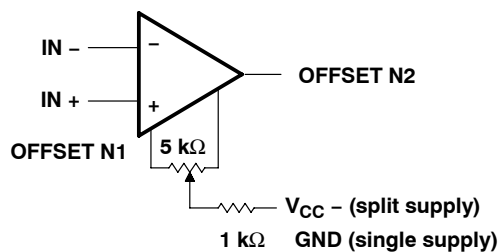


Figure 72. Input Offset Voltage Null Circuit

TLE202x, TLE202xA, TLE202xB, TLE202xY EXCALIBUR HIGH-SPEED LOW-POWER PRECISION OPERATIONAL AMPLIFIERS

SLOS191D – FEBRUARY 1997 – REVISED NOVEMBER 2010

APPLICATION INFORMATION

macromodel information

Macromodel information provided was derived using Microsim *Parts*™, the model generation software used with Microsim *PSpice*™. The Boyle macromodel (see Note 5) and subcircuit in Figure 73, Figure 74, and Figure 75 were generated using the TLE202x typical electrical and operating characteristics at 25°C. Using this information, output simulations of the following key parameters can be generated to a tolerance of 20% (in most cases):

- Maximum positive output voltage swing
- Maximum negative output voltage swing
- Slew rate
- Quiescent power dissipation
- Input bias current
- Open-loop voltage amplification
- Unity-gain frequency
- Common-mode rejection ratio
- Phase margin
- DC output resistance
- AC output resistance
- Short-circuit output current limit

NOTE 5: G. R. Boyle, B. M. Cohn, D. O. Pederson, and J. E. Solomon, "Macromodeling of Integrated Circuit Operational Amplifiers", *IEEE Journal of Solid-State Circuits*, SC-9, 353 (1974).

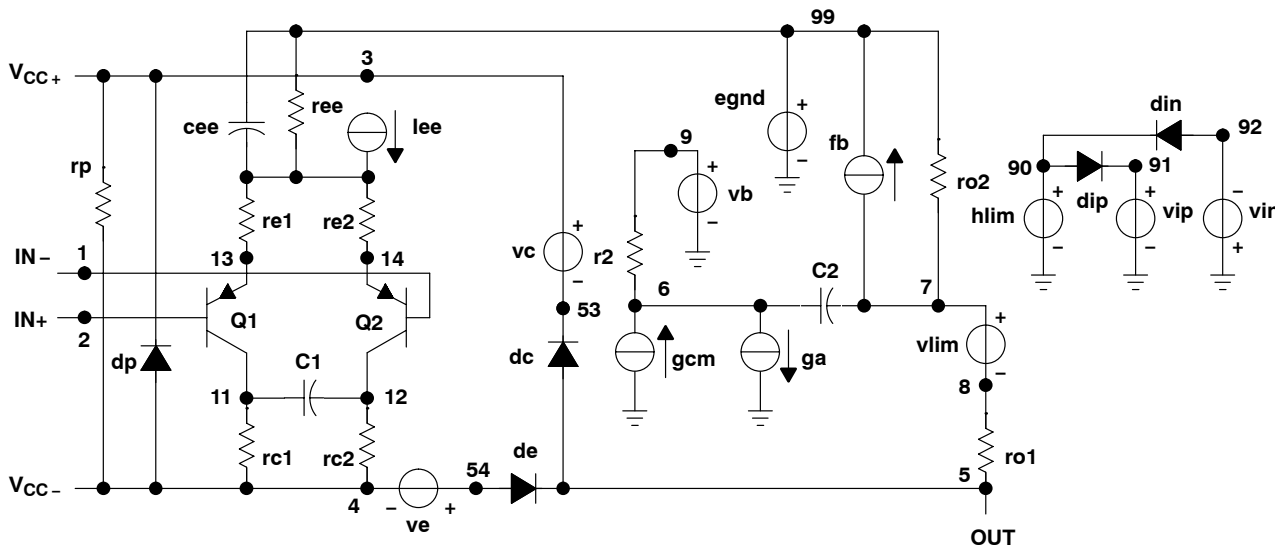


Figure 73. Boyle Subcircuit

PSpice and *Parts* are trademarks of MicroSim Corporation.



POST OFFICE BOX 655303 • DALLAS, TEXAS 75265

TLE202x, TLE202xA, TLE202xB, TLE202xY EXCALIBUR HIGH-SPEED LOW-POWER PRECISION OPERATIONAL AMPLIFIERS

SLOS191D – FEBRUARY 1997 – REVISED NOVEMBER 2010

```
.SUBCKT TLE2021 1 2 3 4 5
*
c1 11 12 6.244E-12
c2 6 7 13.4E-12
c3 87 0 10.64E-9
cpsr 85 86 15.9E-9
dcm+ 81 82 dx
dcm- 83 81 dx
dc 5 53 dx
de 54 5 dx
dlp 90 91 dx
dln 92 90 dx
dp 4 3 dx
ecmr 84 99 (2 99) 1
egnd 99 0 poly(2) (3,0) (4,0) 0 .5 .5
epsr 85 0 poly(1) (3,4) -60E-6 2.0E-6
ense 89 2 poly(1) (88,0) 120E-6 1
fb 7 99 poly(6) vb vc ve vlp vln vpsr 0 547.3E6
+ -50E7 50E7 50E7 -50E7 547E6
ga 6 0 11 12 188.5E-6
gcm 0 6 10 99 335.2E-12
gpsr 85 86 (85,86) 100E-6
grc1 4 11 (4,11) 1.885E-4
grc2 4 12 (4,12) 1.885E-4
gre1 13 10 (13,10) 6.82E-4
gre2 14 10 (14,10) 6.82E-4
hlim 90 0 vlim 1k

hcmr 80 1 poly(2) vcm+ vcm- 0 1E2 1E2
irp 3 4 185E-6
iee 3 10 dc 15.67E-6
iio 2 0 2E-9
i1 88 0 1E-21
q1 11 89 13 qx
q2 12 80 14 qx
R2 6 9 100.0E3
rcm 84 81 1K
ree 10 99 14.76E6
rn1 87 0 2.55E8
rn2 87 88 11.67E3
ro1 8 5 62
ro2 7 99 63
vcm+ 82 99 13.3
vcm- 83 99 -14.6
vb 9 0 dc 0
vc 3 53 dc 1.300
ve 54 4 dc 1.500
vlim 7 8 dc 0
vlp 91 0 dc 3.600
vln 0 92 dc 3.600
vpsr 0 86 dc 0
.model dx d(is=800.0E-18)
.model qx pnp(is=800.0E-18 bf=270)
.ends
```

Figure 74. Boyle Macromodel for the TLE2021

```
.SUBCKT TLE2022 1 2 3 4 5
*
c1 11 12 6.814E-12
c2 6 7 20.00E-12
dc 5 53 dx
de 54 5 dx
dlp 90 91 dx
dln 92 90 dx
dp 4 3 dx
egnd 99 0 poly(2) (3,0) (4,0) 0 .5 .5
fb 7 99 poly(5) vb vc ve vlp vln 0
+ 45.47E6 -50E6 50E6 50E6 -50E6
ga 6 0 11 12 377.9E-6
gcm 0 6 10 99 7.84E-10
iee 3 10 DC 18.07E-6
hlim 90 0 vlim 1k
q1 11 2 13 qx
q2 12 1 14 qx
r2 6 9 100.0E3

rc1 4 11 2.842E3
rc2 4 12 2.842E3
ge1 13 10 (10,13) 31.299E-3
ge2 14 10 (10,14) 31.299E-3
ree 10 99 11.07E6
ro1 8 5 250
ro2 7 99 250
rp 3 4 137.2E3
vb 9 0 dc 0
vc 3 53 dc 1.300
ve 54 4 dc 1.500
vlim 7 8 dc 0
vlp 91 0 dc 3
vln 0 92 dc 3
.model dx d(is=800.0E-18)
.model qx pnp(is=800.0E-18 bf=257.1)
.ends
```

Figure 75. Boyle Macromodel for the TLE2022

PACKAGING INFORMATION

| Orderable part number | Status (1) | Material type (2) | Package Pins | Package qty Carrier | RoHS (3) | Lead finish/ Ball material (4) | MSL rating/ Peak reflow (5) | Op temp (°C) | Part marking (6) |
|---------------------------------|---------------|----------------------|----------------|-----------------------|-------------|--------------------------------------|-----------------------------------|--------------|---|
| 5962-9088101MPA | Active | Production | CDIP (JG) 8 | 50 TUBE | No | SNPB | N/A for Pkg Type | -55 to 125 | 9088101MPA TLE2021M |
| 5962-9088102M2A | Active | Production | LCCC (FK) 20 | 55 TUBE | No | SNPB | N/A for Pkg Type | -55 to 125 | 5962- 9088102M2A TLE2022MFKB |
| 5962-9088102MPA | Active | Production | CDIP (JG) 8 | 50 TUBE | No | SNPB | N/A for Pkg Type | -55 to 125 | 9088102MPA TLE2022M |
| 5962-9088103M2A | Active | Production | LCCC (FK) 20 | 55 TUBE | No | SNPB | N/A for Pkg Type | -55 to 125 | 5962- 9088103M2A TLE2024MFKB |
| 5962-9088103MCA | Active | Production | CDIP (J) 14 | 25 TUBE | No | SNPB | N/A for Pkg Type | -55 to 125 | 5962-9088103MC A TLE2024MJB |
| 5962-9088104Q2A | Active | Production | LCCC (FK) 20 | 55 TUBE | No | SNPB | N/A for Pkg Type | -55 to 125 | 5962- 9088104Q2A TLE2021 AMFKB |
| 5962-9088104QPA | Active | Production | CDIP (JG) 8 | 50 TUBE | No | SNPB | N/A for Pkg Type | -55 to 125 | 9088104QPA TLE2021AM |
| 5962-9088105Q2A | Active | Production | LCCC (FK) 20 | 55 TUBE | No | SNPB | N/A for Pkg Type | -55 to 125 | 5962- 9088105Q2A TLE2022A MFKB |
| 5962-9088105QPA | Active | Production | CDIP (JG) 8 | 50 TUBE | No | SNPB | N/A for Pkg Type | -55 to 125 | 9088105QPA TLE2022AM |
| 5962-9088106Q2A | Active | Production | LCCC (FK) 20 | 55 TUBE | No | SNPB | N/A for Pkg Type | -55 to 125 | 5962- 9088106Q2A TLE2024A MFKB |
| 5962-9088106QCA | Active | Production | CDIP (J) 14 | 25 TUBE | No | SNPB | N/A for Pkg Type | -55 to 125 | 5962-9088106QC A TLE2024AMJB |

| Orderable part number | Status (1) | Material type (2) | Package Pins | Package qty Carrier | RoHS (3) | Lead finish/ Ball material (4) | MSL rating/ Peak reflow (5) | Op temp (°C) | Part marking (6) |
|---------------------------------|------------------|----------------------|----------------|-----------------------|-------------|--------------------------------------|-----------------------------------|--------------|-------------------------------------|
| 5962-9088107Q2A | Active | Production | LCCC (FK) 20 | 55 TUBE | No | SNPB | N/A for Pkg Type | -55 to 125 | 5962-9088107Q2A TLE2021 BMFKB |
| 5962-9088107QPA | Active | Production | CDIP (JG) 8 | 50 TUBE | No | SNPB | N/A for Pkg Type | -55 to 125 | 9088107QPA TLE2021BM |
| 5962-9088108Q2A | Active | Production | LCCC (FK) 20 | 55 TUBE | No | SNPB | N/A for Pkg Type | -55 to 125 | 5962-9088108Q2A TLE2022B MFKB |
| 5962-9088108QPA | Active | Production | CDIP (JG) 8 | 50 TUBE | No | SNPB | N/A for Pkg Type | -55 to 125 | 9088108QPA TLE2022BM |
| 5962-9088109Q2A | Active | Production | LCCC (FK) 20 | 55 TUBE | No | SNPB | N/A for Pkg Type | -55 to 125 | 5962-9088109Q2A TLE2024 BMFKB |
| 5962-9088109QCA | Active | Production | CDIP (J) 14 | 25 TUBE | No | SNPB | N/A for Pkg Type | -55 to 125 | 5962-9088109QC A TLE2024BMJB |
| TLE2021ACD | Obsolete | Production | SOIC (D) 8 | - | - | Call TI | Call TI | - | 2021AC |
| TLE2021ACDR | Last Time Buy | Production | SOIC (D) 8 | 2500 LARGE T&R | Yes | NIPDAU | Level-1-260C-UNLIM | - | 2021AC |
| TLE2021ACP | Active | Production | PDIP (P) 8 | 50 TUBE | Yes | NIPDAU | N/A for Pkg Type | - | TLE2021AC |
| TLE2021AID | Obsolete | Production | SOIC (D) 8 | - | - | Call TI | Call TI | -40 to 85 | 2021AI |
| TLE2021AIDR | Active | Production | SOIC (D) 8 | 2500 LARGE T&R | Yes | NIPDAU | Level-1-260C-UNLIM | - | 2021AI |
| TLE2021AIP | Active | Production | PDIP (P) 8 | 50 TUBE | Yes | NIPDAU | N/A for Pkg Type | - | TLE2021AI |
| TLE2021AMFKB | Active | Production | LCCC (FK) 20 | 55 TUBE | No | SNPB | N/A for Pkg Type | -55 to 125 | 5962-9088104Q2A TLE2021 AMFKB |
| TLE2021AMJGB | Active | Production | CDIP (JG) 8 | 50 TUBE | No | SNPB | N/A for Pkg Type | -55 to 125 | 9088104QPA TLE2021AM |
| TLE2021BMFKB | Active | Production | LCCC (FK) 20 | 55 TUBE | No | SNPB | N/A for Pkg Type | - | 5962-9088107Q2A TLE2021 BMFKB |

| Orderable part number | Status (1) | Material type (2) | Package Pins | Package qty Carrier | RoHS (3) | Lead finish/ Ball material (4) | MSL rating/ Peak reflow (5) | Op temp (°C) | Part marking (6) |
|-------------------------------|------------------|----------------------|----------------|-----------------------|-------------|--------------------------------------|-----------------------------------|--------------|---|
| TLE2021BMJG | Active | Production | CDIP (JG) 8 | 50 TUBE | No | SNPB | N/A for Pkg Type | -55 to 125 | TLE2021 BMJG |
| TLE2021BMJGB | Active | Production | CDIP (JG) 8 | 50 TUBE | No | SNPB | N/A for Pkg Type | - | 9088107QPA TLE2021BM |
| TLE2021CD | Obsolete | Production | SOIC (D) 8 | - | - | Call TI | Call TI | 0 to 70 | 2021C |
| TLE2021CDR | Last Time Buy | Production | SOIC (D) 8 | 2500 LARGE T&R | Yes | NIPDAU | Level-1-260C-UNLIM | 0 to 70 | 2021C |
| TLE2021CP | Active | Production | PDIP (P) 8 | 50 TUBE | Yes | NIPDAU | N/A for Pkg Type | 0 to 70 | TLE2021CP |
| TLE2021CPE4 | Active | Production | PDIP (P) 8 | 50 TUBE | Yes | NIPDAU | N/A for Pkg Type | 0 to 70 | TLE2021CP |
| TLE2021ID | Obsolete | Production | SOIC (D) 8 | - | - | Call TI | Call TI | -40 to 85 | 2021I |
| TLE2021IDR | Active | Production | SOIC (D) 8 | 2500 LARGE T&R | Yes | NIPDAU | Level-1-260C-UNLIM | -40 to 85 | 2021I |
| TLE2021IP | Active | Production | PDIP (P) 8 | 50 TUBE | Yes | NIPDAU | N/A for Pkg Type | -40 to 85 | TLE2021IP |
| TLE2021MD | Active | Production | SOIC (D) 8 | 75 TUBE | Yes | NIPDAU | Level-1-260C-UNLIM | -55 to 125 | 2021M |
| TLE2021MDG4 | Active | Production | SOIC (D) 8 | 75 TUBE | Yes | NIPDAU | Level-1-260C-UNLIM | - | 2021M |
| TLE2021MJG | Active | Production | CDIP (JG) 8 | 50 TUBE | No | SNPB | N/A for Pkg Type | -55 to 125 | TLE2021MJG |
| TLE2021MJGB | Active | Production | CDIP (JG) 8 | 50 TUBE | No | SNPB | N/A for Pkg Type | -55 to 125 | 9088101MPA TLE2021M |
| TLE2022ACD | Obsolete | Production | SOIC (D) 8 | - | - | Call TI | Call TI | 0 to 70 | 2022AC |
| TLE2022ACDR | Active | Production | SOIC (D) 8 | 2500 LARGE T&R | Yes | NIPDAU | Level-1-260C-UNLIM | - | 2022AC |
| TLE2022ACP | Active | Production | PDIP (P) 8 | 50 TUBE | Yes | NIPDAU | N/A for Pkg Type | - | TLE2022AC |
| TLE2022AID | Obsolete | Production | SOIC (D) 8 | - | - | Call TI | Call TI | -40 to 85 | 2022AI |
| TLE2022AIDR | Active | Production | SOIC (D) 8 | 2500 LARGE T&R | Yes | NIPDAU | Level-1-260C-UNLIM | - | 2022AI |
| TLE2022AIP | Active | Production | PDIP (P) 8 | 50 TUBE | Yes | NIPDAU | N/A for Pkg Type | - | TLE2022AI |
| TLE2022AMD | Obsolete | Production | SOIC (D) 8 | - | - | Call TI | Call TI | -55 to 125 | 2022AM |
| TLE2022AMDG4 | Active | Production | SOIC (D) 8 | 75 TUBE | Yes | NIPDAU | Level-1-260C-UNLIM | - | 2022AM |
| TLE2022AMDR | Active | Production | SOIC (D) 8 | 2500 LARGE T&R | Yes | NIPDAU | Level-1-260C-UNLIM | -55 to 125 | 2022AM |
| TLE2022AMDRG4 | Active | Production | SOIC (D) 8 | 2500 LARGE T&R | Yes | NIPDAU | Level-1-260C-UNLIM | - | 2022AM |
| TLE2022AMFKB | Active | Production | LCCC (FK) 20 | 55 TUBE | No | SNPB | N/A for Pkg Type | -55 to 125 | 5962- 9088105Q2A TLE2022A MFKB |
| TLE2022AMJGB | Active | Production | CDIP (JG) 8 | 50 TUBE | No | SNPB | N/A for Pkg Type | -55 to 125 | 9088105QPA TLE2022AM |

| Orderable part number | Status (1) | Material type (2) | Package Pins | Package qty Carrier | RoHS (3) | Lead finish/ Ball material (4) | MSL rating/ Peak reflow (5) | Op temp (°C) | Part marking (6) |
|--------------------------------|---------------|----------------------|----------------|-----------------------|-------------|--------------------------------------|-----------------------------------|---------------|---|
| TLE2022BMFKB | Active | Production | LCCC (FK) 20 | 55 TUBE | No | SNPB | N/A for Pkg Type | -55 to 125 | 5962- 9088108Q2A TLE2022B MFKB |
| TLE2022BMJGB | Active | Production | CDIP (JG) 8 | 50 TUBE | No | SNPB | N/A for Pkg Type | -55 to 125 | 9088108QPA TLE2022BM |
| TLE2022CD | Obsolete | Production | SOIC (D) 8 | - | - | Call TI | Call TI | - | 2022C |
| TLE2022CDR | Active | Production | SOIC (D) 8 | 2500 LARGE T&R | Yes | NIPDAU | Level-1-260C-UNLIM | 0 to 70 | 2022C |
| TLE2022CP | Active | Production | PDIP (P) 8 | 50 TUBE | Yes | NIPDAU | N/A for Pkg Type | - | TLE2022CP |
| TLE2022CPE4 | Active | Production | PDIP (P) 8 | 50 TUBE | Yes | NIPDAU | N/A for Pkg Type | See TLE2022CP | TLE2022CP |
| TLE2022ID | Obsolete | Production | SOIC (D) 8 | - | - | Call TI | Call TI | -40 to 85 | 2022I |
| TLE2022IDR | Active | Production | SOIC (D) 8 | 2500 LARGE T&R | Yes | NIPDAU | Level-1-260C-UNLIM | -40 to 85 | 2022I |
| TLE2022IP | Active | Production | PDIP (P) 8 | 50 TUBE | Yes | NIPDAU | N/A for Pkg Type | - | TLE2022IP |
| TLE2022IPE4 | Active | Production | PDIP (P) 8 | 50 TUBE | Yes | NIPDAU | N/A for Pkg Type | See TLE2022IP | TLE2022IP |
| TLE2022MD | Obsolete | Production | SOIC (D) 8 | - | - | Call TI | Call TI | -55 to 125 | 2022M |
| TLE2022MDR | Active | Production | SOIC (D) 8 | 2500 LARGE T&R | Yes | NIPDAU | Level-1-260C-UNLIM | -55 to 125 | 2022M |
| TLE2022MDRG4 | Active | Production | SOIC (D) 8 | 2500 LARGE T&R | Yes | NIPDAU | Level-1-260C-UNLIM | - | 2022M |
| TLE2022MFKB | Active | Production | LCCC (FK) 20 | 55 TUBE | No | SNPB | N/A for Pkg Type | -55 to 125 | 5962- 9088102M2A TLE2022MFKB |
| TLE2022MJG | Active | Production | CDIP (JG) 8 | 50 TUBE | No | SNPB | N/A for Pkg Type | -55 to 125 | TLE2022MJG |
| TLE2022MJGB | Active | Production | CDIP (JG) 8 | 50 TUBE | No | SNPB | N/A for Pkg Type | -55 to 125 | 9088102MPA TLE2022M |
| TLE2024ACDW | Obsolete | Production | SOIC (DW) 16 | - | - | Call TI | Call TI | - | TLE2024AC |
| TLE2024ACDWR | Active | Production | SOIC (DW) 16 | 2000 LARGE T&R | Yes | NIPDAU | Level-1-260C-UNLIM | - | TLE2024AC |
| TLE2024ACDWR.Z | Active | Production | SOIC (DW) 16 | 2000 LARGE T&R | Yes | NIPDAU | Level-1-260C-UNLIM | -40 to 85 | TLE2024AC |
| TLE2024ACN | Active | Production | PDIP (N) 14 | 25 TUBE | Yes | NIPDAU | N/A for Pkg Type | - | TLE2024ACN |
| TLE2024AIDW | Active | Production | SOIC (DW) 16 | 40 TUBE | Yes | NIPDAU | Level-1-260C-UNLIM | -40 to 85 | TLE2024AI |
| TLE2024AIN | Active | Production | PDIP (N) 14 | 25 TUBE | Yes | NIPDAU | N/A for Pkg Type | - | TLE2024AIN |
| TLE2024AMFKB | Active | Production | LCCC (FK) 20 | 55 TUBE | No | SNPB | N/A for Pkg Type | -55 to 125 | 5962- 9088106Q2A TLE2024A MFKB |

| Orderable part number | Status (1) | Material type (2) | Package Pins | Package qty Carrier | RoHS (3) | Lead finish/ Ball material (4) | MSL rating/ Peak reflow (5) | Op temp (°C) | Part marking (6) |
|--------------------------------|---------------|----------------------|----------------|-----------------------|-------------|--------------------------------------|-----------------------------------|-----------------|---|
| TLE2024AMJB | Active | Production | CDIP (J) 14 | 25 TUBE | No | SNPB | N/A for Pkg Type | -55 to 125 | 5962-9088106QC A TLE2024AMJB |
| TLE2024BMDW | Obsolete | Production | SOIC (DW) 16 | - | - | Call TI | Call TI | -55 to 125 | TLE2024BM |
| TLE2024BMDWG4 | Obsolete | Production | SOIC (DW) 16 | - | - | Call TI | Call TI | -55 to 125 | TLE2024BM |
| TLE2024BMDWR | Active | Production | SOIC (DW) 16 | 2000 LARGE T&R | Yes | NIPDAU | Level-1-260C-UNLIM | -55 to 125 | TLE2024BM |
| TLE2024BMDWR.Z | Active | Production | SOIC (DW) 16 | 2000 LARGE T&R | Yes | NIPDAU | Level-1-260C-UNLIM | -55 to 125 | TLE2024BM |
| TLE2024BMFKB | Active | Production | LCCC (FK) 20 | 55 TUBE | No | SNPB | N/A for Pkg Type | -55 to 125 | 5962- 9088109Q2A TLE2024 BMFKB |
| TLE2024BMJ | Active | Production | CDIP (J) 14 | 25 TUBE | No | SNPB | N/A for Pkg Type | -55 to 125 | TLE2024BMJ |
| TLE2024BMJB | Active | Production | CDIP (J) 14 | 25 TUBE | No | SNPB | N/A for Pkg Type | -55 to 125 | 5962-9088109QC A TLE2024BMJB |
| TLE2024CDW | Obsolete | Production | SOIC (DW) 16 | - | - | Call TI | Call TI | - | TLE2024C |
| TLE2024CDWR | Active | Production | SOIC (DW) 16 | 2000 LARGE T&R | Yes | NIPDAU | Level-1-260C-UNLIM | - | TLE2024C |
| TLE2024CDWR.Z | Active | Production | SOIC (DW) 16 | 2000 LARGE T&R | Yes | NIPDAU | Level-1-260C-UNLIM | See TLE2024CDWR | TLE2024C |
| TLE2024CN | Active | Production | PDIP (N) 14 | 25 TUBE | Yes | NIPDAU | N/A for Pkg Type | - | TLE2024CN |
| TLE2024CNE4 | Active | Production | PDIP (N) 14 | 25 TUBE | Yes | NIPDAU | N/A for Pkg Type | See TLE2024CN | TLE2024CN |
| TLE2024IDW | Obsolete | Production | SOIC (DW) 16 | - | - | Call TI | Call TI | - | TLE2024I |
| TLE2024IN | Active | Production | PDIP (N) 14 | 25 TUBE | Yes | NIPDAU | N/A for Pkg Type | - | TLE2024IN |
| TLE2024MFKB | Active | Production | LCCC (FK) 20 | 55 TUBE | No | SNPB | N/A for Pkg Type | -55 to 125 | 5962- 9088103M2A TLE2024MFKB |
| TLE2024MJB | Active | Production | CDIP (J) 14 | 25 TUBE | No | SNPB | N/A for Pkg Type | -55 to 125 | 5962-9088103MC A TLE2024MJB |

(1) **Status:** For more details on status, see our [product life cycle](#).

(2) **Material type:** When designated, preproduction parts are prototypes/experimental devices, and are not yet approved or released for full production. Testing and final process, including without limitation quality assurance, reliability performance testing, and/or process qualification, may not yet be complete, and this item is subject to further changes or possible discontinuation. If available for ordering, purchases will be subject to an additional waiver at checkout, and are intended for early internal evaluation purposes only. These items are sold without warranties of any kind.

(3) **RoHS values:** Yes, No, RoHS Exempt. See the [TI RoHS Statement](#) for additional information and value definition.

(4) **Lead finish/Ball material:** Parts may have multiple material finish options. Finish options are separated by a vertical ruled line. Lead finish/Ball material values may wrap to two lines if the finish value exceeds the maximum column width.

(5) **MSL rating/Peak reflow:** The moisture sensitivity level ratings and peak solder (reflow) temperatures. In the event that a part has multiple moisture sensitivity ratings, only the lowest level per JEDEC standards is shown. Refer to the shipping label for the actual reflow temperature that will be used to mount the part to the printed circuit board.

(6) **Part marking:** There may be an additional marking, which relates to the logo, the lot trace code information, or the environmental category of the part.

Multiple part markings will be inside parentheses. Only one part marking contained in parentheses and separated by a "~" will appear on a part. If a line is indented then it is a continuation of the previous line and the two combined represent the entire part marking for that device.

Important Information and Disclaimer:The information provided on this page represents TI's knowledge and belief as of the date that it is provided. TI bases its knowledge and belief on information provided by third parties, and makes no representation or warranty as to the accuracy of such information. Efforts are underway to better integrate information from third parties. TI has taken and continues to take reasonable steps to provide representative and accurate information but may not have conducted destructive testing or chemical analysis on incoming materials and chemicals. TI and TI suppliers consider certain information to be proprietary, and thus CAS numbers and other limited information may not be available for release.

In no event shall TI's liability arising out of such information exceed the total purchase price of the TI part(s) at issue in this document sold by TI to Customer on an annual basis.

OTHER QUALIFIED VERSIONS OF TLE2021, TLE2021A, TLE2021AM, TLE2021M, TLE2022, TLE2022A, TLE2022AM, TLE2022M, TLE2024, TLE2024A, TLE2024AM, TLE2024B, TLE2024BM, TLE2024M :

● Catalog : [TLE2021A](#), [TLE2021](#), [TLE2022A](#), [TLE2022](#), [TLE2024A](#), [TLE2024B](#), [TLE2024](#)

● Automotive : [TLE2021-Q1](#), [TLE2021A-Q1](#), [TLE2021A-Q1](#), [TLE2021-Q1](#), [TLE2022-Q1](#), [TLE2022A-Q1](#), [TLE2022A-Q1](#), [TLE2022-Q1](#), [TLE2024-Q1](#), [TLE2024-Q1](#)

● Enhanced Product : [TLE2021-EP](#), [TLE2021A-EP](#), [TLE2021A-EP](#), [TLE2021-EP](#), [TLE2022-EP](#), [TLE2022A-EP](#), [TLE2022A-EP](#), [TLE2022-EP](#), [TLE2024-EP](#), [TLE2024A-EP](#), [TLE2024A-EP](#), [TLE2024-EP](#)

● Military : [TLE2021M](#), [TLE2021AM](#), [TLE2022M](#), [TLE2022AM](#), [TLE2024M](#), [TLE2024AM](#), [TLE2024BM](#)

NOTE: Qualified Version Definitions:

● Catalog - TI's standard catalog product

● Automotive - Q100 devices qualified for high-reliability automotive applications targeting zero defects

- Enhanced Product - Supports Defense, Aerospace and Medical Applications
- Military - QML certified for Military and Defense Applications

TAPE AND REEL INFORMATION

QUADRANT ASSIGNMENTS FOR PIN 1 ORIENTATION IN TAPE


*All dimensions are nominal

| Device | Package Type | Package Drawing | Pins | SPQ | Reel Diameter (mm) | Reel Width W1 (mm) | A0 (mm) | B0 (mm) | K0 (mm) | P1 (mm) | W (mm) | Pin1 Quadrant |
|---------------|--------------|-----------------|------|------|--------------------|--------------------|---------|---------|---------|---------|--------|---------------|
| TLE2021ACDR | SOIC | D | 8 | 2500 | 330.0 | 12.4 | 6.4 | 5.2 | 2.1 | 8.0 | 12.0 | Q1 |
| TLE2021AIDR | SOIC | D | 8 | 2500 | 330.0 | 12.4 | 6.4 | 5.2 | 2.1 | 8.0 | 12.0 | Q1 |
| TLE2021CDR | SOIC | D | 8 | 2500 | 330.0 | 12.4 | 6.4 | 5.2 | 2.1 | 8.0 | 12.0 | Q1 |
| TLE2021IDR | SOIC | D | 8 | 2500 | 330.0 | 12.4 | 6.4 | 5.2 | 2.1 | 8.0 | 12.0 | Q1 |
| TLE2022ACDR | SOIC | D | 8 | 2500 | 330.0 | 12.4 | 6.4 | 5.2 | 2.1 | 8.0 | 12.0 | Q1 |
| TLE2022AIDR | SOIC | D | 8 | 2500 | 330.0 | 12.4 | 6.4 | 5.2 | 2.1 | 8.0 | 12.0 | Q1 |
| TLE2022AMDR | SOIC | D | 8 | 2500 | 330.0 | 12.4 | 6.4 | 5.2 | 2.1 | 8.0 | 12.0 | Q1 |
| TLE2022AMDRG4 | SOIC | D | 8 | 2500 | 330.0 | 12.5 | 6.4 | 5.2 | 2.1 | 8.0 | 12.0 | Q1 |
| TLE2022CDR | SOIC | D | 8 | 2500 | 330.0 | 12.4 | 6.4 | 5.2 | 2.1 | 8.0 | 12.0 | Q1 |
| TLE2022IDR | SOIC | D | 8 | 2500 | 330.0 | 12.4 | 6.4 | 5.2 | 2.1 | 8.0 | 12.0 | Q1 |
| TLE2022MDR | SOIC | D | 8 | 2500 | 330.0 | 12.4 | 6.4 | 5.2 | 2.1 | 8.0 | 12.0 | Q1 |

TAPE AND REEL BOX DIMENSIONS


*All dimensions are nominal

| Device | Package Type | Package Drawing | Pins | SPQ | Length (mm) | Width (mm) | Height (mm) |
|---------------|--------------|-----------------|------|------|-------------|------------|-------------|
| TLE2021ACDR | SOIC | D | 8 | 2500 | 353.0 | 353.0 | 32.0 |
| TLE2021AIDR | SOIC | D | 8 | 2500 | 353.0 | 353.0 | 32.0 |
| TLE2021CDR | SOIC | D | 8 | 2500 | 340.5 | 338.1 | 20.6 |
| TLE2021IDR | SOIC | D | 8 | 2500 | 353.0 | 353.0 | 32.0 |
| TLE2022ACDR | SOIC | D | 8 | 2500 | 353.0 | 353.0 | 32.0 |
| TLE2022AIDR | SOIC | D | 8 | 2500 | 353.0 | 353.0 | 32.0 |
| TLE2022AMDR | SOIC | D | 8 | 2500 | 350.0 | 350.0 | 43.0 |
| TLE2022AMDRG4 | SOIC | D | 8 | 2500 | 353.0 | 353.0 | 32.0 |
| TLE2022CDR | SOIC | D | 8 | 2500 | 353.0 | 353.0 | 32.0 |
| TLE2022IDR | SOIC | D | 8 | 2500 | 353.0 | 353.0 | 32.0 |
| TLE2022MDR | SOIC | D | 8 | 2500 | 350.0 | 350.0 | 43.0 |

TUBE


*All dimensions are nominal

| Device | Package Name | Package Type | Pins | SPQ | L (mm) | W (mm) | T (µm) | B (mm) |
|-----------------|--------------|--------------|------|-----|--------|--------|--------|--------|
| 5962-9088102M2A | FK | LCCC | 20 | 55 | 506.98 | 12.06 | 2030 | NA |
| 5962-9088103M2A | FK | LCCC | 20 | 55 | 506.98 | 12.06 | 2030 | NA |
| 5962-9088104Q2A | FK | LCCC | 20 | 55 | 506.98 | 12.06 | 2030 | NA |
| 5962-9088105Q2A | FK | LCCC | 20 | 55 | 506.98 | 12.06 | 2030 | NA |
| 5962-9088106Q2A | FK | LCCC | 20 | 55 | 506.98 | 12.06 | 2030 | NA |
| 5962-9088107Q2A | FK | LCCC | 20 | 55 | 506.98 | 12.06 | 2030 | NA |
| 5962-9088108Q2A | FK | LCCC | 20 | 55 | 506.98 | 12.06 | 2030 | NA |
| 5962-9088109Q2A | FK | LCCC | 20 | 55 | 506.98 | 12.06 | 2030 | NA |
| TLE2021ACP | P | PDIP | 8 | 50 | 506 | 13.97 | 11230 | 4.32 |
| TLE2021AIP | P | PDIP | 8 | 50 | 506 | 13.97 | 11230 | 4.32 |
| TLE2021AMFKB | FK | LCCC | 20 | 55 | 506.98 | 12.06 | 2030 | NA |
| TLE2021BMFKB | FK | LCCC | 20 | 55 | 506.98 | 12.06 | 2030 | NA |
| TLE2021CP | P | PDIP | 8 | 50 | 506 | 13.97 | 11230 | 4.32 |
| TLE2021CPE4 | P | PDIP | 8 | 50 | 506 | 13.97 | 11230 | 4.32 |
| TLE2021IP | P | PDIP | 8 | 50 | 506 | 13.97 | 11230 | 4.32 |
| TLE2021MD | D | SOIC | 8 | 75 | 505.46 | 6.76 | 3810 | 4 |
| TLE2021MDG4 | D | SOIC | 8 | 75 | 505.46 | 6.76 | 3810 | 4 |
| TLE2022ACP | P | PDIP | 8 | 50 | 506 | 13.97 | 11230 | 4.32 |
| TLE2022AIP | P | PDIP | 8 | 50 | 506 | 13.97 | 11230 | 4.32 |
| TLE2022AMDG4 | D | SOIC | 8 | 75 | 505.46 | 6.76 | 3810 | 4 |
| TLE2022AMFKB | FK | LCCC | 20 | 55 | 506.98 | 12.06 | 2030 | NA |
| TLE2022BMFKB | FK | LCCC | 20 | 55 | 506.98 | 12.06 | 2030 | NA |
| TLE2022CP | P | PDIP | 8 | 50 | 506 | 13.97 | 11230 | 4.32 |
| TLE2022CPE4 | P | PDIP | 8 | 50 | 506 | 13.97 | 11230 | 4.32 |
| TLE2022IP | P | PDIP | 8 | 50 | 506 | 13.97 | 11230 | 4.32 |
| TLE2022IPE4 | P | PDIP | 8 | 50 | 506 | 13.97 | 11230 | 4.32 |
| TLE2022MFKB | FK | LCCC | 20 | 55 | 506.98 | 12.06 | 2030 | NA |
| TLE2024ACN | N | PDIP | 14 | 25 | 506 | 13.97 | 11230 | 4.32 |
| TLE2024AIDW | DW | SOIC | 16 | 40 | 506.98 | 12.7 | 4826 | 6.6 |

| Device | Package Name | Package Type | Pins | SPQ | L (mm) | W (mm) | T (µm) | B (mm) |
|--------------|--------------|--------------|------|-----|--------|--------|--------|--------|
| TLE2024AIN | N | PDIP | 14 | 25 | 506 | 13.97 | 11230 | 4.32 |
| TLE2024AMFKB | FK | LCCC | 20 | 55 | 506.98 | 12.06 | 2030 | NA |
| TLE2024BMFKB | FK | LCCC | 20 | 55 | 506.98 | 12.06 | 2030 | NA |
| TLE2024CN | N | PDIP | 14 | 25 | 506 | 13.97 | 11230 | 4.32 |
| TLE2024CNE4 | N | PDIP | 14 | 25 | 506 | 13.97 | 11230 | 4.32 |
| TLE2024IN | N | PDIP | 14 | 25 | 506 | 13.97 | 11230 | 4.32 |
| TLE2024MFKB | FK | LCCC | 20 | 55 | 506.98 | 12.06 | 2030 | NA |

PACKAGE OUTLINE

JG0008A

CDIP - 5.08 mm max height

CERAMIC DUAL IN-LINE PACKAGE



NOTES:

1. All linear dimensions are in millimeters. Any dimensions in parenthesis are for reference only. Dimensioning and tolerancing per ASME Y14.5M.
2. This drawing is subject to change without notice.
3. This package can be hermetically sealed with a ceramic lid using glass frit.
4. Index point is provided on cap for terminal identification.
5. Falls within MIL STD 1835 GDIP1-T8

EXAMPLE BOARD LAYOUT

JG0008A

CDIP - 5.08 mm max height

CERAMIC DUAL IN-LINE PACKAGE



LAND PATTERN EXAMPLE
NON SOLDER MASK DEFINED
SCALE: 9X

4230036/A 09/2023

GENERIC PACKAGE VIEW

DW 16

SOIC - 2.65 mm max height

7.5 x 10.3, 1.27 mm pitch

SMALL OUTLINE INTEGRATED CIRCUIT

This image is a representation of the package family, actual package may vary.
Refer to the product data sheet for package details.



4224780/A



DW0016A

PACKAGE OUTLINE

SOIC - 2.65 mm max height

SOIC



4220721/A 07/2016

NOTES:

1. All linear dimensions are in millimeters. Dimensions in parenthesis are for reference only. Dimensioning and tolerancing per ASME Y14.5M.
2. This drawing is subject to change without notice.
3. This dimension does not include mold flash, protrusions, or gate burrs. Mold flash, protrusions, or gate burrs shall not exceed 0.15 mm, per side.
4. This dimension does not include interlead flash. Interlead flash shall not exceed 0.25 mm, per side.
5. Reference JEDEC registration MS-013.

EXAMPLE BOARD LAYOUT

DW0016A

SOIC - 2.65 mm max height

SOIC



LAND PATTERN EXAMPLE
SCALE:7X



SOLDER MASK DETAILS

4220721/A 07/2016

NOTES: (continued)

6. Publication IPC-7351 may have alternate designs.

7. Solder mask tolerances between and around signal pads can vary based on board fabrication site.

EXAMPLE STENCIL DESIGN

DW0016A

SOIC - 2.65 mm max height

SOIC



SOLDER PASTE EXAMPLE
BASED ON 0.125 mm THICK STENCIL
SCALE:7X

4220721/A 07/2016

NOTES: (continued)

8. Laser cutting apertures with trapezoidal walls and rounded corners may offer better paste release. IPC-7525 may have alternate design recommendations.
9. Board assembly site may have different recommendations for stencil design.

GENERIC PACKAGE VIEW

FK 20

LCCC - 2.03 mm max height

8.89 x 8.89, 1.27 mm pitch

LEADLESS CERAMIC CHIP CARRIER

This image is a representation of the package family, actual package may vary.
Refer to the product data sheet for package details.



4229370VA\

J 14

GENERIC PACKAGE VIEW
CDIP - 5.08 mm max height
CERAMIC DUAL IN LINE PACKAGE



Images above are just a representation of the package family, actual package may vary.
Refer to the product data sheet for package details.

4040083-5/G

J0014A



PACKAGE OUTLINE

CDIP - 5.08 mm max height

CERAMIC DUAL IN LINE PACKAGE



NOTES:

1. All controlling linear dimensions are in inches. Dimensions in brackets are in millimeters. Any dimension in brackets or parenthesis are for reference only. Dimensioning and tolerancing per ASME Y14.5M.
2. This drawing is subject to change without notice.
3. This package is hermetically sealed with a ceramic lid using glass frit.
4. Index point is provided on cap for terminal identification only and on press ceramic glass frit seal only.
5. Falls within MIL-STD-1835 and GDIP1-T14.

EXAMPLE BOARD LAYOUT

J0014A

CDIP - 5.08 mm max height

CERAMIC DUAL IN LINE PACKAGE



LAND PATTERN EXAMPLE
NON-SOLDER MASK DEFINED
SCALE: 5X



4214771/A 05/2017



D0008A

PACKAGE OUTLINE

SOIC - 1.75 mm max height

SMALL OUTLINE INTEGRATED CIRCUIT



4214825/C 02/2019

NOTES:

- Linear dimensions are in inches [millimeters]. Dimensions in parenthesis are for reference only. Controlling dimensions are in inches. Dimensioning and tolerancing per ASME Y14.5M.
- This drawing is subject to change without notice.
- This dimension does not include mold flash, protrusions, or gate burrs. Mold flash, protrusions, or gate burrs shall not exceed $.006$ [0.15] per side.
- This dimension does not include interlead flash.
- Reference JEDEC registration MS-012, variation AA.

EXAMPLE BOARD LAYOUT

D0008A

SOIC - 1.75 mm max height

SMALL OUTLINE INTEGRATED CIRCUIT



LAND PATTERN EXAMPLE
EXPOSED METAL SHOWN
SCALE:8X



SOLDER MASK DETAILS

4214825/C 02/2019

NOTES: (continued)

- 6. Publication IPC-7351 may have alternate designs.
- 7. Solder mask tolerances between and around signal pads can vary based on board fabrication site.

EXAMPLE STENCIL DESIGN

D0008A

SOIC - 1.75 mm max height

SMALL OUTLINE INTEGRATED CIRCUIT



SOLDER PASTE EXAMPLE
BASED ON .005 INCH [0.125 MM] THICK STENCIL
SCALE:8X

4214825/C 02/2019

NOTES: (continued)

8. Laser cutting apertures with trapezoidal walls and rounded corners may offer better paste release. IPC-7525 may have alternate design recommendations.
9. Board assembly site may have different recommendations for stencil design.

P (R-PDIP-T8)

PLASTIC DUAL-IN-LINE PACKAGE



- NOTES:
- A. All linear dimensions are in inches (millimeters).
 - B. This drawing is subject to change without notice.
 - C. Falls within JEDEC MS-001 variation BA.

N (R-PDIP-T**)

PLASTIC DUAL-IN-LINE PACKAGE

16 PINS SHOWN



- NOTES:
- A. All linear dimensions are in inches (millimeters).
 - B. This drawing is subject to change without notice.
 - Falls within JEDEC MS-001, except 18 and 20 pin minimum body length (Dim A).
 - The 20 pin end lead shoulder width is a vendor option, either half or full width.

IMPORTANT NOTICE AND DISCLAIMER

TI PROVIDES TECHNICAL AND RELIABILITY DATA (INCLUDING DATA SHEETS), DESIGN RESOURCES (INCLUDING REFERENCE DESIGNS), APPLICATION OR OTHER DESIGN ADVICE, WEB TOOLS, SAFETY INFORMATION, AND OTHER RESOURCES "AS IS" AND WITH ALL FAULTS, AND DISCLAIMS ALL WARRANTIES, EXPRESS AND IMPLIED, INCLUDING WITHOUT LIMITATION ANY IMPLIED WARRANTIES OF MERCHANTABILITY, FITNESS FOR A PARTICULAR PURPOSE OR NON-INFRINGEMENT OF THIRD PARTY INTELLECTUAL PROPERTY RIGHTS.

These resources are intended for skilled developers designing with TI products. You are solely responsible for (1) selecting the appropriate TI products for your application, (2) designing, validating and testing your application, and (3) ensuring your application meets applicable standards, and any other safety, security, regulatory or other requirements.

These resources are subject to change without notice. TI grants you permission to use these resources only for development of an application that uses the TI products described in the resource. Other reproduction and display of these resources is prohibited. No license is granted to any other TI intellectual property right or to any third party intellectual property right. TI disclaims responsibility for, and you will fully indemnify TI and its representatives against, any claims, damages, costs, losses, and liabilities arising out of your use of these resources.

TI's products are provided subject to [TI's Terms of Sale](#) or other applicable terms available either on [ti.com](#) or provided in conjunction with such TI products. TI's provision of these resources does not expand or otherwise alter TI's applicable warranties or warranty disclaimers for TI products.

TI objects to and rejects any additional or different terms you may have proposed.

Mailing Address: Texas Instruments, Post Office Box 655303, Dallas, Texas 75265
Copyright © 2025, Texas Instruments Incorporated